Jurassic Calcareous Nannofossils and Environmental Cycles

Edward Benedict Walsworth-Bell

University College London
PhD Thesis 2000

UCL

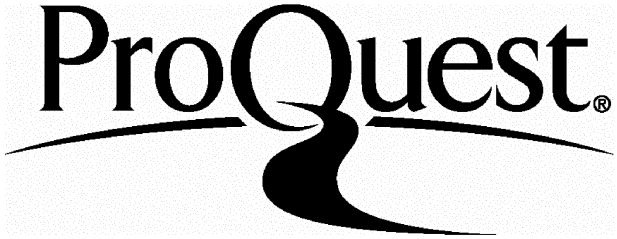

Title page illustrations. Foreground: Cross-polarised light micrograph of a Jurassic calcareous nannofossil (x3000). *Crucirhabdus primulus* was one of the first coccolithophores, and is the only member of this group known to have survived the terminal Triassic extinction event (Bown 1998a). This species is thus thought to be ancestral to Jurassic (and possibly all) coccolithophores (Bown & Young 1998a). **Background:** A section of the Belemnite Marls (Jurassic, UK). The decimetre- and metre-scale bedding rhythms which characterise these marine sediments record orbitally-forced (Milankovitch) environmental fluctuations (Weedon & Jenkyns 1999)

To see a world in a grain of sand
And a heaven in a wild flower,
Hold infinity in the palm of your hand
And eternity in an hour.

William Blake

Abstract

Calcareous nannofossils are microscopic remains of the calcite-secreting nannoplankton, a marine phytoplankton group which originated in the Late Triassic (Bown & Young 1998a). The ecology of the extant representatives of this group is reasonably well known, and the vastly abundant, geographically extensive and stratigraphically continuous fossil record of these organisms thus provides much in the way of palaeoceanographic, as well as biostratigraphic, information.

This thesis considers the distribution of nannofossils through three British Jurassic hemipelagic mudrock formations: the Black Ven Marls (Sinemurian), the Belemnite Marls (Pliensbachian) and the Oxford Clay (Callovian-Oxfordian). All three formations exhibit sedimentary cyclicity; the Belemnite Marls and the Oxford Clay are thought to record orbital (Milankovitch) periodicities (Weedon & Jenkyns 1999; Hudson & Martill 1994; Coe pers. comm. 1998), whilst the Black Ven Marls contains putative sequence cycles (Hesselbo & Jenkyns 1998). However, the processes linking environmental change and sedimentation in Jurassic epicontinental marine settings remain enigmatic, largely due to a paucity of detailed investigations. In this study high-resolution, quantitative nannofossil assemblage data were collected and subjected to various statistical analyses. Absolute abundance and diversity fluctuations are compared to lithological evidence, and interpreted in terms of palaeoenvironmental processes. Responses to palaeoenvironmental fluctuations allow suggestions to be made concerning the little-known ecological preferences of the early nannoplankton. The Belemnite Marls dataset is of sufficient length for time-series analysis (Weedon 1993, in prep.); the presence of regular cycles is detected, and located within the Milankovitch spectrum using Weedon & Jenkyns' (1999) cyclostratigraphic time-scale for the formation. In addition, the unusually high resolution of the nannofossil datasets allows the biostratigraphy of all three formations to be reconsidered.

This study reaffirms the potential for nannofloral investigation of the cyclostratigraphic record (Young *et al.* 1994). It is the first to apply time-series analysis to Jurassic nannofossil cycles.

Contents

List of Figures and Tables

2 Calcareous nannofossils

3 Cyclostratigraphy

4 The Belemnite Marls

5 The Oxford Clay

6 The Black Ven Marls

Appendix 1 Sample Curation

Appendix 2 Reproducibility of data

Appendix 4 Belemnite Marls data

Appendix 5 Biostratigraphy of the Belemnite Marls

Appendix 7 Oxford Clay Data

Appendix 8 Biostratigraphy of the Oxford Clay

Appendix 9 Black Ven Marls Data

Acknowledgements

I am greatly indebted to Paul Bown and Graham Weedon for helpful and good-humoured supervision throughout these 3 years of PhD research. Without their inspiring attention my work would have been substantially less productive; just as importantly, it would have been far less enjoyable.

I am also grateful to all my other colleagues, at UCL and beyond, who have provided thoughtful advice and discussion above and beyond the call of duty. In particular I would like to mention: Emma Bowden, Andy Howard, Jackie Lees, Emanuela Mattioli, Chris Street, Doorke Tervoort and Jeremy Young.

Jim Davy and Toby Stiles have been unflinching as ever in meeting my demands for technical support in laboratory work and reprographics. John Street helped out with the diversity analysis software.

The Natural Environment Research Council funded this project (award reference GT/04/97/191/ES). UCL and its Micropalaeontology Unit (Department of Geological Sciences) provided a supportive environment for research.

Finally, my family and friends deserve thanks for their constant encouragement and (professed!) interest in what I've been up to. In particular Ella Delderfield, for invaluable proof-reading and for surviving the traumas of my writing-up period.

1

Introduction

1.1 BACKGROUND

Calcareous nannofossils are microscopic remains of the calcite-secreting nannoplankton, a marine phytoplankton group which originated in the Late Triassic and has contributed significantly to pelagic carbonate sedimentation since the Early Jurassic (Bown & Young 1998a). Over the past 50 years the vastly abundant, geographically extensive and stratigraphically continuous fossil record of these organisms has proven exceptionally useful for biostratigraphy (Bown & Young 1998a). In addition, the ecology of the extant representatives of this group is reasonably well known, and in recent decades studies of relationships between nannofossil and lithofacies distribution through time and space have yielded much in the way of palaeoceanographic information (Burnett *et al.* 2000). The last decade or so has seen the appearance and rapid development of a promising new research area, that of nannofloral cyclicity (Young *et al.* 1994). Quantitative analyses of nannofossil distribution through sedimentary cycles in the orbital (Milankovitch) spectrum have proven particularly interesting, although cycles studied have ranged from sub-annual laminae (e.g. Thomsen 1989) to sequence cycles (e.g. Ineson *et al.* 2000). In allowing both quantification of sedimentary fluctuations and investigation of the palaeoenvironmental processes responsible, such approaches have provided increasingly refined data regarding palaeoceanographic and -climatic processes. Responses to palaeoenvironmental change have also shed light on the ecological preferences of fossil nannoplankton, about which little was previously known.

1.2 OBJECTIVES

This thesis considers the distribution of nannofossils through three British Jurassic hemipelagic mudrock formations: the Black Ven Marls (Sinemurian), the Belemnite Marls (Pliensbachian) and the Oxford Clay (Callovian-Oxfordian). All three formations exhibit sedimentary cyclicity, yet none have previously been subjected to detailed palaeoenvironmental analysis using microfossils. As a result the processes which linked environmental change and sedimentation in Jurassic epicontinental marine settings have remained largely enigmatic.

The rhythmic bedding of the Belemnite Marls has recently been shown to record Milankovitch periodicities (Weedon & Jenkyns 1999). This formation represents the focus of the present study. High-resolution, quantitative nannofloral data were collected and subjected to various statistical analyses. Time-series analysis allows the presence of regular cycles in the dataset to be detected (Weedon 1993, in prep.). Preservation, absolute abundance and diversity fluctuations are compared with lithological parameters, and interpreted in terms of palaeoenvironmental processes.

It has been suggested that the Oxford Clay also records Milankovitch cyclicity (Hudson & Martill 1994; Coe pers. comm. 1998). In the present study these sediments were subjected to extensive nannofloral and geochemical investigation, with a view to determining their potential for cyclostratigraphic analysis. The Black Ven Marls contains putative sequence cycles (Hesselbo & Jenkyns 1998); a detailed reconnaissance of this unit was undertaken in order to ascertain whether such lithological fluctuations are also expressed by nannofloral parameters.

1.3 PREVIOUS WORK

Although nannofossils have proven useful in palaeoceanographic studies reaching back as far as the Mesozic (e.g. Burnett *et al.* 2000), little attention has been paid to the oceanic history of the Jurassic as traced by nannoplankton (with several notable exceptions, e.g. Mattioli 1997). Previous nannofloral studies of sedimentary cycles, albeit relatively few in number, have ranged from the

Quaternary (e.g. Okada & Matsuoka 1996) to the Jurassic (e.g. Mattioli 1997; where pertinent, these are discussed in the text). However, the time-significance of Mesozoic stratigraphic cycles has rarely been well constrained, and Mesozoic nannofloral studies involving cyclostratigraphic techniques have been limited to the Cretaceous (e.g. Erba *et al.* 1992). As such the present study, which includes nannofloral time-series analysis, represents the first of its kind to focus on the Jurassic.

2

Calcareous Nannofossils

2.1 INTRODUCTION

Calcareous nannofossils are the remains of calcite-secreting plankton (Bown & Young 1998a). The term 'nannofossil' derives from the exigencies of plankton/micropalaeontological sampling, preparation and observation techniques, rather than from any observation of biological affinity; it represents all organically-precipitated calcite remains smaller than 30μm in size (and thus the smallest fossils that are routinely studied). This polyphyletic grouping includes coccolithophorid algae (coccolithophores), numerous *incertae sedis* taxa, and (more rarely) calcareous dinoflagellates, juvenile foraminifera and ascidian spicules of tunicates. It is the coccolithophores which are predominant in most nannofossil assemblages.

The living representatives of all these groups are included under the heading 'calcareous nannoplankton/nannoflora'. The study of their fossil record is referred to as 'nannopalaeontology/nannofacies analysis'. For a useful review of this field, see Bown & Young (1998a).

2.1.1 Nannoplankton biology and ecology

Coccolithophore biology. Coccolithophores are unicellular marine phytoplankton. The biology of their extant representatives is reasonably well known (Pienaar 1994). Coccolithophores are characterised by the secretion of a sub-spherical outer cell covering (coccosphere; Fig. 2.1; see Young *et al.* (1997) for morphological terminology) of calcite scales (coccoliths), the function of which is not fully understood (Young 1994). Classification has largely been based on the species-specific nature of coccolith morphology, resulting in a reliable taxonomy for the whole evolutionary history of the group (Bown & Young 1998a).

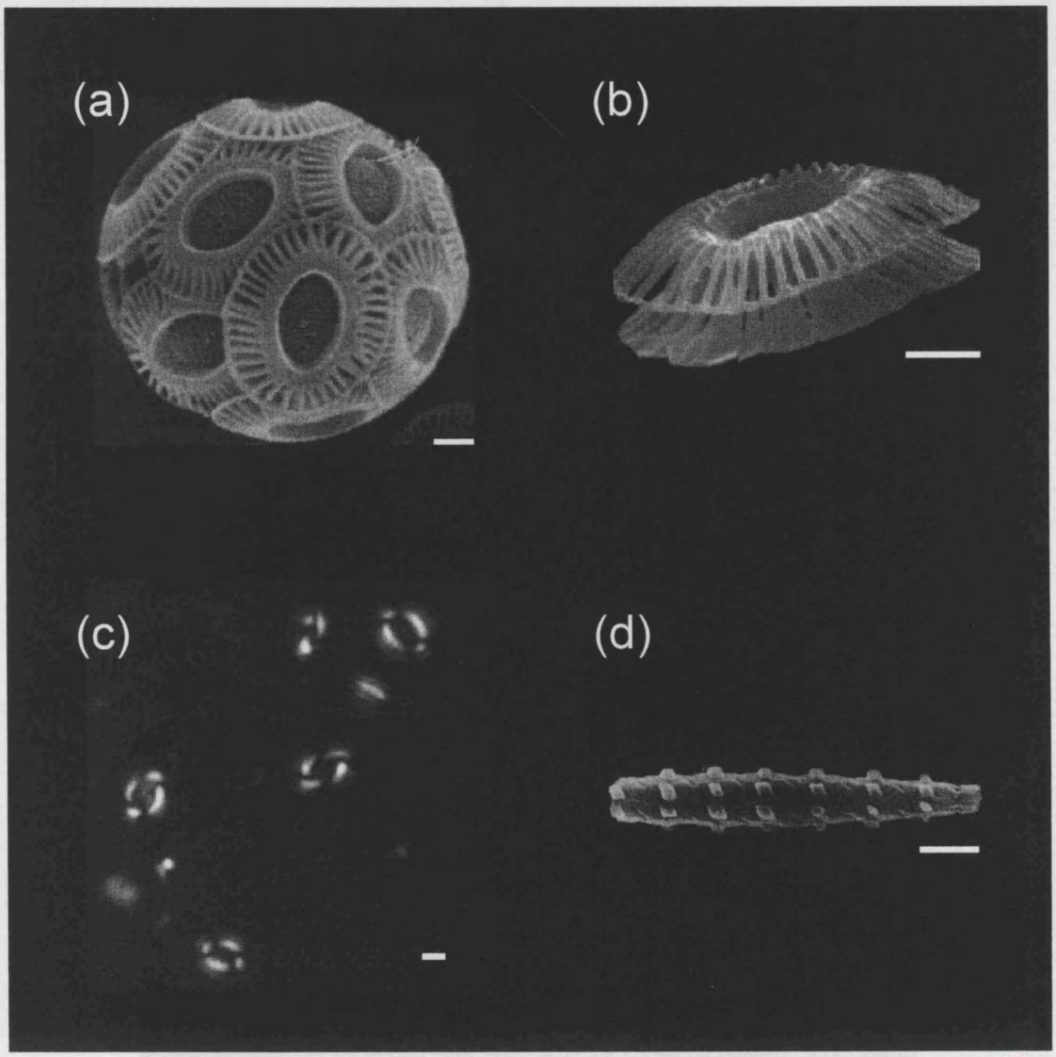

Fig. 2.1 (a) Scanning electron micrograph of a coccosphere and **(b)** a coccolith of the extant coccolithophore *Emiliania huxleyi* (modified from *www.soc.soton.ac.uk/soes/staff/tt/eh*); **(c)** cross-polarised light micrograph of several *E. huxleyi* coccoliths; **(d)** scanning electron micrograph of *Microrhabdulus belgicus*, a Cretaceous nannolith (modified from *www.bugware.com*). Scale bars = 1μm

Coccolithophore ecology. Together with diatoms and dinoflagellates, coccolithophores comprise a significant component of the present-day marine phytoplankton (Brand 1994; Fig. 2.2). The majority of extant species are essentially global in distribution, although diversity generally diminishes between tropical and polar waters (Winter *et al.* 1994). Ecologically, coccolithophores are similar to other phytoplankton groups (Brand 1994), the most significant difference being that most coccolithophore species are more specialised in their adaptation to specific ecological niches. Much of the following discussion of

coccolithophore ecology is based on the syntheses provided by Brand (1994) and Winter *et al.* (1994).

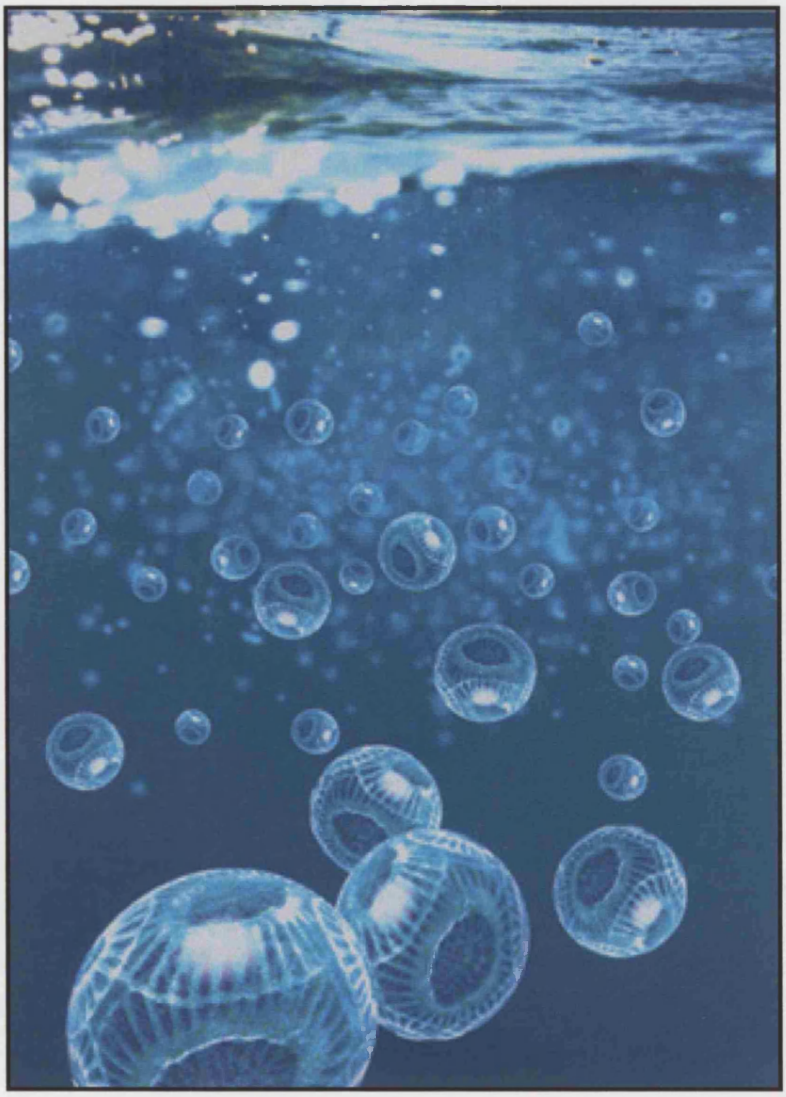

Fig. 2.2 Artist's impression of a coccolithophore (*Emiliania huxleyi*) bloom in marine surface waters. From *www.soc.soton.ac.uk/soes/staff/tt/eh*

The majority of coccolithophores are ecological specialists. Surface-water nutrient concentration appears to be the primary factor influencing coccolithophore distribution and productivity, whilst temperature exerts a major secondary influence. Specialised species are adapted to warm, low nutrient conditions (to the extent that these 'K-selected' taxa do not respond significantly to nutrient enrichment events).

A few species exhibit the higher levels of environmental tolerance characteristic of opportunistic strategies. These more 'r-selected' species have wider temperature tolerances, and display high maximum growth rates which allow them to respond to nutrification. Their abundances are however more easily limited by low nutrient concentrations.

This effectively continuous spectrum of environmental responses results in predictable spatial and temporal patterns in extant coccolithophore distribution. In terms of geographical distribution, most coccolithophore species inhabit the stratified waters of the temperate and tropical regions. As such, coccolithophore diversity is highest in warm, low-productivity (oligo-/mesotrophic) 'blue water' regions, such as subtropical oceanic gyre centres and restricted areas of circulation (e.g. the Red Sea). These zones are characterised by relatively low nannoplankton productivity, but high species diversity.

Lower diversity values are typical of cooler, more fertile surface waters in well-mixed temperate oceanic and subpolar regions, as assemblages are dominated by r-selected taxa. Diversity is also low in coastal waters. However, coccolithophore concentrations may be high in these settings. For instance, *Emiliania huxleyi*, the most ubiquitous and abundant coccolithophore in today's oceans (often occurring at a relative abundance of 60-80%), tends to become very abundant in cooler, nutrient-enriched waters on the margins of the subtropical oceanic gyres and in upwelling regions[1]. In the well-stratified waters of the central gyres this species is present but in much lower abundances, whilst assemblages are rich in other species which remain low in abundance in elevated nutrient settings. Under highly eutrophic conditions, low-diversity (essentially monospecific) blooms may occur, involving huge concentrations of cells (e.g. *E. huxleyi* in the Norwegian Fjords; Figs. 2.2 & 2.3. In some *E. huxleyi* blooms as many as 100 million coccoliths are present per litre of seawater).

[1] Another explanation for the low diversity found in upwelling areas is that upwelled metals (e.g. copper) might be toxic to phytoplankton. Supporting this idea is the fact that *E. huxleyi*, the coccolithophore most commonly found in upwelling areas, is able to tolerate higher concentrations of copper than other species. This effect of toxic metals on diversity is thought to be subordinate to the major limiting factors of nutrient enrichment and temperature.

Fig. 2.3 Satellite image of a coccolithophore (*Emiliania huxleyi*) bloom in the western Atlantic (off Newfoundland, Canada). From *www.soc.soton.ac.uk/soes/staff/tt/eh*

Temporal variations in distribution also reflect coccolithophore ecology well. For instance, during winter periods of vertical mixing in the open ocean, opportunistic species such as *E. huxleyi* flourish, whilst specialists become rare. During summer stratification, a diverse community of specialists becomes dominant, and the population of *E. huxleyi* diminishes.

Nannoliths. Also significant in nannofossil assemblages are 'nannoliths' (Fig. 2.1), the remains of extinct organisms of unknown biological affinity. Classification of these organisms is based on their diverse morphologies. It has been speculated that a number of nannolith species may represent derived coccolith morphologies (Bown & Young 1998a). Based on morphology and distribution it is believed that nannolith species were also phytoplanktonic, and displayed environmental responses analogous to those of the coccolithophores.

2.1.2 The fossil record

Sedimentation. Coccolithophores represent a significant component of preservable marine phytoplankton, and are major producers of calcareous

sediments (Berger 1976). Such deep-sea carbonate oozes are one of the most widespread sediment types on the planet, covering approximately half the floor of the modern oceans or a third of the surface of the Earth (nannofossils are only preserved in sediments which accumulate above the calcite compensation depth (CCD), unless transported by turbidites; Roth 1994).

Coccoliths sink towards the sea-floor in the faecal pellets of grazing zooplankton and in marine snow (Steinmetz 1994). This rapid sedimentation engenders nannofossil biocoenoses which are compositionally analogous to populations in the overlying surface waters (Roth 1994; although some level of disparity is always evident due to the lower preservation potential of fragile taxa).

The geological record. The nannofossil record dates from the Late Triassic (Bown 1998a; although the first appearance of nannofossils in Triassic rocks may not represent nannoplankton origins, but merely the earliest instance of their biomineralisation and/or preservation). The early nannoplankton shifted carbonate production from marine shelves into pelagic environments for the first time, and this group has contributed significantly to pelagic carbonates since the Early Jurassic; nannofossil limestones are common and extensive in the sedimentary record (e.g. the Upper Cretaceous white chalk facies, which occurs across most of northern Europe and has equivalents around the world). As such the nannoplankton have one of most abundant and continuous fossil records of any organism. The evolutionary development of nannoplankton through geological time is presented by various authors *in* Bown (1998b).

Palaeoecology. It is believed that nannoplankton have displayed ecological tolerances broadly similar to those of the extant coccolithophores throughout their geological history (Bown & Young 1998a). This assumption is based on various temporal and spatial scales of approach to the fossil record, including: distribution through sub-annual laminae (e.g. Thomsen 1989); distribution through larger-scale sedimentary (e.g. Milankovitch) cycles (e.g. Erba *et al.* 1992); distribution through the stratigraphic record as a whole and comparison with records of long-term global environmental (climate and sea-level) change (e.g. Burnett *et al.* 2000); and nannofossil palaeobiogeography (e.g. Street & Bown 2000). The environmental preferences of certain fossil species have been hazarded (e.g.

Mattioli 1997). Naturally understanding of nannofossil ecology diminishes with increasing geological antiquity, as a consequence of the vagaries of the fossil record and taxonomic 'distance' from living counterparts.

2.2 APPLICATIONS

Biostratigraphy. Nannofossils are amongst the most useful biostratigraphic marker fossils (Bown & Young 1998a), being planktonic in origin, and thus essentially facies independent; generally cosmopolitan in geographical distribution; both rapidly evolving and found in stratigraphic continuity (unlike ammonites), allowing narrow subdivision of geological time; minute, and thus recoverable from the smallest samples (e.g. side-wall cores); often vastly abundant in marine sediments, allowing high-resolution stratigraphic study; and relatively simple to process and identify. Biostratigraphy represents the most common application of nannofossils to date. Extensive scientific and industrial studies in recent decades have generated increasingly refined biozonation schemes, based on data from both on- and off-shore sections (unlike ammonites, which are known almost exclusively from the former). Problems with nannofossil biostratigraphy include the vagaries of preservation (under certain circumstances nannofossils are susceptible to dissolution, overgrowth and recrystallisation), the risk of contamination due to their diminutive size (in both the field (e.g. caving in boreholes) and laboratory), reworking, and occasional palaeobiogeographical constraints (e.g. absent marker species and event-horizon diachroneity).

Preservation analysis. Nannofossils allow estimation of the quality of carbonate preservation (Thierstein & Roth 1991). Experimental studies (Thierstein 1980) have shown that assemblage composition is strongly influenced by dissolution; species with small and delicate elements are susceptible to destruction, whilst those that are solidly constructed from large elements are more resistant. Syndepositional processes (e.g. the action of corrosive bottom waters) and/or postdepositional diagenetic alteration may result in overgrowth of resistant taxa at the expense of dissolution of fragile taxa (it is important to note that etching and overgrowth of specimens may be found within the same horizon). Mechanical

attrition of nannofossils may also occur due, for instance, to bioturbation. Nannofossil preservation has occasionally been used to assess the metamorphic history of metasediments (e.g. Volin *et al.* 1998).

Palaeobiology. The availability of large nannofossil populations in stratigraphic continuity provides excellent potential for palaeobiology, including studies of nannofossil ontogeny (e.g. Young & Bown 1991), phylogeny (e.g. Young 1990), palaeoecology (see below) and the nature of large-scale bio-events in Earth history (e.g. MacLeod *et al.* 1997). It may also be possible to use nannopalaeontological data in the investigation of major issues in evolutionary theory, such as the much-debated relative frequency of phyletic gradualism and punctuated equilibrium in speciation (e.g. Gibbs 2000; Knappertsbusch 2000).

Palaeoceanography and palaeoclimatology. Due to their environmental sensitivity, modern nannofloral assemblage composition corresponds with physical and chemical surface water-mass conditions (Brand 1994; Winter *et al.* 1994). Due to their protected and accelerated sedimentation in faecal pellets and/or marine snow (Steinmetz 1994), these spatial and temporal distribution patterns are translated into a remarkably representative sedimentary record (Roth 1994).

The fossil record suggests that the environmental controls on nannoplankton distribution have changed little over time (Section 2.1.2). Relationships between ancient nanno- and litho-facies may thus be considered in these palaeoecological terms and, when preservational controls are taken into account, ancient nannofloral geographic and stratigraphic distribution provide useful palaeoceanographic proxy data. Nannofossils have facilitated palaeoceanographic studies reaching as far back as the Mesozoic (e.g. Burnett *et al.* 2000; Gale *et al.* 2000; Street & Bown 2000).

Cyclostratigraphy. Nannofossils have particular potential for the investigation of sedimentary cyclicity, as they often constitute a significant component of rhythmic pelagic lithotypes. For instance, quantitative nannofloral distribution studies have allowed recognition of Milankovitch cyclicity and consideration of the environmental mechanisms responsible (e.g. Erba *et al.* 1992). Scales of

cyclicity that are not visually evident may be revealed, allowing the detection of palaeoenvironmental cycles from lithologically complex/monotonous sequences. In exceptional circumstances, nannofossils may allow cyclic palaeoenvironmental variations to be observed at the scale of laminae (e.g. Thomsen 1989). Nannofloral studies of sequence cycles have also been undertaken (e.g. Ineson *et al.* 2000).

Art history, archaeology and forensics. There have been a number of applications of nannofossils to art history (e.g. von Salis 1995), archaeology (e.g. Quinn 1999, 2000), and rare examples of nannofloral analysis in forensic science (not documented in the literature; Lord pers. comm. 2000). These have primarily relied on the biostratigraphic value of these fossils (see above) for correlation of a nannofossil-bearing sample (e.g. paint/a ceramic artefact/mud from the scene of a crime) with the exposure of its geological source. Preservation analysis is also useful in the study of historical manufacturing technologies (e.g. ceramic firing temperatures).

2.3 TECHNIQUES

In this section the standard techniques of nannofossil analysis are discussed. Methods that are particular to this study are presented in the relevant chapters. For additional background on nannopalaeontological techniques see Bown & Young (1998b).

2.3.1 Fieldwork

Nannofossils may be present in abundances of billions of specimens per gram of sediment; therefore samples collected need only be very small (in the order of a few mm^3; several cm^3 is the ideal size, allowing ease of handling and sub-sampling). Samples should not be collected from sediments that have been exposed to dissolution and contamination by weathering; it is better to expose and collect from a fresh surface.

2.3.2 Laboratory techniques

Nannofossils are routinely studied under the light microscope (LM). The birefringent properties of calcite in cross-polarised light (XPL) allow observation of both morphological and underlying crystallographic features; taxa exhibiting low birefringence may be studied using phase-contrast illumination. A magnification of *ca.* x1000 is typically employed. The diminutive size of nannofossils prevents extraction of individual specimens from sediments, and they are generally viewed in sediment smear/strew slides.

Smear and strew slides. In the preparation of a smear slide, a small amount of sediment is powdered onto a glass slide (nannofossils are too small to suffer comminution from this process) and mixed with a drop of water, using a flat-sided toothpick. The resulting smear is dried prior to affixation of the coverslip (various optical mounting media are available for this purpose).

Strew slides are similar in principle, but here the sediment is suspended in water and flooded onto the slide.

As nannofossils are dust-sized, there is substantial risk of sample contamination by stray specimens. This may be avoided by operating a dust-free laboratory, using distilled water (mains water may contain nannofossils, or cause specimen etching/overgrowth), cleaning all glassware in dilute HCl, and, where practical, employing disposable materials (e.g. plastic pipettes).

Random settling technique. More complex and specialised techniques are available which allow random settling of nannofossils onto a slide. The procedure outlined below is based on that of Geisen *et al.* (1999).

A small quantity of sediment is oven-dried, in order to facilitate disaggregation, and powdered. A 1l flask of water is buffered to a neutral pH (7.5-8), ideal for the prevention of specimen etching. A test-tube is filled from this flask, and *ca.* 10-50mg (accurately recorded weight) of powder is suspended inside it; this suspension is briefly subjected to ultrasound, ensuring complete sediment disaggregation. The contents of the test-tube are then added to the flask, and the suspension homogenised. The resulting suspension is poured into a settling apparatus (Fig. 2.4) until the water-level is 2-3cm (accurately recorded

height) above the surface of the slide. The apparatus is left in a quiet environment at room temperature for 24hrs, allowing all particles to settle out from suspension, before the water is removed using the drain valve. Once the slide has dried the coverslip can be mounted in the usual way.

(a)

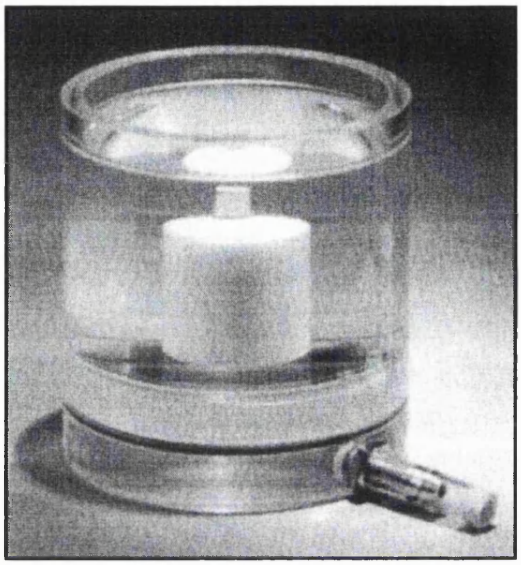

(b)

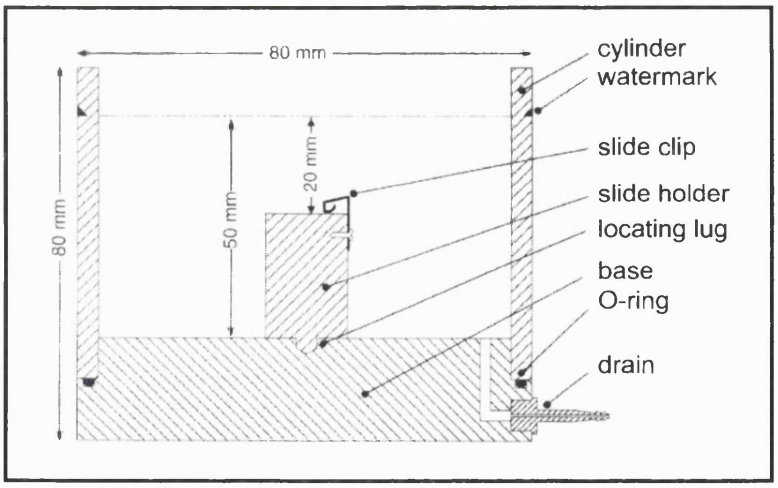

Fig. 2.4 (a) Photograph and **(b)** diagram of a random settling apparatus. Modified from Geisen *et al.* (1999)

Thin sections. Thin sections are rarely used in nannofossil studies, as specimens are typically too small to resolve using this method. Exceptionally, data for larger taxa have been collected in this fashion from highly-indurated limestones (e.g. Bronnimann 1955).

SEM preparations. The simplest method for viewing nannofossils in the SEM is to mount a small rock chip with a freshly exposed surface onto a stub. If specimens are to be viewed in isolation, a coverslip may be prepared using the smear/strew technique. A more sophisticated technique involves centrifugal 'cleaning' of suspended samples; this removes particles outside the size range of nannofossils, facilitating location and observation of specimens.

The appearance of nannofossils in the SEM is often worse than might be expected from their appearance in the LM. This is often due to fine particles (e.g. clay) obscuring specimens, even after centrifugation. This problem may be alleviated by encouraging sediment disaggregation through oven-drying and ultrasonic vibration of the suspension (a deflocculant (e.g. sodium hexametaphosphate) may be added at this stage).

Sample centrifugation may result in distorted assemblage composition, whilst SEM observation is time-consuming. As a consequence, use of the SEM is typically restricted to taxonomic studies (e.g. Bown 1987) or the detailed assessment of preservational state (e.g. Mattioli 1997), and rarely applied in the collection of population count data. SEM study is however occasionally essential to specialised investigations of nannofloral dynamics (e.g. distribution through laminae, more easily observed '*in situ*' on rock chips than in slide preparations under the LM; e.g. Thomsen 1989).

2.3.3 Data collection

Preservation. Nannofossil preservation is highly variable, and an indication of preservational state is necessary to indicate the integrity of any dataset. Preservation is difficult to quantify, as both etching and overgrowth may be observed in the same sample, and is typically the subject of qualitative estimates based on the predominant preservational state. Table 2.1 represents a suggestion for a system of standardised categories (Roth 1983).

Population counts. Nannofossil distribution studies have often been qualitative in nature, relying on broad categorisations of sample character (e.g. Crux 1987a). There is currently a trend towards collecting quantitative data, which are more suitable for detailed biostratigraphic (e.g. Raffi 1999) and palaeoceanographic

(e.g. Gale *et al.* 2000; Street & Bown 2000) studies. This requires the collection of population count data which adequately represent the natural proportions of a sample. A random count of 300 specimens is usually sufficient (Thierstein *et al.* 1977), allowing 95% confidence that all taxa constituting more than 1% of the population have been recorded. This is adequate for even detailed analysis, providing a useful compromise between time spent and precision required.

E-3	Heavily etched (much fragmented material, only solution-resistant taxa left)
E-2	Moderately etched (irregular outlines, delicate structures dissolved)
E-1	Slightly etched (serrate outlines, partial dissolution of delicate structures)
X	Excellent (structures are pristine)
O-1	Slightly overgrown (extended elements, thickened structures)
O-2	Moderately overgrown (delicate structures obscured)
O-3	Heavily overgrown (specimens so overgrown that identification is difficult)

Table 2.1 Typical nannofossil preservation categories (after Roth 1983)

2.3.4 Data analysis

Biostratigraphy. Samples may be assigned an age by comparing assemblage composition with recent nannofossil zonation schemes (e.g. various authors *in* Bown 1998b). Zones are typically based on first and last occurrences (FOs and LOs), relying on simple presence/absence data. However, increasing use is being made of population dynamics (e.g. acme intervals), requiring collection of quantitative data (e.g. Raffi 1999).

Relative abundance. Nannofloral data analysis typically involves the generation of percentage figures representing the relative (%) abundances of taxa (or biogenic calcite and detrital particles) in a sample. There is however a 'closed sum' problem with %abundance calculation; for instance, an increase in the %abundance of one taxon may cause an apparent decline in taxa which did not actually decrease in absolute abundance. Such interdependence of data must be taken into account when interpreting %abundance data; signal (genuine change in the abundance of a group) must be distinguished from echo (passive response to change in the %abundance of another group).

It has been suggested that preparations of the smear/strew variety are unsuitable for quantitative analysis (e.g. Geisen *et al.* 1997), as they do not yield an even distribution of particles. Slides produced by random settling are considered by some (e.g. Geisen *et al.* 1997) to be the more appropriate method. Notwithstanding this objection, the application of smear/strew slides in the collection of meaningful %abundance data is well established (e.g. Gale *et al.* 2000; Street & Bown 2000).

Absolute abundance. It is preferable to collect absolute abundance as well as %abundance data; the absolute abundance of a taxon is not affected by that of other taxa in the sample, as each is computed independently. Such estimates allow nannofossils to be investigated in terms of their behaviour as both population components and sediment particles.

Smear/strew preparations are increasingly used in the quantification of absolute abundances (e.g. Backman & Raffi 1997). The number of specimens per unit area of slide is proportional to the number of specimens per unit volume of sediment (assuming that care has been taken (as with all the techniques described here) to apply standardised procedures; in the case of smear/strew slides this involves achieving a largely consistent sediment density across all slides).

Diversity. Taxonomic diversity is a useful parameter in the investigation of palaeoecology (Ludwig & Reynolds 1988). Diversity indices may be generated through the application of various statistical techniques to population count data. Taxonomic richness is the simplest measure of diversity, representing the number of taxa in an assemblage. Evenness (equitability) is a measure of dominance within an assemblage, taking into account the distribution of individuals between taxa, and is calculated by finding the ratio between the actual distribution of individuals and the maximum distribution possible, given the taxonomic richness. A true diversity index encompasses both taxonomic richness and equitability.

3

Cyclostratigraphy

3.1 MILANKOVITCH CYCLES

The Earth experiences complex but predictable cyclic perturbations in the geometry of its orbit around the Sun (Fig. 3.1). These 'Milankovitch cycles' have periods ranging from tens to hundreds of thousands of years, and are driven by the changing gravitational environment of the Earth as dictated by the positions of the other planets in the solar system. For a useful introduction to these and other concepts underlying cyclostratigraphy, see Fischer *et al.* (1990). The historical development of the subject is reviewed by Imbrie & Imbrie (1979).

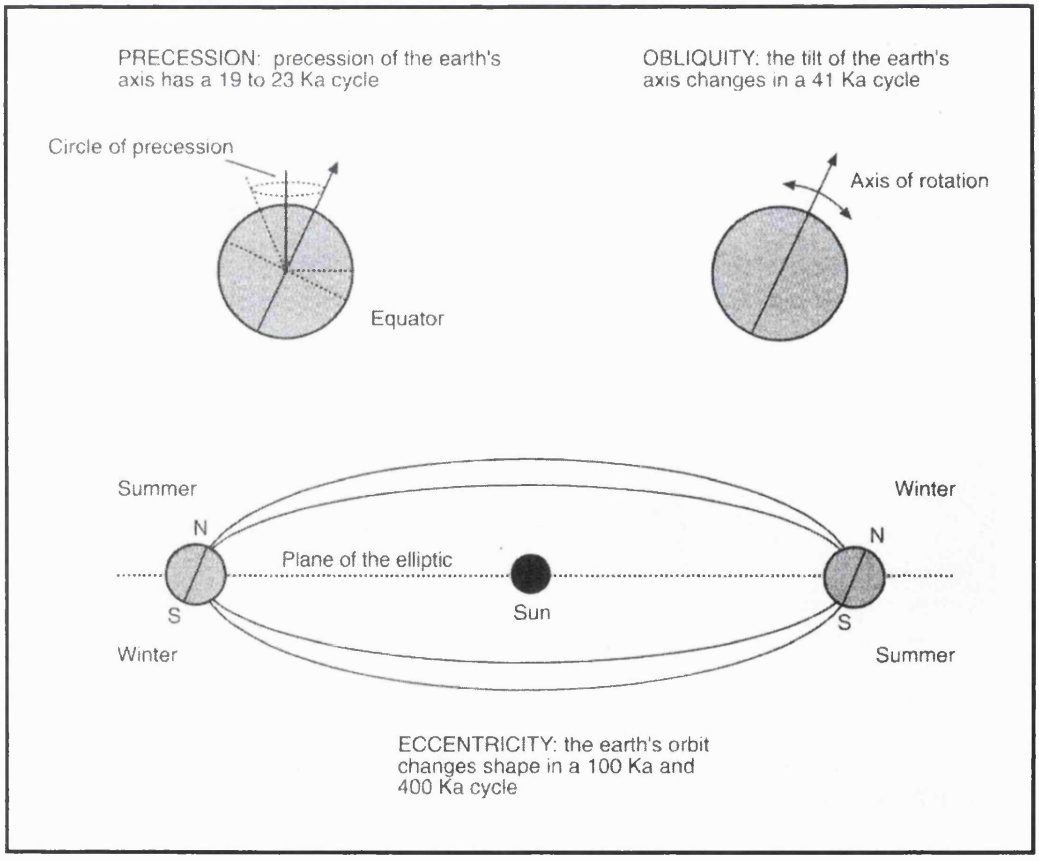

Fig. 3.1 Diagram of the Earth-Moon-Sun system and the oscillations that produce Milankovitch cycles. From Gale (1998)

The precession cycle. Earth's axis of rotation experiences a cyclic 'wobble' in space known as 'precession'. The periodicity of this cycle is bimodal, with present-day frequency peaks at 19 and 23ka (all cycle durations given are approximate).

The obliquity cycle. Earth's angle of axial tilt (obliquity) experiences cyclic variations with a present-day period of 41ka.

The eccentricity cycle. The Earth's orbit is deformed from more circular to more elliptical. Two major cycles characterise this process, with periods of 100 and 400ka.

The decreasing spin rate of the Earth has caused the periods of precession and obliquity to increase slowly through geological time (Berger *et al.* 1989). The durations of the eccentricity cycles have not changed.

3.1.1 Orbital forcing of climate

Orbital cycles mainly affect the latitudinal and seasonal distribution of Earth's insolation (solar energy input; Fig. 3.2). Insolation is the major energy input into the atmosphere-ocean system, and it is the motions of this system that are manifested as climate. Earth's irregular orbital geometry thus triggers climatic changes of global extent.

Precession and climate. Precession alters the structure of the seasonal cycle, shifting climatic belts between the hemispheres. This alters the total radiative heating in each season. Effects are especially pronounced at mid-latitudes.

Obliquity and climate. Obliquity affects both the intensity of the seasonal cycle and the latitudinal insolation gradient. This climatic effect is most pronounced in the polar regions.

Eccentricity and climate. Eccentricity affects the total amount of solar radiation received on the Earth's surface.

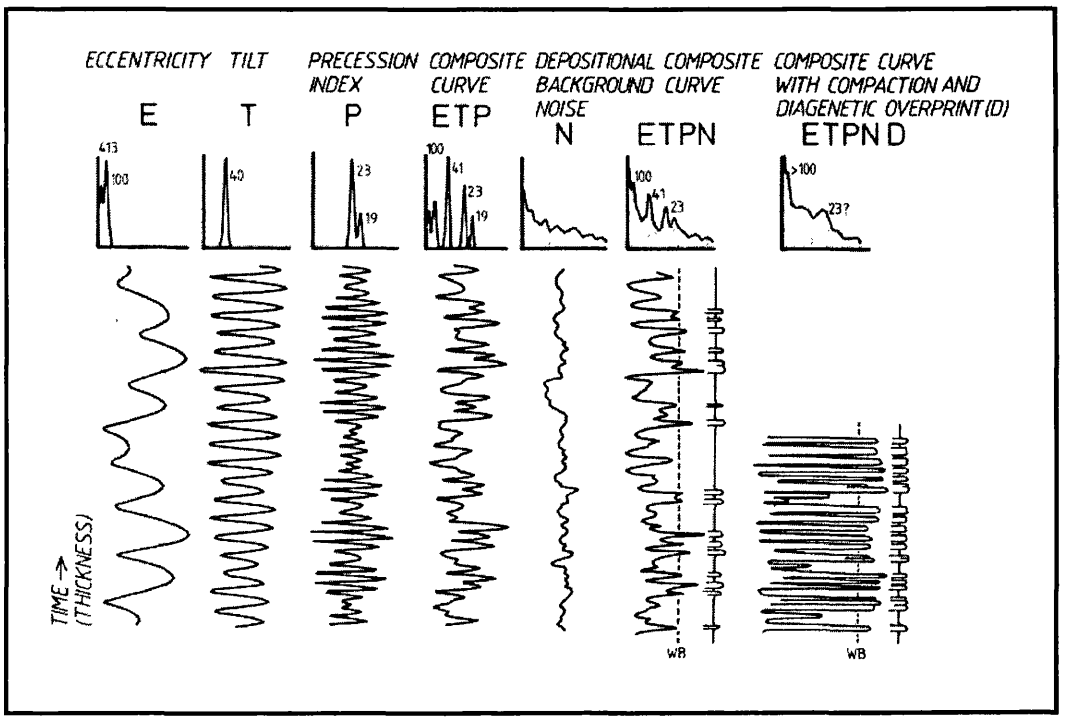

Fig. 3.2 Schematic diagram showing the Milankovitch frequencies (eccentricity, obliquity (tilt) and precession) and the generation of sedimentary cycles through the superposition of various parameters (orbital frequencies, depositional noise and diagenesis). The ETP curve, the sum of the orbital frequencies, is a measure of insolation. The ETPN curve is the sedimentary manifestation of the ETP curve; the ETPND curve is the signal as preserved in the stratigraphic record. Simplified weathering profiles are shown for the ETPN and ETPND curves, assuming that only those signals translated into carbonate contents above the weathering boundary (WB) result in limestones. From Einsele & Ricken (1991)

The precession-eccentricity syndrome. The effect of eccentricity alone on climate is minimal. Meanwhile, precession would have no climatic effect if the Earth's orbit were circular. The intensity of the precession cycle in climate is modulated by eccentricity; the effect of this 'precession-eccentricity syndrome' is considerable. Both the durations of the seasons, and the intensity of solar radiation received during the seasons, are affected (i.e. in each hemisphere there is alternation between, for instance, periods of long warm summers and periods of short hot summers).

3.1.2 Orbital-climatic forcing of sedimentation

The relatively weak Milankovitch variations in insolation are amplified by climate and oceanic circulation, and may consequently produce strong sedimentary

signals which are preserved in the stratigraphic record (Fig. 3.2; Einsele *et al.* 1991). Orbital-climatic explanations have been advanced for examples of sedimentary cyclicity throughout the geological column, and from a wide range of facies world-wide. The study of such cyclic sections is known as 'cyclostratigraphy' (Fischer *et al.* 1990). Discussion of the mechanisms by which climatic cycles affect sedimentation is provided by Fischer *et al.* (1990).

Orbital cyclicity may be expressed by numerous and diverse stratigraphic parameters, but marine calcareous mudrocks displaying regular bedding cycles at Milankovitch frequencies are especially common (Weedon 1993). These are associated with a number of different palaeogeographic settings, and typically comprise carbonate-rich/-poor alternations. Such carbonate rhythmites form the focus of this study, and the mechanisms involved in their formation are discussed below.

The processes linking climate with sedimentation are complex. Producing models to explain how climatic change may cause sedimentary cyclicity is not problematic, whilst identifying the correct climatic and sedimentological processes responsible for individual cases is difficult. A number of models have been proposed for the formation of marine carbonate rhythms (Fischer *et al.* 1990), all of which may involve climate (and as such represent 'primary' mechanisms). Numerous variables may affect any one sedimentary environment; often one process predominates, but interaction with others may be significant.

Productivity. Productivity models invoke periodic fluctuations in the abundance of calcareous-walled plankton, superimposed on a steady influx of fine terriginous clastics. This may represent a response to variations in surface-water conditions (e.g. changes in nutrient supply driven by variable upwelling).

Dilution. Dilution models describe the opposite scenario, where steady production of biogenic carbonate is overprinted by a fluctuating input of terrestrial detritus. Fluctuation in detrital supply may result from a number of processes (e.g. variable run-off).

Winnowing. Variable winnowing of fines may result in lithological alternations.

This may, for example, be connected to shifts in the intensity of marine circulation.

Dissolution. Dissolution models propose constant production of biogenic carbonate and a steady supply of terriginous sediment, but periodic syndepositional dissolution of carbonate (e.g. as a result of variations in the CCD).

Redox cycles. 'Redox' cycles produce variations in the preservation of organic matter, resulting in alternating dark, organic-rich shales and light, bioturbated marls. They may be caused by fluctuations in the supply of organic carbon and/or oxygen to bottom waters.

Diagenesis. The possible effects of diagenetic overprinting, involving post-depositional ('secondary') redistribution of carbonate, must also be taken into account. Diagenetic modification has been the cause of controversy over the genesis of sedimentary cycles, although it is now generally considered to be of importance only as a secondary enhancer of pre-existing carbonate rhythms (Weedon 1985).

3.2 CYCLOSTRATIGRAPHIC ANALYSIS

The effects of precession, obliquity and eccentricity combine to produce a complex insolation curve (Fig. 3.2). The translation of this curve, via climate, into the stratigraphic record is distorted by the random processes inherent to syn- and post-depositional environments. As a result, rhythmic sedimentary sequences are composed of a number of different wavelength oscillations, and visual inspection alone does not allow reliable recognition of regular cyclicity. A number of quantitative methods have been developed to assist with the detection and analysis of regular cycles.

For an introduction to cyclostratigraphic methods, see Gale (1998). A more detailed account is provided by Einsele *et al.* (1991) and Weedon (1993, in prep.). For a case-study, see Section 4.1.1.

3.2.1 Simple quantitative methods

Cycle counting. The occurrence of sedimentary cycles of regular thickness suggests that a regular cycle in time was responsible for their formation. Establishing that this cyclicity falls within the Milankovitch band can be attempted by dividing the duration of an interval dated with reference to radiometric methods by the number of bedding couplets (e.g. limestone-shale alternations); the result represents the approximate time interval recorded by each cycle. This technique of 'cycle counting' does not always produce reliable results. Only a very approximate frequency is yielded, as changing accumulation rates/the presence of hiatuses can significantly skew the result, and radiometric dates are imprecise. Also, some of the 'cycles' in question may represent event beds (e.g. related to tectonic events).

The ratio method. If multiple scales of sedimentary cyclicity are observed, the presence of distinctive ratios between the frequencies involved may assist in their identification. For instance, a frequency ratio of 5:1 would be commensurate with a record of precession (average period 21ka) and the short eccentricity cycle (100ka). This 'ratio method' is unreliable for the same reasons as discussed for the cycle counting method. Furthermore, the variety of possible cycle combinations allows for a confusing spectrum of wavelength ratios.

3.2.2 Time-series analysis

A more reliable approach to the assessment of sedimentary cycles is the collection and analysis of 'time series' representing small-scale parameter fluctuations. A time series is a sequence of parameter values collected at constant intervals of time/space (e.g. cumulative rock thickness). The techniques applied to the study of such data are referred to as 'time-series analysis'. Much of the following discussion of time-series analysis is based on the work of Weedon (1993, in prep.).

Field procedures

A number of conditions must be met, and procedural decisions made, before time series are generated from cyclic sequences: (1) Not all stratigraphic sections are suitable for time-series analysis. The interval must be free from major facies changes; by the same logic, any fossils under examination must be free from major evolutionary events. A time series which exhibits an overall trend towards higher/lower values is described as 'non-stationary', and may complicate detection of regular frequencies. (2) There must be a largely consistent relationship between stratigraphic thickness and time if what is essentially a 'depth series' is to be treated as a time series. (3) It is important that the data collected are reasonably reproducible and accurate. The recorded variable need not be restricted to lithology, and this significantly widens the scope of potential investigations. However, the variable must have had an unambiguous relationship with some fluctuating aspect of the environment throughout the time interval represented (albeit establishing the relationship between a particular environmental factor and the measured variable may be problematic). It would, for instance, be pointless to use a measurement determined by diagenetic processes alone. (4) Time-series analysis requires data points that are evenly spaced. Closely-spaced sampling with reference to the frequency under investigation is imperative, as the frequency resolution generated partially depends upon this factor; if samples are too far apart then small-scale variations are incompletely recorded, and spurious long-wavelength oscillations are created. Such inappropriately collected data are referred to as 'aliased'. A minimum of 4 sampling points per cycle (bedding couplet) is desirable; ideally, the sampling interval would be substantially smaller than the thinnest bed, allowing all oscillations to be defined by values that change smoothly from point to point. (5) In order to detect a particular wavelength, the time series must include numerous cycle repetitions; the frequency resolution generated partially depends upon this factor. Naturally it is desirable to obtain the longest possible time series, as more points give higher resolution. Most series are limited by the length of continuous stratigraphic exposure. Ideally, an absolute minimum of 5 cycles would be represented.

Spectral analysis

The standard method of identifying regular cyclicity within time series is 'spectral analysis'. Spectral analysis is an objective, statistical procedure, the most widely-used methods being based upon Fourier analysis. According to Fourier's Theorem any time series, regardless of its shape, is constructed from a combination of regular sine and cosine waves of specific phases, wavelengths and amplitudes. Fourier analysis allows the identification and quantification of cyclicity within a dataset.

In time-series analysis, the initial procedure typically involves the application of Fourier analysis to the dataset in order to produce a 'power spectrum'. Power spectra graphically portray the presence and relative significance of any frequency components. These 'spectral peaks' occur at frequencies corresponding to component wavelengths.

Confidence intervals are used to distinguish spectral peaks due to random fluctuations from those due to regular cyclicity. If a spectral peak occurs below the lowest reasonable confidence level (e.g. 90%), it cannot be considered statistically distinct from the background 'noise', and regular cyclicity cannot be inferred.

The frequency resolution of each spectral peak (bandwidth) is also calculated. Time-series oscillations may be considered demonstrably regular when the uncertainty in wavelength is less than a factor of two (Weedon & Jenkyns 1999).

Cross-spectral analysis

Another way to extract information from cyclostratigraphic data is through the application of 'cross-spectral analysis' ('coherency' and 'phase' spectra) to parallel time-series (e.g. wt%$CaCO_3$ and TOC determined for the same samples). Coherency spectra reveal the degree of correlation between the amplitudes of two time series at particular frequencies. Significant coherence at the frequency of a regular cycle would imply that the same environmental factor(s) controlled both parameters. Phase spectra are used to measure the phase relationship between two time series for different frequencies, and thus the relative timing of the oscillations

in the time series. Phase difference (phase) ranges from 180 to -180°; a phase of 0° would indicate simultaneous variations in the two parameters, whilst a phase of ±180° would indicate that the two parameters varied inversely.

Establishing the time-significance of cycles

Random depositional processes (e.g. variations in sedimentation rate) typically distort the stratigraphic record of palaeoenvironmental change, resulting in time series with measurements obtained at inconstant intervals in time. Significantly, these processes all destroy rather than create regularity (Weedon 1991). If regular cyclicity is detected through time-series analysis in the thickness domain, it can be concluded that a regular cycle in time was the cause. It is then reasonable to estimate cycle periods using cycle counting and/or ratio methods; a result falling within the Milankovitch spectrum may be considered a convincing case for orbital-climatic control (the supporting arguments in favour of this are the well-documented Pleistocene precedents, and the absence of other processes, known to be sufficiently regular for millions of years, that have the correct periods; Weedon 1993).

The absence of significant spectral peaks does not necessarily indicate an original absence of regular cyclicity, but perhaps only that time-depth distortions have masked signals.

3.3 APPLICATIONS

Correlation. The mechanisms involved in the formation of the cyclostratigraphic record are regionally synchronous. As such, the identification of Milankovitch frequencies in coeval sections allows refined lithostratigraphic correlation across wide geographic areas (e.g. Gale 1998). Individual bedding rhythms can sometimes be traced for thousands of kilometres, and can thus be applied to fine-scale basin reconstruction. These techniques produce data of a far higher resolution than those obtained using other stratigraphic techniques.

Cyclochronology. The identification of Milankovitch signals in the sedimentary

record enables increasingly accurate numerical dates to be assigned to bio- and chronostratigraphic timescales (e.g. Weedon & Jenkyns 1999; various authors *in* Shackleton *et al.* 1999). Such 'cyclochronology' is allowing the study of increasingly large parts of Earth history in 'real' time (i.e. on a scale of tens or hundreds of thousands of years; results obtained in this fashion may thus be several orders of magnitude more accurate than those yielded using radiometric timescales).

Environmental change prediction. Analysis of the stratigraphic record of long-term global environmental (e.g. climatic) processes allows clearer understanding of modern environments in the context of change within the Milankovitch spectrum (e.g. glacial/interglacial cycles; Imbrie & Imbrie 1979).

4

The Belemnite Marls

4.1 INTRODUCTION TO THE FORMATION

Incipient fragmentation of Pangaea in the Late Triassic and Early Jurassic, together with global marine transgression, resulted in extension of a new epicontinental seaway into the heart of the supercontinent (Fig. 4.1; Donovan & Howarth *in* Bradshaw *et al.* 1992). Marine conditions were established over part of previously continental north-western Europe. During the early Pliensbachian, the hemipelagic sediments of the Belemnite Marls Formation (Dorset, southern UK) accumulated in the Wessex Basin, which lay within this epeiric sea, largely enclosed by Pangaea, at a latitude of *ca.* 35°N (Hesselbo & Jenkyns 1995). Sea-floor relief was negligible, with water depths in the region of tens of to a few hundred metres (Hallam 1975; Sellwood & Jenkyns 1975). The formation is well exposed in cliffs on the south coast of England (Figs. 4.2 & 4.3). Lang *et al.* (1928) produced the first systematic bio- and lithostratigraphic treatment of the formation. Detailed sedimentological observations were provided by Sellwood (1972). More recently, work of a cyclostratigraphic nature has been presented by Weedon & Jenkyns (1999).

The complete formation is *ca.* 24m in thickness (Fig. 4.4). It consists principally of calcareous mudstones (marls), comprised of varying quantities of carbonate, clay, organic matter, pyrite, and a relatively low abundance of macrofossils. There are also minor millimetre-laminated carbon-rich shales. The carbonate is largely micritic and therefore of conjectural origin (Walker 1991), although nannoplankton contributed significantly (Sellwood 1972). The organic matter is chiefly marine, with minor terrestrial components (Fleet *et al.* 1987), and the clays are considered terrestrial in origin (Sellwood 1970).

The sequence is characterised by light- and dark-marl bedding couplets at the decimetre scale. These beds are clearly visible in coastal exposures, and are

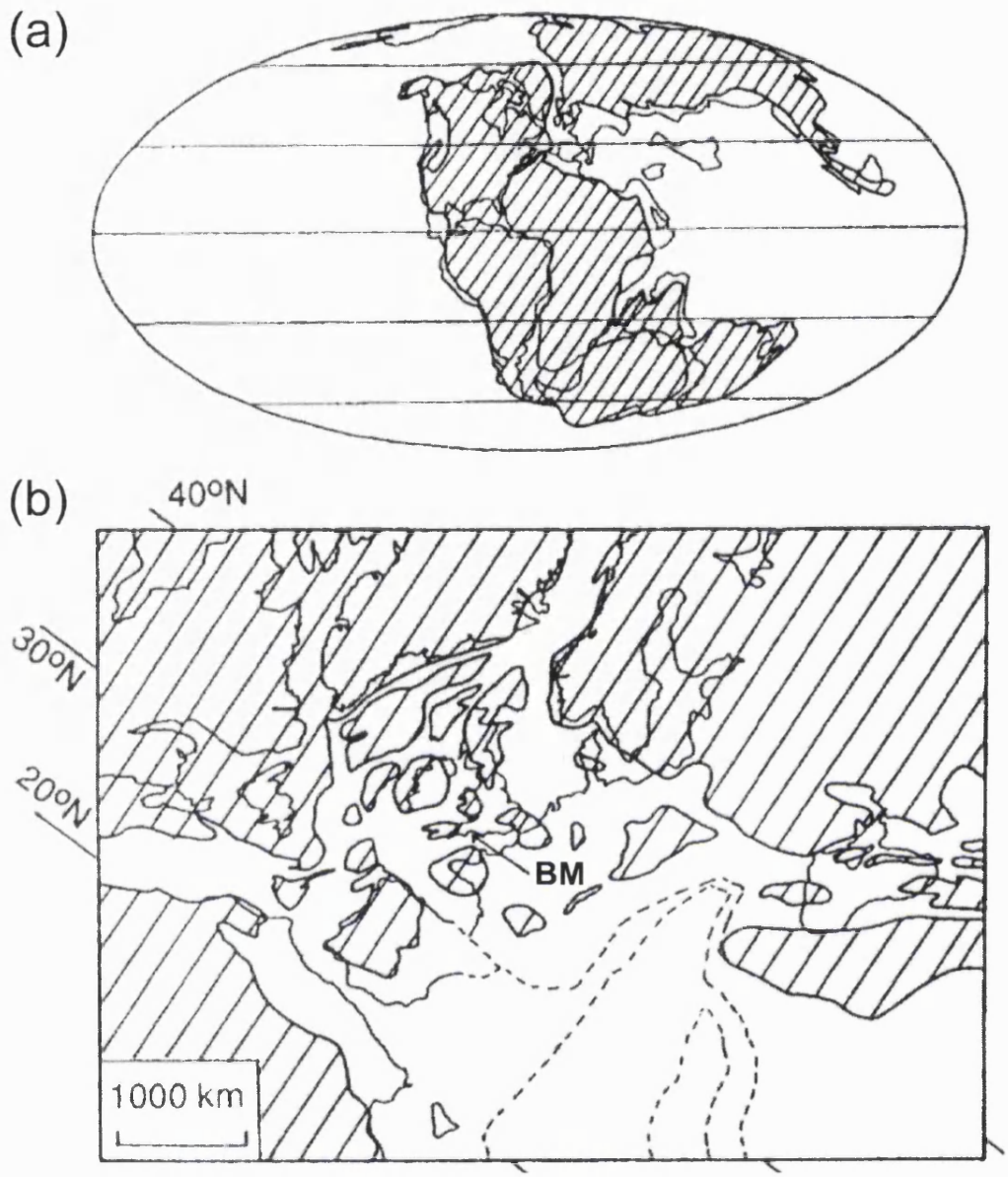

Fig. 4.1 (a) Main Pangaean coastlines of the Pliensbachian. Land areas are hatched. **(b)** European Pliensbachian coastlines. The location of the Belemnite Marls (BM) is indicated. Note approximate lines of palaeolatitude. Present-day coastlines shown for guidance. Modified from Weedon & Jenkyns (1999)

laterally continuous over several kilometres. They represent large variations in carbonate, clay and organic matter content (Fig. 4.5). There are also metre-scale fluctuations in the abundance of these components throughout the formation, giving rise to a conspicuous 'bundling' of the couplets. These couplets and bundles represent primary compositional variations, as supported by the following observations: (1) Extensive burrow mottling exists at bed contacts, with dark sediment piped into light and *vice versa* (Sellwood 1970). (2) Both carbonate

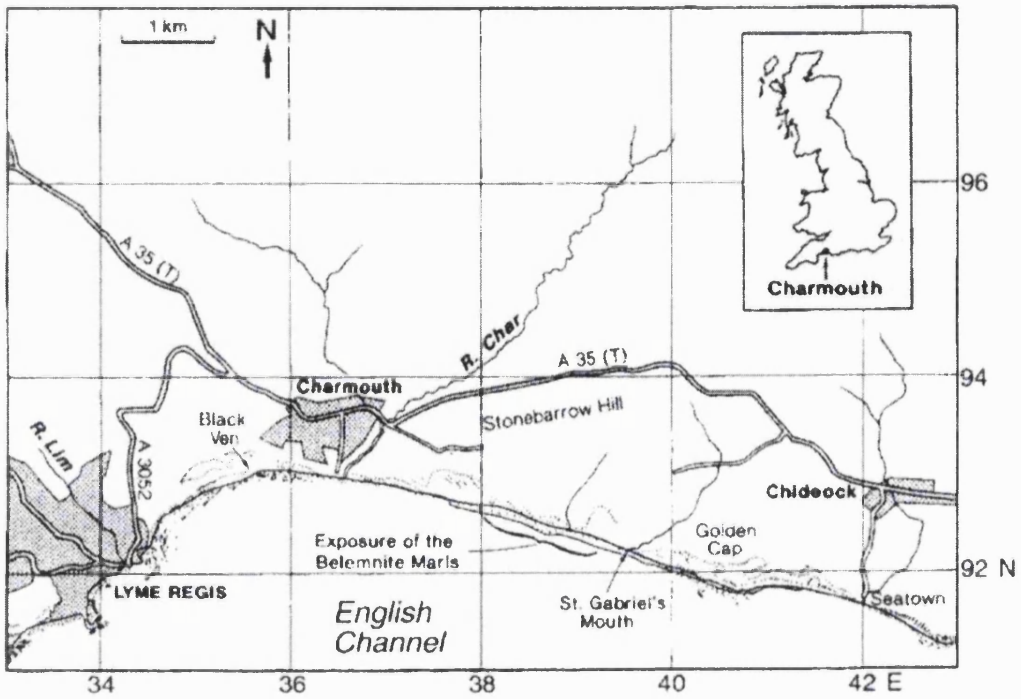

Fig. 4.2 Location of the Belemnite Marls exposure near Charmouth, southern UK. Numbers refer to the Ordnance Survey SY 100,000m grid square. From Weedon & Jenkyns (1999)

content and organic carbon content (expressed on a carbonate-free basis) vary between lithologies (Weedon & Jenkyns 1990). Closed-system carbonate redistribution cannot explain the inverse correlation between these parameters; instead, the large variations represented by the couplet cycles are best interpreted as primary. The bundle cycles also appear to be primary, as their lowest carbonate contents are associated both with beds that have above-average organic-carbon contents, and with the occurrence of laminated shales (sediments which record original accumulation of organic-rich deposits; Weedon & Jenkyns 1990). (3) There is no sedimentological evidence for significant redistribution of carbonate (Weedon & Jenkyns 1999; Munnecke *et al.* in press). Burrows are always partially compacted, three-dimensional aragonitic fossil moulds are absent, and there are no limestone nodules, early diagenetic limestones or stylolites. (Nonetheless the presence of pyrite throughout the sequence indicates that the labile organic matter led to some sulphate reduction at every stratigraphic level. This suggests that some of the carbonate microspar formed during early diagenesis. Furthermore, at least some diagenetic dissolution is suggested by the

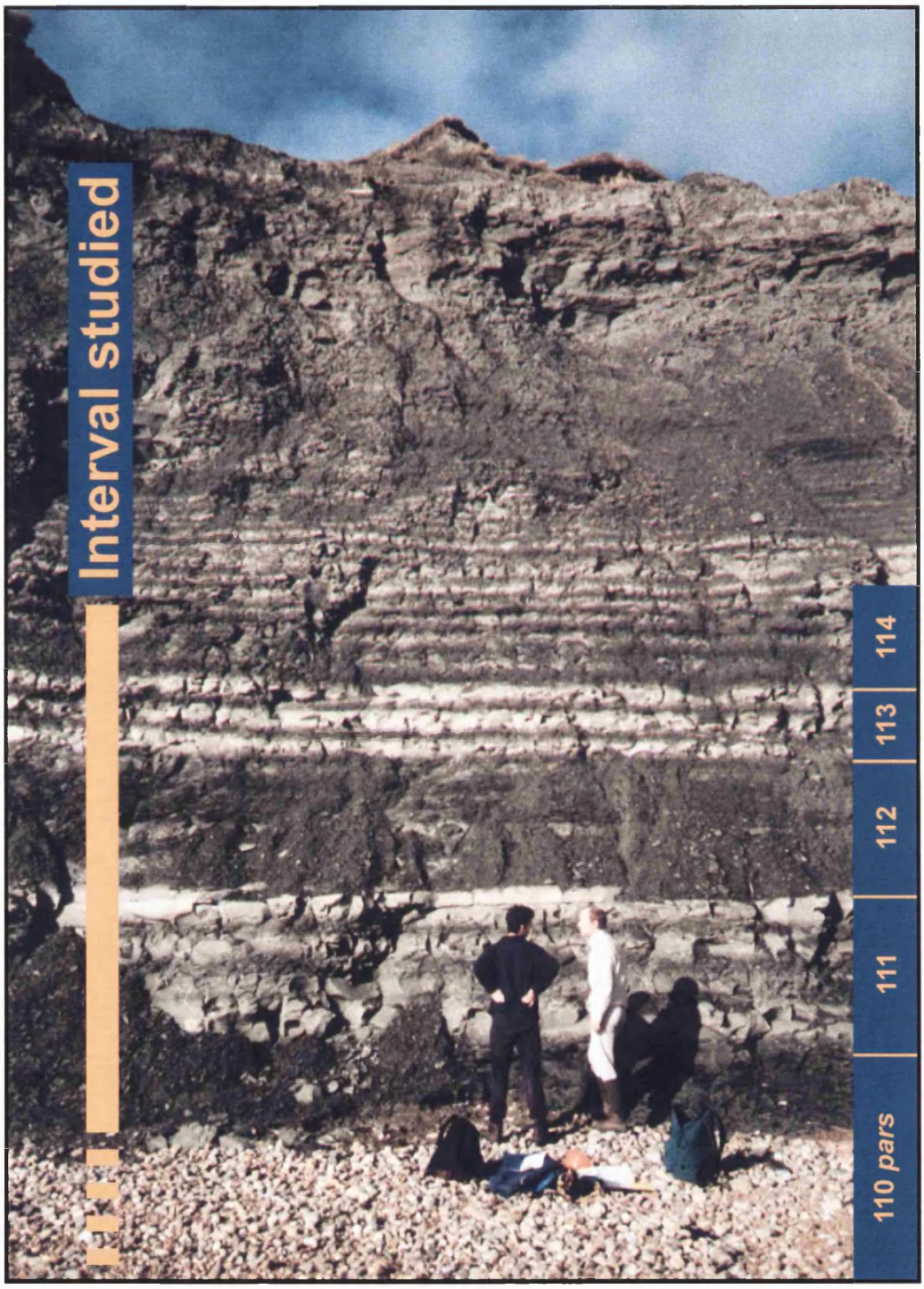

Fig. 4.3 Partial exposure (Beds 110-5) of the Belemnite Marls below Stonebarrow Hill. The main interval studied is shown

absence of fossils that would have possessed aragonitic shells; Weedon & Jenkyns 1999).

There is a gradual up-section decrease in the thickness of both couplet and bundle variations; this may be due to a decrease in mean sedimentation rate, as it

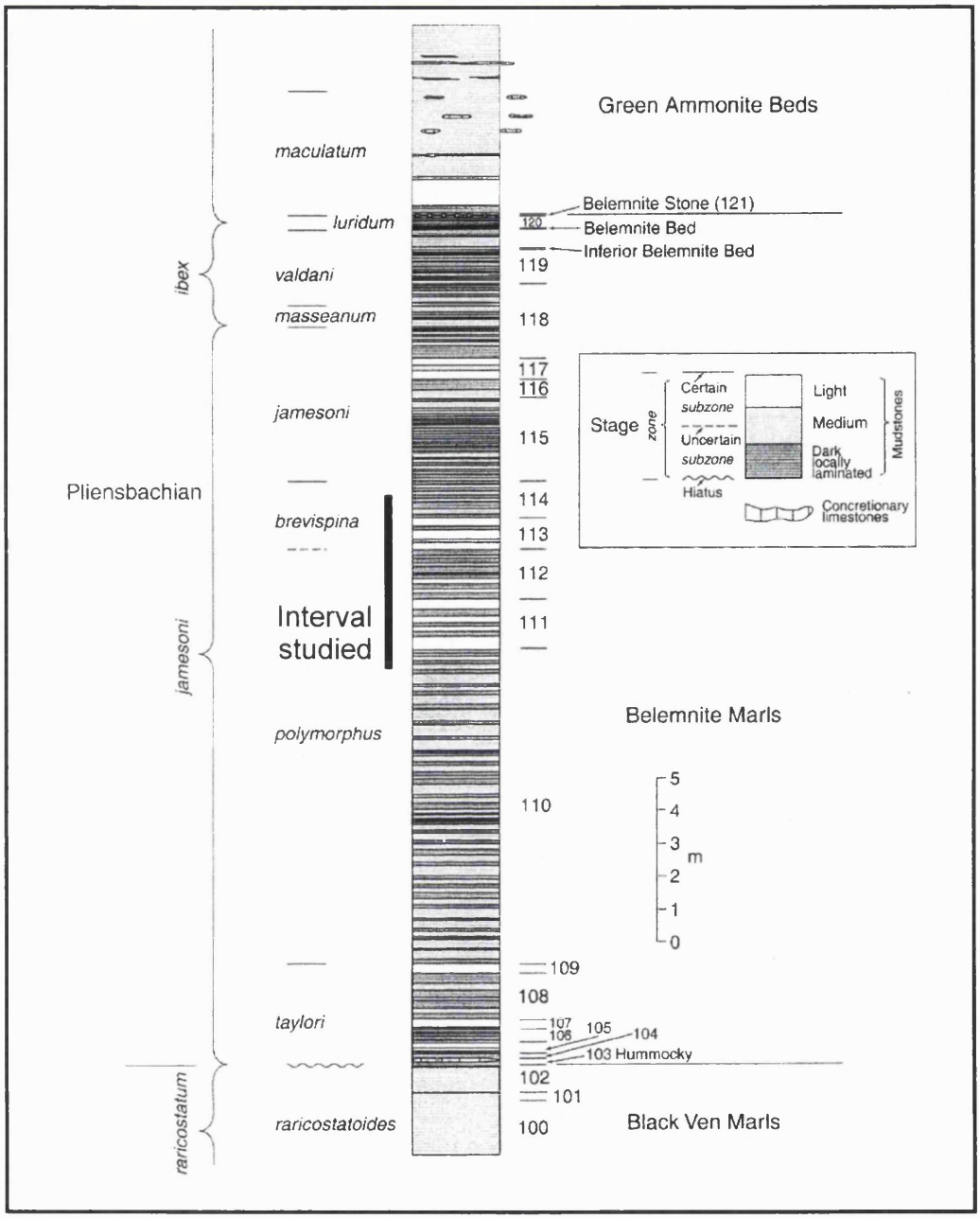

Fig. 4.4 Summary of the lithostratigraphy and ammonite stratigraphy of the Belemnite Marls and part of the adjacent formations. The main interval studied is shown. Modified from Weedon & Jenkyns (1999)

is accompanied by an increase in the concentration of macrofossils (Weedon & Jenkyns 1999).

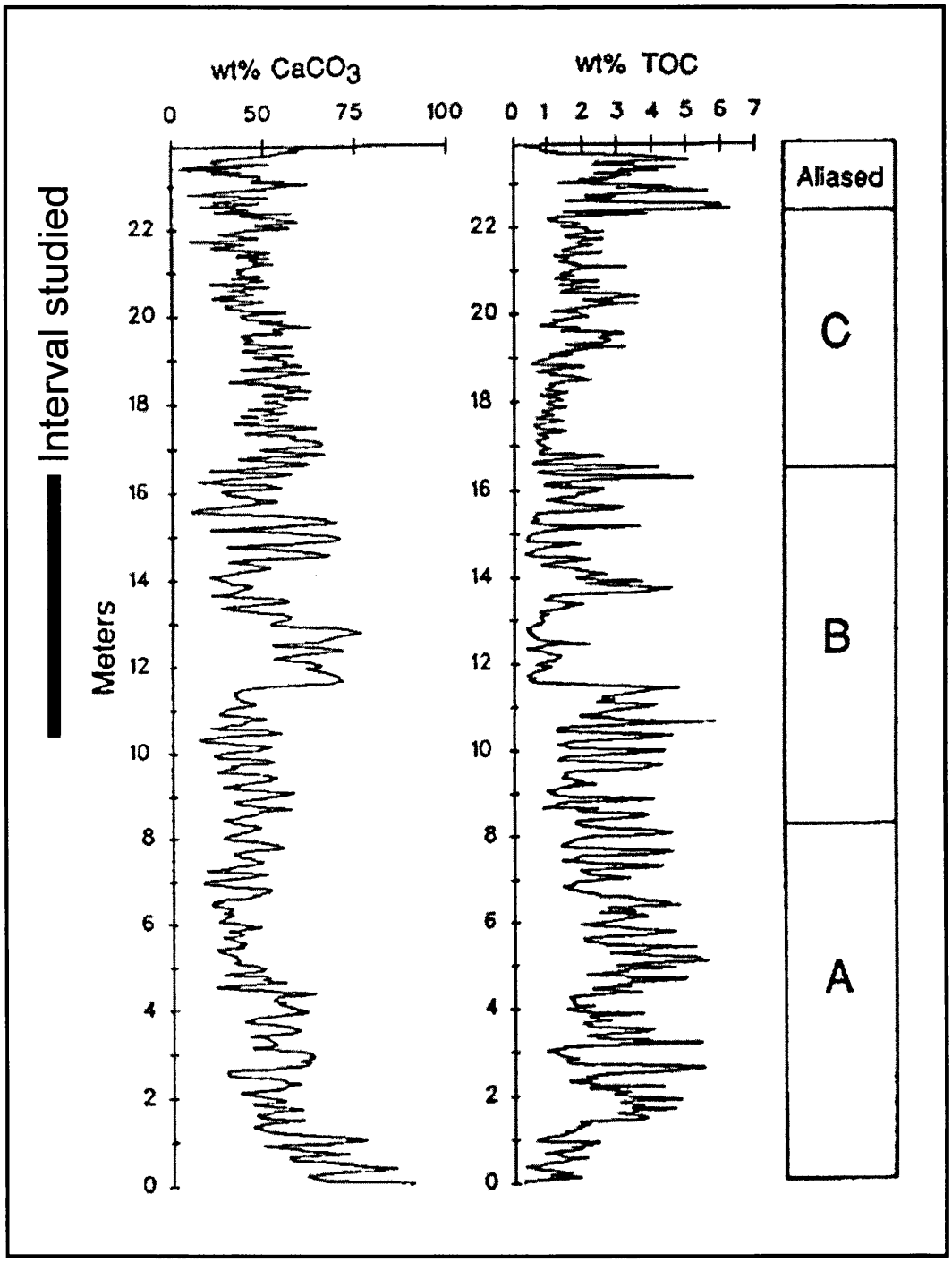

Fig. 4.5 Complete time series of wt%$CaCO_3$ and TOC from the Belemnite Marls. The lettered segments are those used for spectral analysis by Weedon & Jenkyns (1999); the topmost interval was not used due to the likelihood that the data have been aliased using the 3cm sampling interval. The main interval studied is shown. Modified from Weedon & Jenkyns (1999)

4.1.1 Cyclostratigraphy – previous work

The Belemnite Marls thus represents, for its age, an unusually accurate record of fluctuating sedimentation. The following represents a summary of Weedon & Jenkyns' (1999) cyclostratigraphy of the formation.

Time series

Weedon & Jenkyns generated geochemical determinations (weight-percent calcium carbonate and total organic carbon) for the whole of the Belemnite Marls, using a sampling interval of 3cm (Fig. 4.5). These time series possess a relatively simple structure, characterised by sinusoidal variations. Wt%TOC shows a general non-linear inverse correlation with wt%$CaCO_3$, even when expressed on a carbonate-free basis. Decimetre-scale variations in both parameters correspond to couplets of light marl (carbonate-rich and organic-poor) with dark marl or laminated shale (carbonate-poor and organic-rich). Modulating couplet compositions are metre-scale variations in average $CaCO_3$ and TOC, producing bundles of beds.

Time-series analysis

Weedon & Jenkyns investigated these observations further using spectral and cross-spectral analysis. A substantial decrease in sedimentation rate was found to occur two thirds of the way through the formation (at 16.41m); the time series were therefore split into three reasonably stationary segments of subequal length (A-C) for spectral analysis. The data from the topmost interval were thought to be aliased, and were omitted from the analysis.

The power spectra for the $CaCO_3$ data from the lower two segments (A and B; Fig. 4.6) contain significant spectral peaks corresponding to a wavelength of 0.37m. The regular cycle represented is consistent with the decimetre-scale of the bedding couplets. The same scale of variation is present in Segment B of the TOC data. However, in Segment A of the TOC data, the spectral peak represents a wavelength of 0.29m. The TOC time series from Segments A and B is thus not strictly stationary, unlike the $CaCO_3$ record.

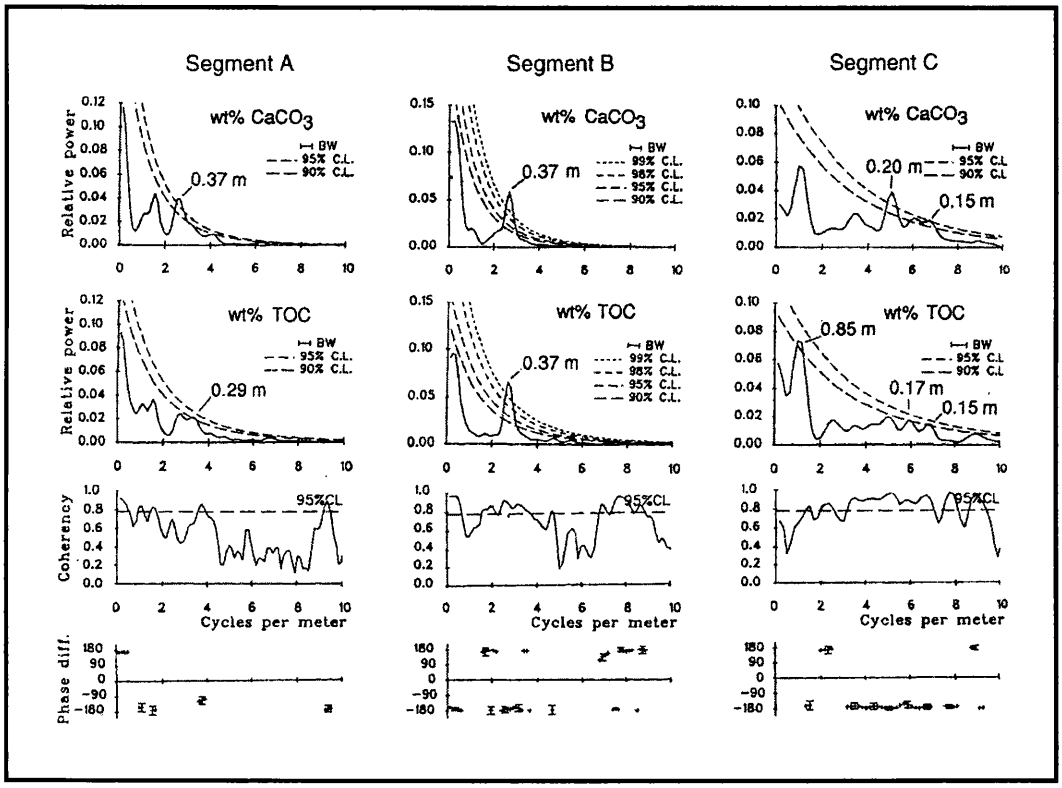

Fig. 4.6. Top: Power spectra of wt%$CaCO_3$ and TOC time series from Segments A to C of the Belemnite Marls (see Fig. 4.5; from Weedon & Jenkyns 1999). BW = bandwidth; CL = confidence level. **Middle:** Coherency spectra for the time series represented by the power spectra above. **Bottom:** Phase-difference spectra for the time series represented by the power spectra above. Phase difference values (+ symbols) are only plotted for frequencies where coherency is significant. The uncertainty of the phase estimates is indicated using vertical bars (±95% confidence intervals) at the frequencies of coherence maxima; for frequencies where the coherency is not significant, the uncertainty in phase difference becomes too large for the values to be useful

The relationship between $CaCO_3$ and TOC in Segments A and B was further investigated using cross-spectral analysis. For Segment B, the two parameters are significantly coherent at the frequency of the couplet cycles. The phase difference is consistent with an inverse relationship between the datasets. However, in Segment A there is no coherence between these parameters at the frequency of either the 0.37m $CaCO_3$ variations or the 0.29m TOC variations. Thus both the frequency of TOC variability, and the relationship of TOC to $CaCO_3$, changes from Segment A to B.

The spectrum for the $CaCO_3$ data from Segment C reveals two regular cycles with wavelengths of 0.20cm and 0.15cm. The smaller scale of these couplet cycles records the decreasing accumulation rate; the pair of spectral peaks is probably caused by the progressive nature of this decrease. The spectrum for TOC

in this segment shows essentially the same shape as the $CaCO_3$ spectrum (although the significant couplet cycles range from 0.17m to 0.15m).

In summary, the spectral results indicate that the bedding couplets express a regular cycle in carbonate deposition. Burial and/or preservation of organic carbon changed character during the interval represented by Segment A, and organic-carbon content shows an inverse non-linear relationship with carbonate content throughout the bulk of the formation. A substantial decrease in the wavelength of the couplets in the upper third of the formation is associated with the decrease in accumulation rate.

Although all spectra for Segments A and B exhibit a peak corresponding to a wavelength of about 3m, the scale of the bundle cycles, in no case is this statistically distinct from the environmental noise represented by the background spectrum. The TOC spectrum for Segment C contains a significant peak corresponding to a wavelength of 0.85m, representing a regular bundle cycle (the shortened wavelength being the effect of decreased accumulation rate). The $CaCO_3$ spectrum for this segment reveals the same peak, albeit statistically indistinguishable from the background spectrum. These results indicate that a longer period environmental cycle, which may have been regular in time, produced the bundle cycles in carbonate and organic-carbon contents.

Time-significance of cycles

Weedon & Jenkyns constrained the periods of these regular cycles in Belemnite Marls deposition using the cycle counting method (although the lack of reliable chronometrical tie points in the Lower Jurassic (Gradstein *et al.* 1994) implies that there are large uncertainties in their estimates). According to the latest chronometrical timescale (Gradstein *et al.* 1994) the duration of the Pliensbachian was 5.7my. The stage contains 15 ammonite subzones (ASZs; Cope *et al.* 1980), and the mean duration of an ASZ may be estimated at 0.4my. The Belemnite Marls, which contains 7 ASZs, thus apparently represents a time interval of 2.7My. Taking into account the stratigraphic gaps bounding the unit, the average period of each of the 89 couplets constituting the sequence represents less than 30ky (if the section contains undetected hiatuses, the cycles would have shorter durations). This result is consistent with the 20ky period of Early Jurassic

variations in orbital-precession[1] (and inconsistent with the 39.6ky period of Early Jurassic obliquity).

Although the bundle cycle is not demonstrably regular in the thickness domain, replotting the data on a cyclostratigraphic timescale based on the 20ky couplet period yielded a spectral peak at 140ky. Taking into account the error of period determination, this probably corresponds with the 100ky orbital-eccentricity cycle (the ratio between the two cycles (7:1) is closer to being consistent with short eccentricity:precession (5:1) than with short eccentricity:obliquity (2.5:1).

The amplitude of the precession cycle in climate is modulated by the eccentricity cycle. If the bundles record eccentricity and the couplets precession, a similar relationship between these cycles should exist. However, although the amplitude of the couplets varies at the same frequency as the bundle cycles, there is no consistent relationship (coherence) between the amplitude of the couplet and bundle cycles. This mismatch can be explained in terms of non-linear behaviour of a climatic system which had a varying response time.

The cyclostratigraphic analysis of Weedon & Jenkyns (1999) has thus suggested that the bedding cycles in the Belemnite Marls record orbital-climatic forcing at the Milankovitch scale. The couplets are inferred to record variations in orbital-precession, and the bundles orbital-eccentricity (short cycle). The data were not found to contain any evidence for obliquity cycles.

4.1.2 Previous studies of Belemnite Marls nannofossils

Rood *et al.* (1973) were the first to describe nannofossils from the Belemnite Marls (although Sellwood (1972) had previously noted the presence of coccoliths in the sediments); their taxonomic and biostratigraphic study was concerned with the Lower and Middle Jurassic as a whole. There have subsequently been a limited number of nannofossil studies of the Belemnite Marls, and these have also been primarily of a taxonomic and biostratigraphic nature; Barnard & Hay (1974)

[1] The Early Jurassic precession cycle had component periods of 18.1 and 21.6ky, or a mean period of 19.8ky. This figure was rounded to 20ky for the purposes of this study.

and Hamilton (1982) sampled the formation in their wider studies of the Jurassic, whilst Bown *in* Lord & Bown (1987) and Crux (1987a) present more detailed data for the formation itself. There has been no palaeoenvironmental approach to Belemnite Marls nannofacies to date.

4.2 MATERIALS AND METHODS

4.2.1 Sampling

Samples studied by Weedon & Jenkyns (1999) were employed here[1], permitting stratigraphic comparison of data collected for both studies. Such procedural consistency in the production of time series for multiple parameters is highly desirable if a coherent cyclostratigraphy is to be established. These samples represent the coastal cliff-forming exposure of the Belemnite Marls below Stonebarrow Hill, east of Charmouth (between Ordnance Survey grid reference points SY 380 927 and SY 392 924; Figs. 4.2 & 4.3).

The samples were collected by Weedon & Jenkyns at constant 3cm intervals, in order to adequately represent the decimetre-scale couplet cycles; this scale of analysis was also applied in the present study. The recording of compositional anomalies was minimised by the application of channel sampling (sediment was collected from complete 3cm stratigraphic intervals, avoiding visible fossils, and homogenised by crushing. Qualitative comparison of these samples with fresh samples collected as part of this study but without crushing, for control purposes, revealed no difference in nannofloral preservation).

A *ca.* 6m section of the middle part of the Belemnite Marls (Beds 110a-114 of Lang *et al.* (1928); Fig. 4.3, 4.4 & 4.5) was selected for time-series analysis. This interval was chosen on the grounds of reasonably constant sedimentation rate (Weedon & Jenkyns 1999), thus simplifying time-series analysis, and a clear inverse relationship between carbonate and organic-carbon content (Weedon & Jenkyns 1999), permitting palaeoenvironmental controls on nannofossil

[1] See Appendix 1 for details of the curation of all samples discussed in this thesis.

distribution to be considered. The interval represents *ca.* 15 couplet cycles, which is adequate for the detection of regular cyclicity.

A very short (0.45m) section representing a single couplet in the basal Belemnite Marls (Bed 108), and a short (1.17m) interval of the upper Belemnite Marls (Beds 118-119) were also subjected to high-resolution study. These provide 'snapshots' of nannofloral distribution through the oldest and youngest parts of the formation. Ian Bailey assisted with data collection from Bed 108 as part of a University College London (UCL) MSci project (Bailey 2000).

Clearly it would be preferable to obtain nannofossil time series representing the entire formation. The strategy employed here represents a useful compromise between the sampling requirements for time-series analysis (a small sampling interval in relation to cycle wavelength, with numerous cycles represented) and the time-consuming nature of nannofossil data collection.

4.2.2 Data collection

Samples were analysed in random stratigraphic order in order to minimise the possibility of subjective researcher bias. Nannofloral data collection involved standard techniques. Smear slides were studied under the light microscope (Norland Optical Adhesive[1] was employed for affixation of coverslips, on account of its ease of use and permanence), and at least 300 random specimens recorded per sample. %abundance data were generated, and an index of absolute abundance calculated by relating count data to the number of fields of view (FOV) examined. When tested for reproducibility, these methods were found to yield results of reasonable precision (Appendix 2).

Numerous measures of taxonomic diversity have been proposed. Hill's diversity numbers (Hill 1973) and the modified Hill's ratio (Alatalo 1981) are considered to be amongst the most reliable (Ludwig & Reynolds 1988). Hill's diversity numbers are:

[1] Norland Products Inc., New Brunswick, NJ 08902, USA

Number 0 (N0) = S

where S is the total number of species;

Number 1 (N1) = $e^{H'}$

where

$$H' \text{ (Shannon's index)} = -\sum_{i=1}^{s^*} (p_i \ln p_i)$$

where the assemblage is made up of S^* species with known proportional abundances $p1, p2, p3, \ldots, p_{s^*}$; and

Number 2 (N2) = $1/\lambda$

where

$$\lambda \text{ (Simpson's index)} = \sum_{i=1}^{s} p_i^2$$

where p_i is the proportional abundance of the i^{th} species, given by

$$p_i = \frac{n_i}{N}, \qquad i = 1, 2, 3, \ldots, S$$

where n_i is the number of individuals of the i^{th} species, and N is the known total number of individuals for all S species in the population.

The modified Hill's ratio is:

$$\text{Evenness index 5 (E5)} = \frac{(1/\lambda) - 1}{e^{H'} - 1} = \frac{\text{N2} - 1}{\text{N1} - 1}$$

where λ is Simpson's index (see above) and H' is Shannon's index (see above).

N0 represents taxonomic richness; N1 the number of taxa (expressed in taxonomic units) that are abundant in an assemblage; and N2 the number of taxa (in taxonomic units) that are very abundant. E5 is a measure of evenness; the lower the value of this index, the lower the evenness and *vice versa*. In this study all four of these indices were used to quantify diversity.

A visual estimation of preservational state was made through application of the scheme of Roth (1983). In general, broken nannofossils were only counted where more than half the specimen was present, in which case they were recorded as complete. This avoids duplicating counts, and minimises bias towards taxa for which recognition from fragmented material is straightforward.

Consistent and objective nannofossil data collection often calls for conventions to be observed which are specific to a particular stratigraphic interval, facies or research objective. Several such conventions were required in this study, and are listed under the relevant taxonomic headings in Appendix 3. Taxonomic assignments were confirmed using the SEM.

Random settling techniques were attempted during the initial stages of this study, but in all cases produced an uneven distribution of sediment across the slide. This may have been due to a number of different factors, and repeated experimentation may have yielded improved results. Further investigation was forestalled by the time-consuming nature of the techniques and the satisfactory results yielded by the simple smear technique.

4.2.3 Time-series analysis

Spectral analysis was used to test for regular cyclicity in the nannofossil data, and cross-spectra to examine relationships between datasets. The spectral and cross-spectral methods employed are those of Weedon & Jenkyns (1999), with the exception that confidence levels were located using the procedure of Mann & Lees (1996).

4.3 RESULTS

4.3.1 General

All horizons sampled yielded abundant, well-preserved nannofloras typical of open-marine settings in the Pliensbachian of the Boreal Realm (Bown & Cooper 1998). All taxa encountered are listed in Appendix 3; species common in Belemnite Marls assemblages are illustrated in Fig. 4.7. All data are listed in Appendix 4; a selection of the nannofossil time series generated for the middle section of the Belemnite Marls is illustrated in Fig. 4.8, together with the previously published geochemical data (Weedon & Jenkyns 1999). The nannofossil biostratigraphy of the formation is discussed in Appendix 5.

In the middle part of the formation *Crepidolithus crassus* is the numerically dominant coccolith species in many samples, representing 47.77% of all specimens recorded. The relative abundances of this species and others display striking variations at the scales of both the bedding couplets and bundles; nannofloral composition thus appears to fluctuate along with the distribution of carbonate, clay and organic carbon throughout the sequence. The validity of this observation was assessed through the application of time-series analysis.

4.3.2 Time-series analysis

Relative abundance

Power spectra. The power spectrum for the %*C. crassus* data contains a significant spectral peak corresponding to the 0.38m wavelength of the bedding couplets (Weedon & Jenkyns 1999; Fig. 4.9). The bandwidth indicates that the uncertainty in wavelength is less than a factor of two; therefore the decimetre-scale cycle in %*C. crassus* can be described as regular.

The same scale of regular cyclicity is found in the %*Mitrolithus elegans*, %*Parhabdolithus liasicus* and diversity (e.g. E5, which takes into account N0, N1 and N2) data. Again, in all cases the spectral peak is significant at a frequency corresponding to the couplet cycles.

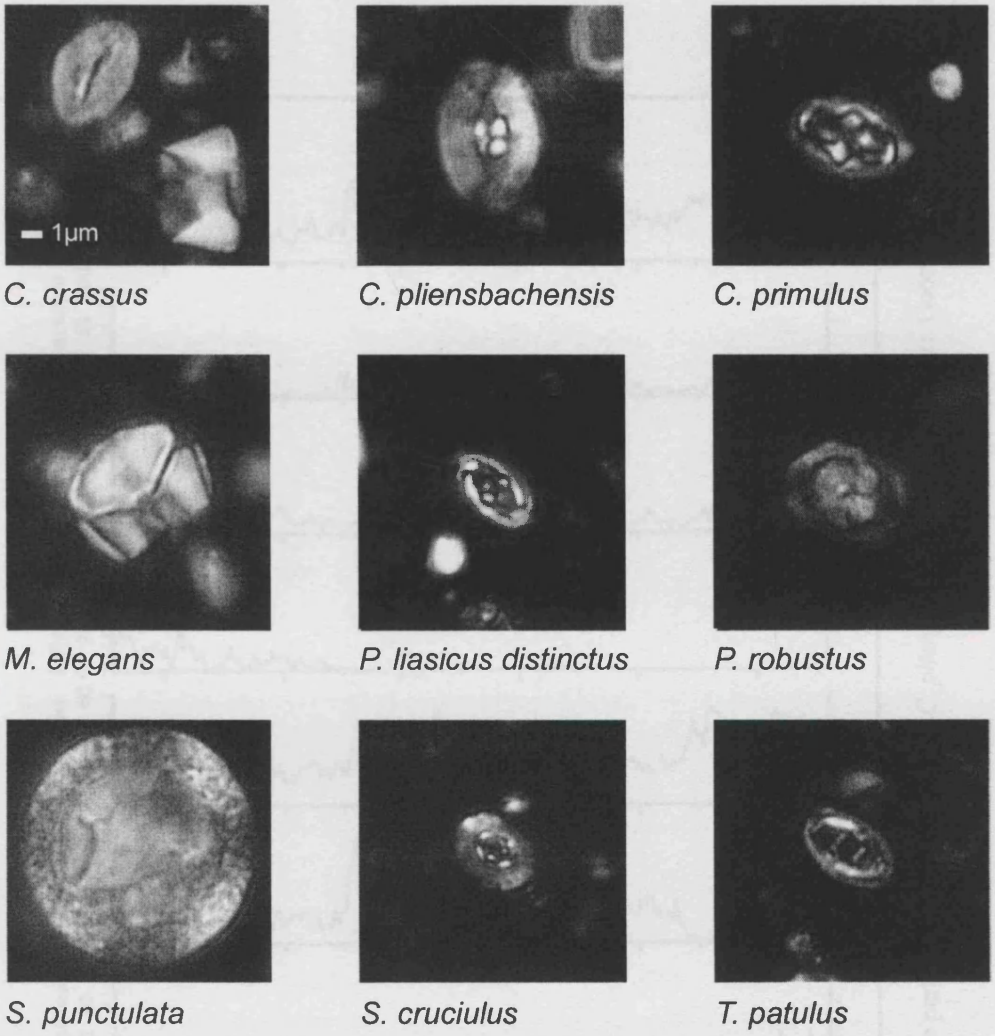

Fig. 4.7 Cross-polarised light micrographs of common Belemnite Marls nannofossils

Cross spectra. The %*Crepidolithus crassus* and wt%$CaCO_3$ time series are significantly coherent at the 2.67 cycles/m frequency of the couplet cycles. Phase is indistinguishable from 0°; this is consistent with a covariation of %*C. crassus* and wt%$CaCO_3$.

%*Mitrolithus elegans*, %*Parhabdolithus liasicus* and diversity (e.g. E5) are also coherent with wt%$CaCO_3$ at the couplet frequency, but in all cases phase is close to 180°. These parameters thus vary in phase with organic carbon.

Other parameters

Significant peaks were not present in power spectra generated from any other time series relating to the above species (i.e. %abundance calculated on a *Crepidolithus*

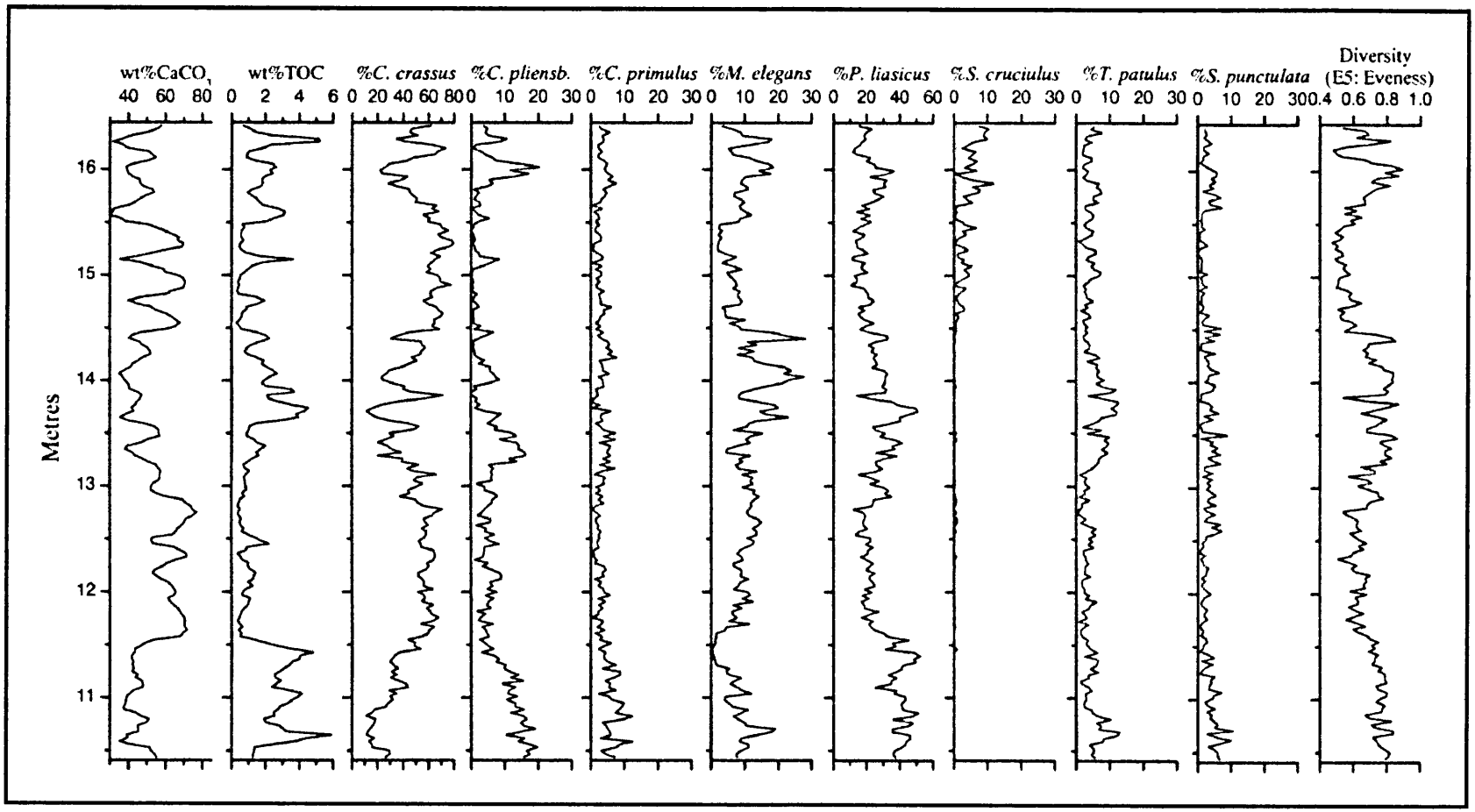

Fig. 4.8 Selected geochemical and nannofossil time series from the middle part of the Belemnite Marls. *C. pliensbach.* = *C. pliensbachensis*. Geochemical data from Weedon & Jenkyns (1999)

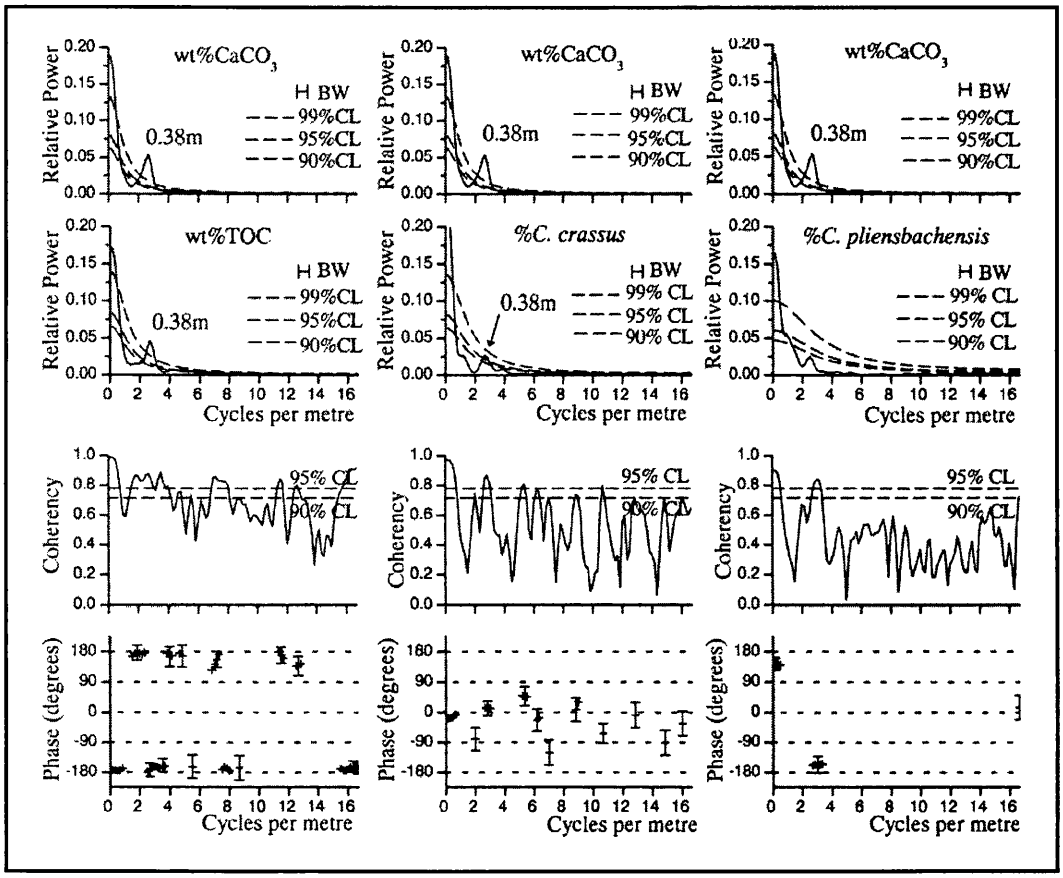

Fig. 4.9a. Top: Power spectra of selected Belemnite Marls geochemical and nannofossil time series. BW = bandwidth; CL = confidence level. **Middle:** Coherency spectra for the time series represented by the power spectra above. **Bottom:** Phase-difference spectra for the time series represented by the power spectra above. Phase difference values (+ symbols) are only plotted for frequencies where coherency is significant. The uncertainty of the phase estimates is indicated using vertical bars (±95% confidence intervals) at the frequencies of coherence maxima; for frequencies where the coherency is not significant, the uncertainty in phase difference becomes too large for the values to be useful. Geochemical data from Weedon & Jenkyns (1999)

crassus-free basis; absolute abundance; preservation). Regular cycles were not found in datasets relating to other species (although %*C. pliensbachensis* exhibits significant coherence with wt%$CaCO_3$, with phase close to 180°) or overall assemblage preservation. 'Tuning' these datasets to the cyclostratigraphic time-scale of Weedon & Jenkyns (1999), followed by interpolation in time and spectral analysis, did not yield further significant spectral peaks.

Visual examination of the datasets reveals the presence of a metre-scale bundling of the couplet cycles. These lower-frequency cycles appear to correlate well with the eccentricity bundles identified in the geochemical data (Weedon &

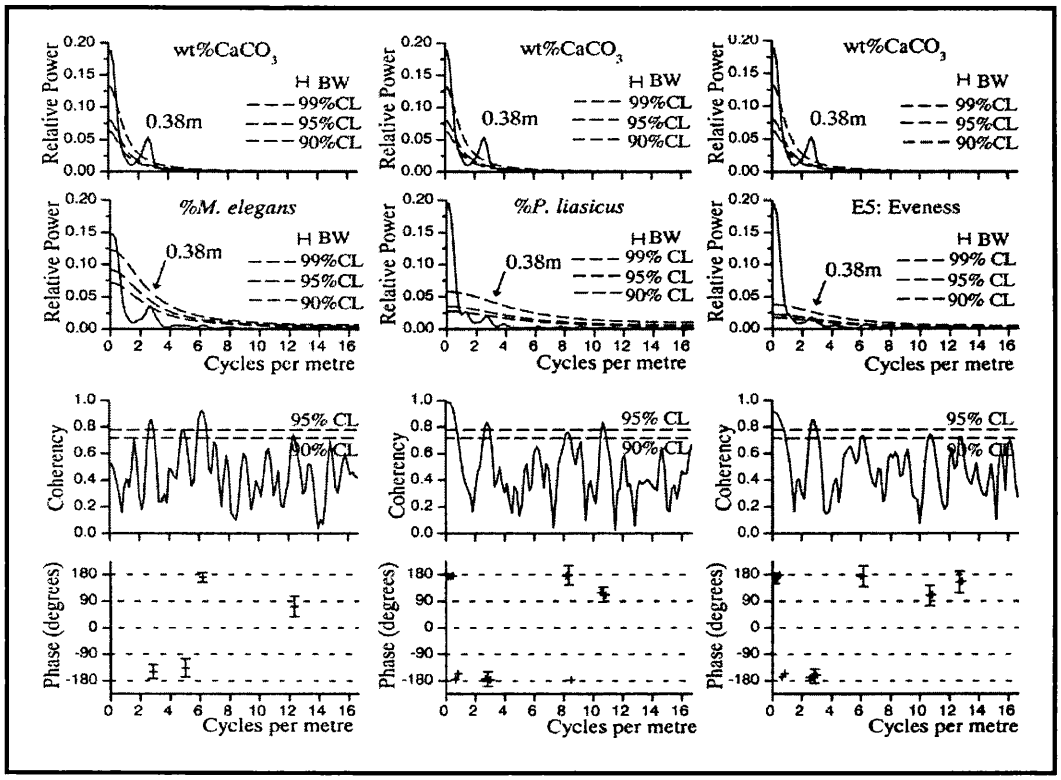

Fig. 4.9b. Top: Power spectra of selected Belemnite Marls geochemical and nannofossil time series. BW = bandwidth; CL = confidence level. **Middle:** Coherency spectra for the time series represented by the power spectra above. **Bottom:** Phase-difference spectra for the time series represented by the power spectra above. Phase difference values (+ symbols) are only plotted for frequencies where coherency is significant. The uncertainty of the phase estimates is indicated using vertical bars (±95% confidence intervals) at the frequencies of coherence maxima; for frequencies where the coherency is not significant, the uncertainty in phase difference becomes too large for the values to be useful. Geochemical data from Weedon & Jenkyns (1999)

Jenkyns 1999). However, the time series are too short in relation to the wavelength of the bundle cycles to confirm periodicity.

4.4 DISCUSSION

4.4.1 Carbonate sedimentology

Establishing the genesis of micritic carbonate in Jurassic marine basinal deposits is an enduring problem in sedimentology (Hinnov & Park 1999; Mattioli 2000). The two main putative sources are platform-derived carbonate mud from nearby shelf environments, or pelagic (nannofossil) ooze. It has been suggested that the

primary micrite in the Belemnite Marls was for the most part supplied by diagenetically altered coccoliths (Sellwood 1970; Weedon & Jenkyns 1999). This hypothesis is considered misleading in the light of the present study, on the basis of the following observations: (1) Reference to the term 'coccolith' is erroneous in this context, as the non-coccolithophorid *Schizosphaerella punctulata* was undoubtedly a major contributor to the supply of pelagic carbonate[1]. (2) There is no significant relationship between absolute nannofossil abundance and carbonate content (Fig. 4.10). (3) Nannofossil preservation is good and does not vary between the dark- and light-marl horizons (Fig. 4.11). Hence the high carbonate content of the light marls cannot represent original abundance maxima of nannofossils, now destroyed by diagenesis. (4) Qualitative evaluation of the microcarbonate fraction in the smear slides reveals that much of the micrite is in the form of anhedral particles (Fig. 4.11). These are much more abundant in the light marls than in the dark. The large size of these carbonate particles (relative to whole and disintegrated nannofossils), together with the rare occurrence of microspar, indicates that this carbonate is not of nannoplanktonic or diagenetic origin.

A more probable scenario is that a relatively constant supply of nannoplanktonic carbonate was periodically diluted by major contributions of platform-derived carbonate mud into the basin. This interpretation is supported by Sellwood's (1972) observation that a significant component of the carbonate in the light marls is accounted for by fragments of crinoids, echinoids, foraminifera and ostracods. It is also consistent with recent work on the origin of the microcarbonate fraction in other Mesozoic (including Lower Jurassic) rhythmites (Hinnov & Park 1999; Mattioli *et al.* 2000).

[1] The numerical dominance of *Crepidolithus crassus* in the coccolith assemblages from the middle part of the Belemnite Marls, where it represents *ca.* 50% of all specimens, does however confirm Sellwood's (1972) observation that *Crepidolithus* represents a significant component of the carbonate.

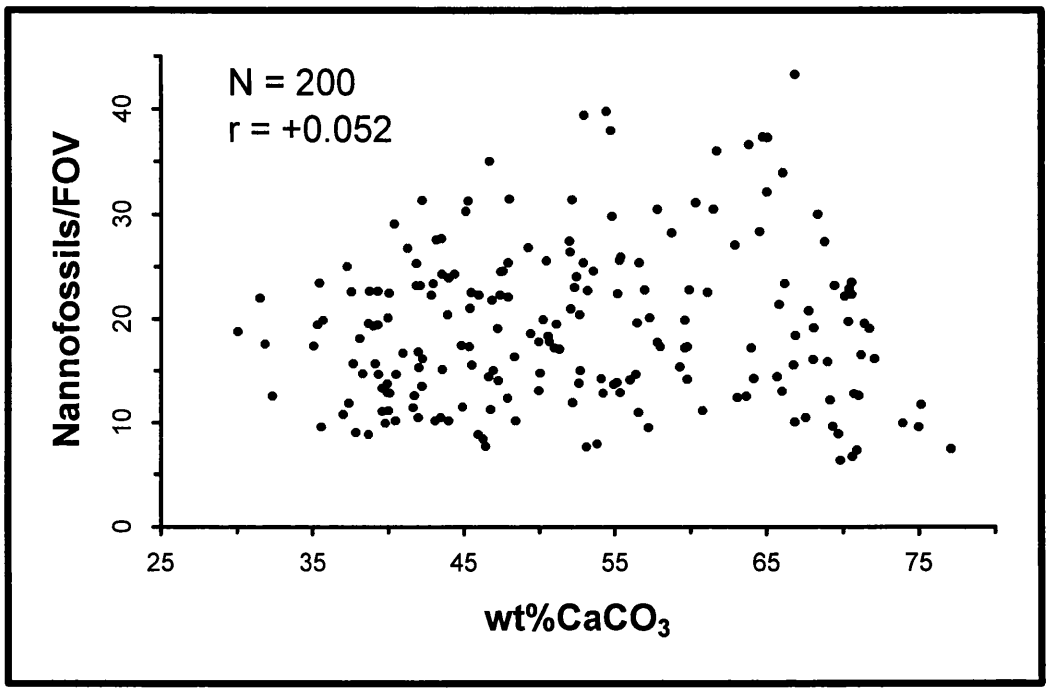

Fig. 4.10 Graph showing no significant relationship between nannofossil abundance (FOV = field of view) and carbonate content in the middle part of the Belemnite Marls. $CaCO_3$ data from Weedon & Jenkyns (1999)

4.4.2 Palaeoenvironmental implications

Nannofloral cycles - original or taphonomic?

Vital to the interpretation of geological time series is the extent to which the data reflect primary, environmental (as opposed to secondary, preservational) signals (Einsele & Ricken 1991). The primary nature of lithological cyclicity in the Belemnite Marls has already been demonstrated (Weedon & Jenkyns 1999; Munnecke *et al.* in press). The present study finds that nannofossil preservation is good throughout the formation (all assemblages are characterised by specimens that are slightly overgrown by calcite, rather than etched), in both the dark and light marls. The abundance of *Schizosphaerella*, thought to be a dissolution-resistant taxon (Mattioli 1997), does not exhibit passive enhancement by diagenesis in the light marls. Thus taphonomy cannot be invoked to explain the scale of nannofloral variability discussed below. In any case, small-scale taphonomic variations would probably have had little effect on coccolith

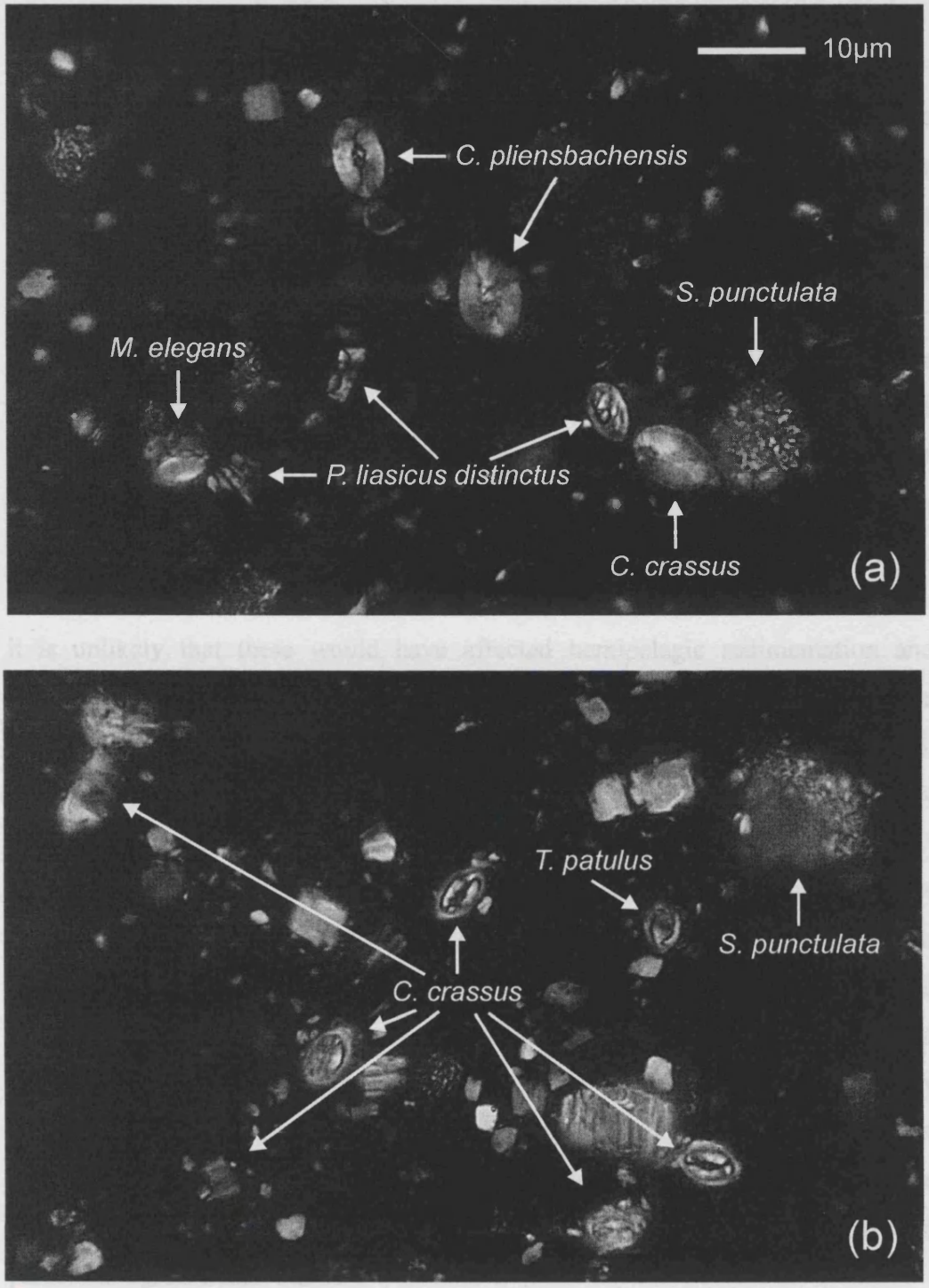

Fig. 4.11 Cross-polarised light micrographs of characteristic Belemnite Marls nannofossil assemblages from **(a)** a dark- and **(b)** a light-marl bed

assemblage composition, as it is contended here that most early Pliensbachian taxa were robust and of similar preservation potential.

Previous work on the Belemnite Marls

The site of Belemnite Marls deposition was ideally situated to record the precessional climate variability characteristic of central Pangaea during the early Pliensbachian (Kutzbach 1994). Deposition of all the major components of the sediments (carbonate, clay and organic matter) was potentially influenced by climate.

Numerous and diverse mechanisms link climate and sedimentation (Fischer *et al.* 1990). In the case of the Belemnite Marls, the effect of eustatic sea level change is discounted (Weedon & Jenkyns 1999). Global ice volumes were apparently low at this time, with little or no polar ice (Frakes *et al.* 1992); although it is possible that small sea-level changes at the Milankovitch scale arose from varying freshwater storage in continental basins (Jacobs & Sahagian 1995), it is unlikely that these would have affected hemipelagic sedimentation and nannoplankton population dynamics significantly. Local tectonic/subsidence control of water depth have also been discounted (Weedon & Jenkyns 1999), based on the regularity and estimated period of the couplet cycles and the symmetrical, sinusoidal shape of both couplet and bundle cycles.

Rather it has been suggested that the formation records fluctuations in one or a combination of the following factors: the productivity of calcareous *v.* organic-walled plankton, in connection with the nutrient supply from terrestrial run-off/marine circulation; fluvial argillaceous input, linked to precipitation; and bottom-water oxygenation levels, driven by variable surface-water productivity and/or density (salinity and/or thermal) stratification of the water-column (Walker 1991; Hesselbo & Jenkyns 1995; Weedon & Jenkyns 1999). These models have been based on a variety of inconclusive sedimentological, geochemical and palaeontological observations.

The present study represents the first quantitative micropalaeontological analysis of the Belemnite Marls, and allows new palaeoenvironmental conclusions to be drawn.

Palaeoenvironmental model

Bedding rhythms in the Belemnite Marls are accompanied by cycles in

nannofossil species diversity. This may be interpreted in the light of the generally inverse relationship between modern nannoplankton diversity and surface-water nutrient concentrations (Section 2.1.1). The dark marls yield assemblages of high diversity; given the adaptation of most extant nannoplankton species to oligotrophic settings, clay- and organic-rich accumulation thus appear to have been accompanied by low-fertility conditions in surface waters. The light marls are characterised by relatively low-diversity assemblages that are numerically dominated by *Crepidolithus crassus* (*C. crassus* is known to be dissolution-resistant (Bown 1987), but a taphonomic origin for the variations in abundance of this species is discounted here; see above). Such low diversity in modern assemblages is typical of zones of elevated productivity, suggesting that intervals of carbonate-rich sedimentation in the Early Jurassic Wessex Basin coincided with relatively high fertility in the photic zone.

It is suggested that these variations in productivity were not driven by nutrients supplied by terrestrial run-off, as beds recording high-nutrient conditions (low species-diversity) are richer in carbonate than clay (Ricken 1991). This carbonate enrichment is unlikely to have resulted from dilution of clay input by pelagic carbonate, as the light beds are not significantly thicker than the dark, and the bulk of the carbonate does not appear to be of planktonic origin.

Rather the diversity cycles may record variations in surface-water nutrification, as a result of fluctuating intensity of vertical mixing in the water column (Fig. 4.12). According to this scenario carbonate-rich mud may have accumulated during intervals of vigorous circulation, when enhanced recycling of nutrient-rich bottom waters into the photic zone led to an elevation of surface-water fertility, and nannoplankton species diversity declined. Such increased water-column turbulence may explain the increased supply of platform-derived carbonate mud into the basin. The dominant species in these horizons, *C. crassus*, is likely to have increased in absolute as well as %abundance during these intervals; however, the enhanced contribution of this species to sedimentation was diluted by this simultaneous influx of micrograde carbonate from the basin margins.

Clay- and organic-rich deposition may have accompanied water-column stratification and reduced bottom-water ventilation. This may have been linked to the supply of low-salinity water from run-off, as the clays are largely terrestrial in

origin. Surface-waters were typically oligotrophic, with any nutrient supply from run-off quickly exhausted. Certainly, reduced bottom-water oxygenation was not produced by enhanced surface-water productivity, as the organic-rich marls are associated with the high nannoplankton diversity typical of a low-fertility setting. Reduced bottom-water oxygenation during intervals of dark marl deposition is supported by the paucity of burrows piping dark marl into light (compared to those piping light into dark), a high organic-carbon content in the carbonate-free fraction and occasional laminated shale intervals (Weedon & Jenkyns 1999).

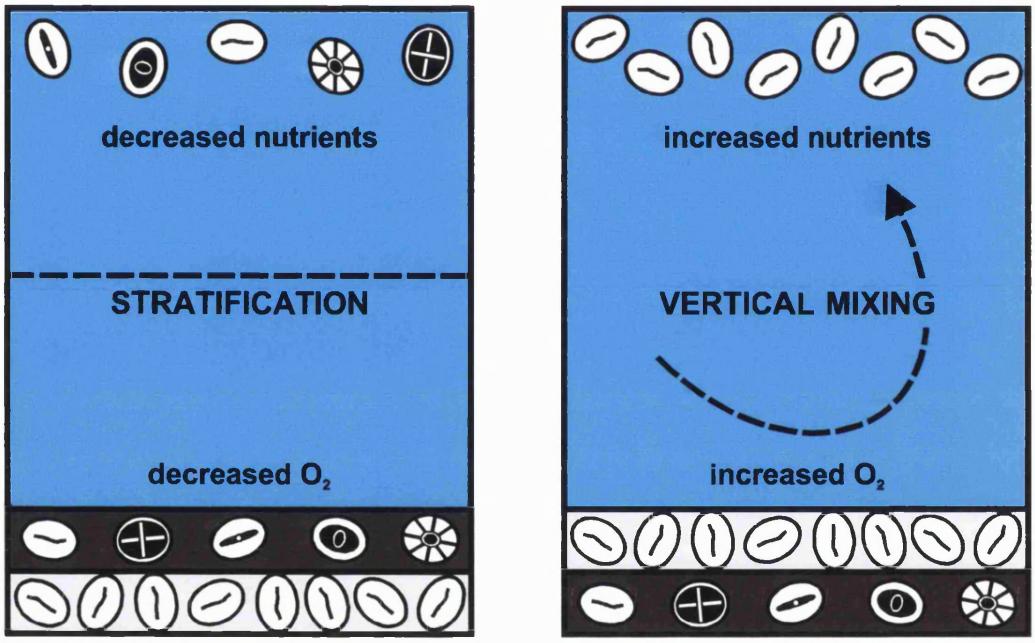

Fig. 4.12 Model linking nannoplankton species diversity with marine circulation

The model advanced above can also be applied to the bundling of the nannofloral data. The degree of eccentricity of the Earth's orbit is known to modulate the climatic effect of precession; this may have resulted in longer-term fluctuations in the intensity of marine circulation.

'Snapshot' intervals

Lower interval. Although the dataset from the basal Belemnite Marls (Fig. 4.13) is too short to allow conclusions to be drawn about regular cycles in nannofloral composition, it is nonetheless of interest that species diversity exhibits an inverse relationship with carbonate content, as observed in the middle part of the

formation. This is despite striking differences in assemblage composition, which are probably evolutionary in origin[1]. *Crepidolithus crassus*, which originated during deposition of the underlying Black Ven Marls Formation (Bown & Cooper 1998; Appendix 10), was not yet established as a major species; rather *Parhabdolithus liasicus* appears to be numerically dominant through this interval, especially in the light marls.

Upper interval. The patterns observed in the middle section of the Belemnite Marls were not evident in the data from the upper part of the formation (Fig. 4.14). This may be due to one or a number of factors: (1) The upper dataset, too short to allow time-series analysis, may not be long enough to allow overall trends to be visually discernible. (2) This interval represents a significant change in general nannofloral composition. *Crepidolithus crassus*, greatly diminished in abundance, has been replaced by *Similiscutum cruciulus* as the dominant coccolith species. Significant abundance shifts also characterise other species (e.g. *Parhabdolithus robustus*, rare in the middle samples, is common here).

These changes are probably evolutionary in origin. For instance, *Similiscutum cruciulus* originated during deposition of the lower part of the Belemnite Marls, and steadily increases in abundance up-section. By the interval represented by the upper part of the formation this species had clearly become a major component of the nannoplankton, presumably through direct competition with other taxa (e.g. *Crepidolithus crassus*). Such evolutionary change may have altered patterns of nannofloral response to environmental cycles. (3) The decreased sedimentation rate represented by this uppermost interval may record increased winnowing of fines (Weedon & Jenkyns 1999). This could have distorted the composition of sediment assemblages.

Other studies

The palaeoenvironmental model advanced here for Belemnite Marls nannofloral distribution is not universally applicable to rhythmic marine carbonates. This can

[1] It is also possible however that this long-term shift in nannofloral composition represents a low-frequency environmental cycle (e.g. sea-level change).

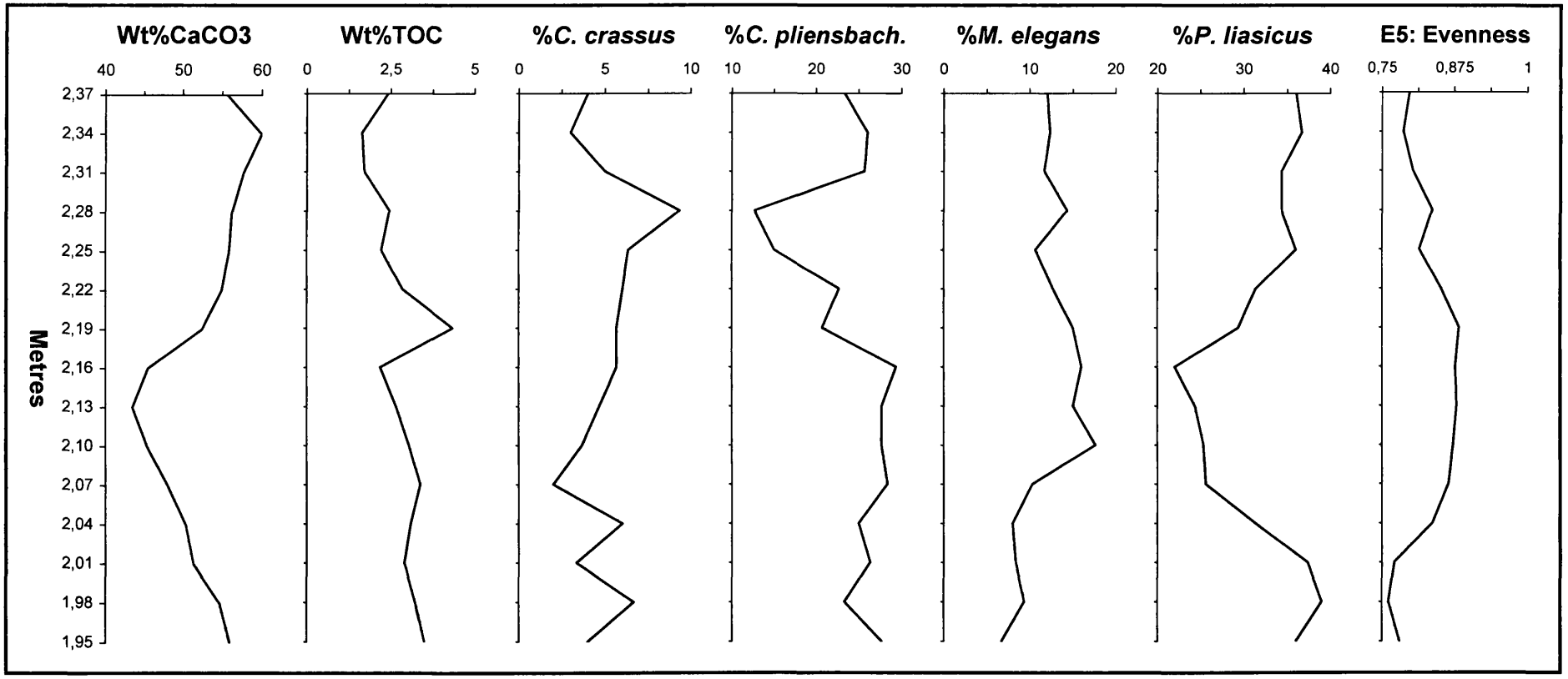

Fig. 4.13 Selected geochemical and nannofossil series from the lower interval of the Belemnite Marls. *C. pliensbach.* = *C. pliensbachensis*. Geochemical data from Weedon & Jenkyns (1999)

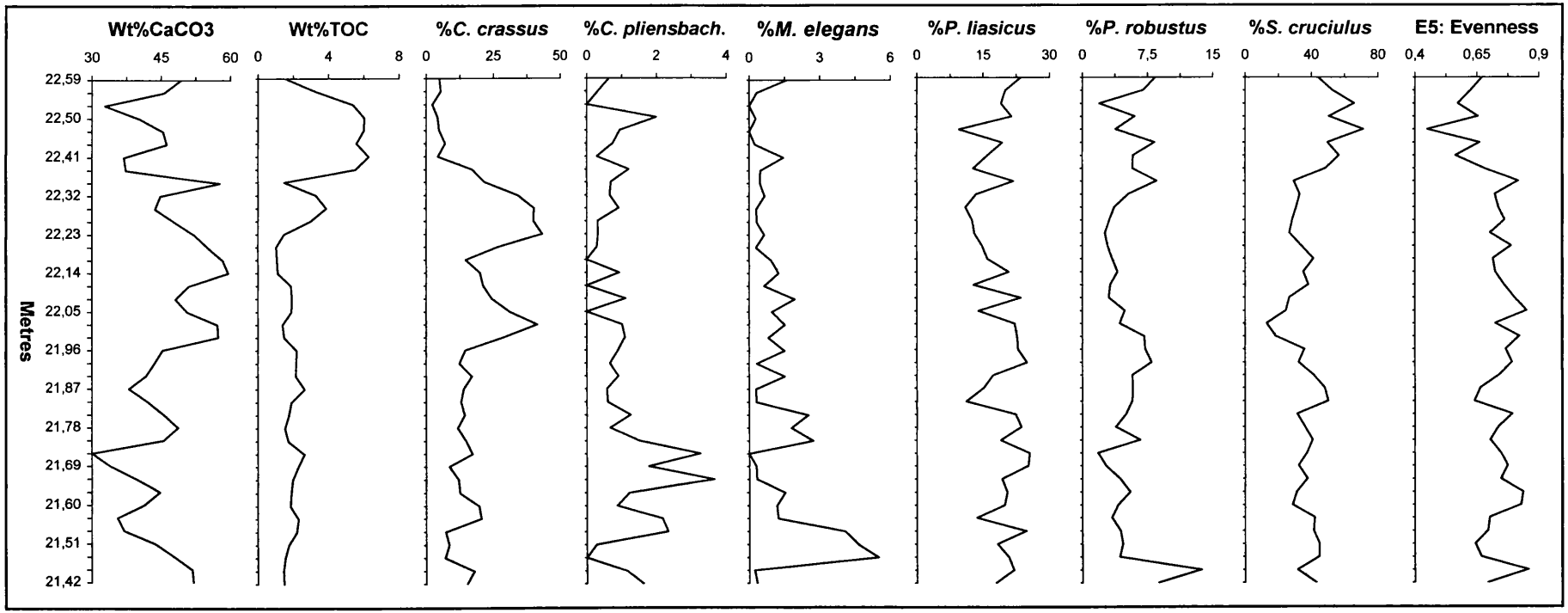

Fig. 4.14 Selected geochemical and nannofossil series from the upper interval of the Belemnite Marls. *C. pliensbach.* = *C. pliensbachensis*. Geochemical data from Weedon & Jenkyns (1999)

be illustrated by comparison with other Mesozoic studies (Fig. 4.15): (1) Nannofossils from various Lower Cretaceous sites in northern Germany and the eastern UK (Hauterivian and Barremian; Mutterlose & Ruffel 1999), from Cenomanian-Turonian sediments in south-western Morocco (da Gama 2000), from the Greenhorn Limestone (Cenomanian-Turonian, central USA; Watkins 1989), and from Turonian sequences in south-western Africa and north-eastern Brazil (Scarparo Cunha 2000) appear to record the opposite scenario, with oligotrophic conditions during carbonate-rich sedimentation and eutrophic conditions during shale deposition. (2) The Gault Clay nannoflora (Albian, southern UK; Erba *et al.* 1992) records trophic cyclicity that is not in phase with sedimentary fluctuations. (3) Nannofossil analysis of various Lower Cretaceous Atlantic and Pacific DSDP sections (Hauterivian, upper Barremian, lower Aptian, upper Albian; Thierstein & Roth 1991) suggests that surface water conditions remained stable, whilst lithological cyclicity records the action of diagenesis on originally homogenous sediments.

This spectrum of scenarios reflects the complex nature of the processes underlying cyclostratigraphic records. Any rhythmite is likely to represent a unique interaction between factors as diverse as palaeogeography, -climate, -oceanography, -biology and taphonomy. Nonetheless, interpretations which are broadly similar to that advanced here for the Belemnite Marls have been proposed for the Fiuminuta section (Toarcian-Aalenian, central Italy; Mattioli 1997), the upper Aptian of southern France (Herrle & Hemleben 2000) and various Cenomanian sections from southern France and the south-eastern UK (Windley 1995).

4.4.3 Nannoplankton palaeoecology

Crepidolithus crassus is the numerically dominant coccolith in the low-diversity nannofloras from the middle part of the Belemnite Marls, representing nearly 50% of all specimens recorded. This species is thus considered to have been an

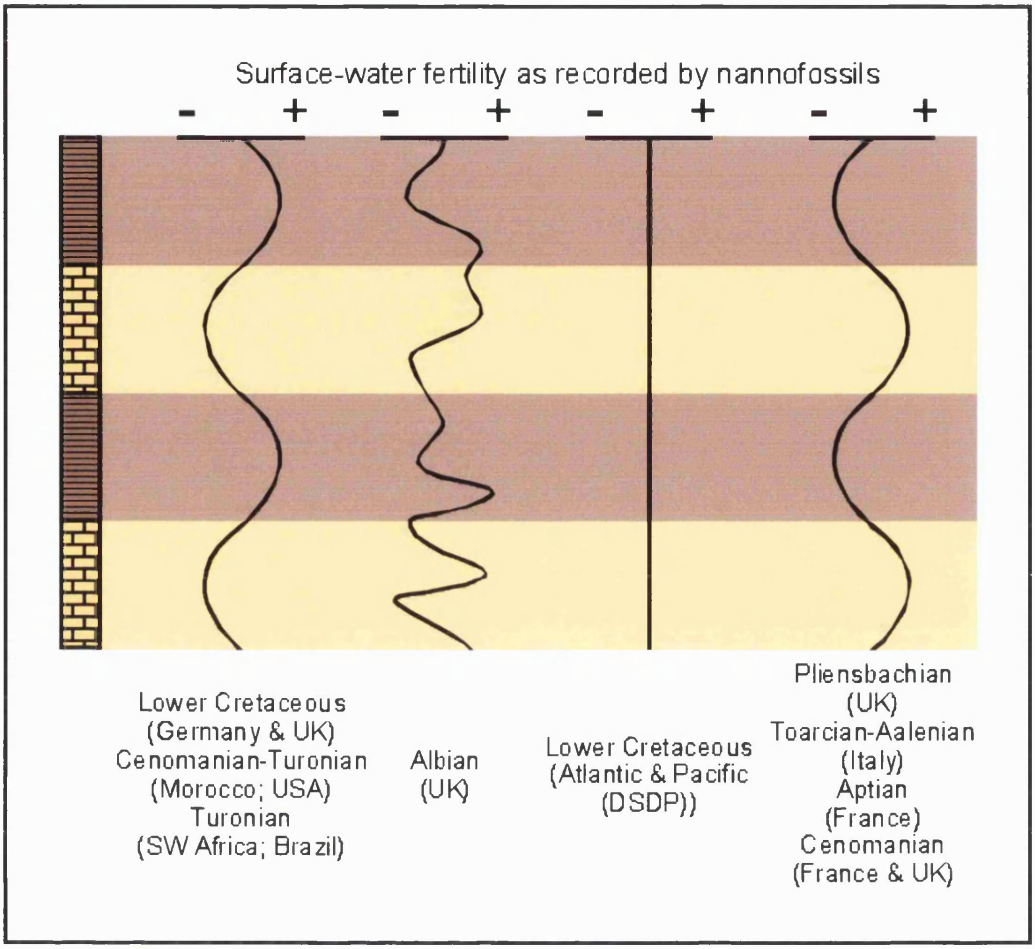

Fig. 4.15 Schematic representation of different relationships between lithology and nannofloral records of surface-water fertility as observed in various Mesozoic sequences (Mutterlose & Ruffel 1999; da Gama 2000; Watkins 1989; Scarparo Cunha 2000; Erba *et al.* 1992; Thierstein & Roth 1991; this study; Mattioli 1997; Herrle & Hemleben 2000; Windley 1995). Two decimetre-scale carbonate-rich/-poor alternations are shown

ecological opportunist during this interval in the Boreal Realm[1], flourishing during periods of high surface-water fertility. Opportunistic species are characterised by long evolutionary lifespans, and *C. crassus* has one of the longest ranges (Sinemurian-Tithonian) of all Early Jurassic species.

C. pliensbachensis, *Mitrolithus elegans* and *Parhabdolithus liasicus* display a positive relationship with carbonate-poor, organic-rich sedimentation in

[1] In any discussion of nannoplankton palaeoecology, it is necessary to take into account that the environmental preferences of individual taxa are liable to change through time as a result of genetic drift (Brand 1994).

the middle part of the formation. These may have been specialists, strongly exhibiting a preference (typical of extant nannoplankton) for low-fertility waters.

Data for other species in the middle part of the Belemnite Marls do not display such a clear relationship with the record of environmental change. It may be that these species display a somewhat broader range of environmental tolerances than those exhibiting regular cyclicity (although this could also represent relatively large counting errors for less abundant taxa).

It is significant that nannofloral composition was characterised by high levels of unevenness throughout the minimum of 1.78My that the Belemnite Marls apparently represents (Weedon & Jenkyns 1999). Unevenness has been a feature of nannoplankton communities throughout their evolutionary history (Street & Bown 2000), and may reflect the tendency of opportunistic species to numerically dominate assemblages. It may thus be tentatively suggested that *Parhabdolithus liasicus* (dominant during deposition of the basal part of the formation) and *Similiscutum cruciulus* (dominant in the upper beds) were somewhat oriented towards elevated nutrient conditions during these respective intervals. *Parhabdolithus liasicus* thus appears to have shifted in terms of environmental responses before deposition of the middle part of the formation. It is of interest that *S. cruciulus* was ancestral to the Biscutaceae, including the genus *Biscutum*, frequently cited as an indicator of high surface-water fertility in the Cretaceous (e.g. Gale *et al.* 2000, Street & Bown 2000). Unfortunately *S. cruciulus* is too rare through much of the Belemnite Marls for statistical consideration.

It is tentatively suggested here that *Mitrolithus elegans* was adapted to life in the lower euphotic zone, characterised during oligotrophic intervals by lower inter-species competition, relatively high nutrient availability (unlike the upper photic zone, where nutrients would have been rapidly depleted) and water-column transparency. Such an adaptation is unusual amongst coccolithophores, but is, for example, demonstrated by the extant species *Florisphaera profunda* (Brand 1994); the abundance of *F. profunda* exhibits an inverse relationship with the intensity of vertical mixing in the water column, resulting in stratigraphic fluctuations which correspond to Milankovitch (glacial-interglacial) cycles (Okada & Matsuoka 1996). Although little is known of coccolith functional

morphology (Young 1994), the heavy spine that characterises *Mitrolithus elegans* may have provided the ballast essential to such a strategy. It is possible to speculate regarding the morphological similarities between the crystal elements which characterise the *M. elegans* spine and those of *Florisphaera profunda* coccoliths. Otherwise unusual amongst coccolithophores, it has been suggested that such sub-rectangular calcite plates may function to refract light into the cell, a useful adaptation to low light levels at the nutricline (Young 1994).

It is of interest that Bed 120a, sampled for biostratigraphic purposes (Sample 266), contains a 'flood' of *M. elegans* (otherwise rare in this upper part of the Belemnite Marls) and a dearth of *Similiscutum cruciulus* (which is otherwise dominant). This bed is a laminated shale horizon (rare in this succession), and may represent an interval of unusually developed water-column stratification, supporting a large *Mitrolithus elegans* population. Certainly the unusually low ratio of *M. elegans* spine fragments to *M. elegans* coccoliths in this horizon suggests that the depositional environment was exceptionally quiet.

Schizosphaerella, a nannolith taxon (considered by some to be of dinoflagellate origin; Kälin & Bernouilli 1984), has been associated with enhanced productivity in the Early Jurassic Tethys (Mattioli 1997), where it sometimes occurred in rock-forming abundance. *S. punctulata* was not found to exhibit any meaningful relationship with lithology in the Belemnite Marls. This may be due to inadequacy of the data collected for this taxon, as considerable disaggregation of this species is evidenced by the ubiquitous abundance of small fragments. However, care was exercised in the collection of representative data. Rather it seems that *Schizosphaerella*, albeit a significant contributor to carbonate sedimentation, did not display Tethyan abundances or ecological affinities in the early Pliensbachian Boreal Realm.

4.5 FURTHER WORK

This study could be usefully developed by extension of the nannofossil time series to represent the entire Belemnite Marls, allowing more detailed time-series analysis. It would also be useful to apply an integrated micropalaeontological

investigation (i.e. including foraminifera, ostracods and palynomorphs) to further understanding of the genesis of the sedimentary cycles. A multidisciplinary approach including detailed sedimentology, stable carbon and oxygen isotope analysis and biogeochemistry would doubtless provide much information on the nature of the palaeoenvironments concerned. A comparative study of coeval nannofossiliferous rhythmites in Portugal (Brenha Road section; Hamilton 1977) would potentially shed further light on Pliensbachian environmental cycles and nannofloral palaeoecology.

5

The Oxford Clay

5.1 INTRODUCTION TO THE FORMATION

The Oxford Clay Formation is a marine argillaceous unit of middle Callovian to early Oxfordian (latest Middle-earliest Late Jurassic) age. These sediments accumulated beneath the transgressive shallow epicontinental sea covering most of Britain and northern Europe at that time (Fig. 5.1; Rawson *in* Bradshaw *et al.* 1992). Sedimentological and faunal evidence suggest that water depths were in the region of several tens of metres (Hudson & Martill 1994).

The location of the site at the edge of a major sedimentary basin resulted in only moderate burial (to a maximum of 500m in central England; Hudson & Martill 1991). The consequently mild thermal and diagenetic history of the deposits has allowed near-pristine preservation of original sediment composition. The formation crops out in central and southern England (Fig. 5.2), and is well exposed in both coastal cliff and ephemeral brick-pit sections.

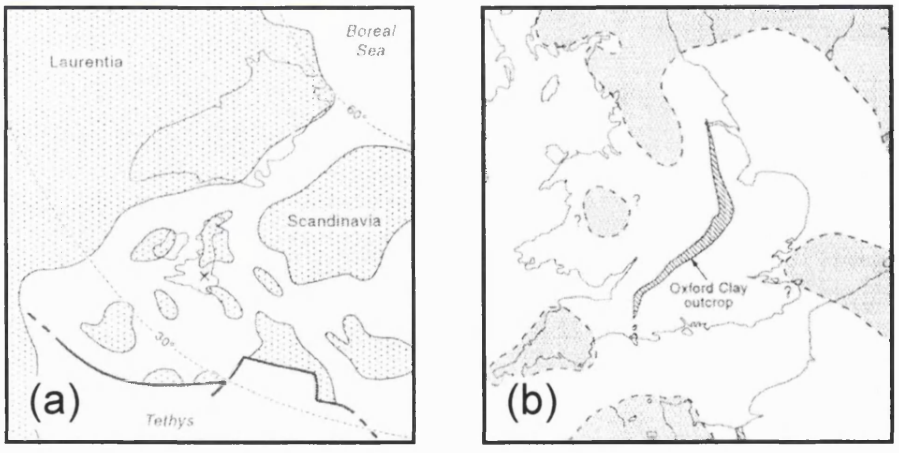

Fig. 5.1 (a) Generalised map of the NW European epeiric sea in Callovian times, showing latitudes. Present-day coastlines of the British Isles and Greenland shown for guidance. X = central England. The heavy line is the Alpine front. **(b)** Callovian geography of central and southern England, showing approximate distribution of landmasses. Modified from Hudson & Martill (1994)

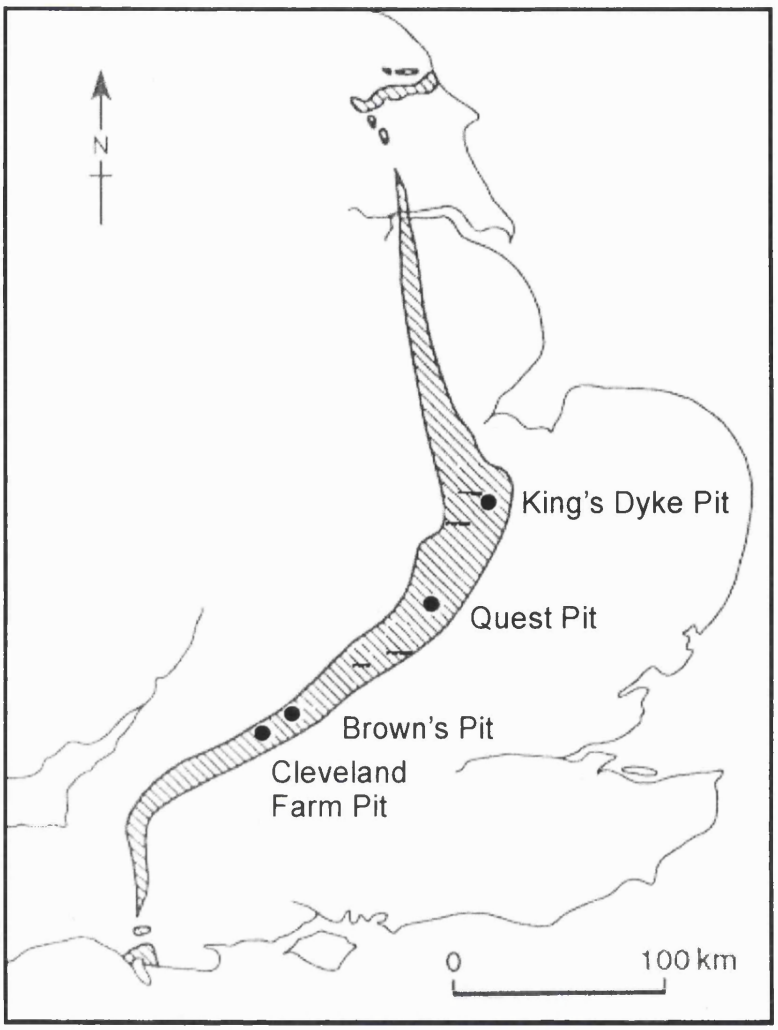

Fig. 5.2 Schematic map showing onshore outcrop of the Oxford Clay in England, and locations mentioned in the text. Modified from Kenig *et al.* (1994)

The Peterborough Member of the Oxford Clay has received particular attention in recent years (Hudson 1994; MacQuaker & Howell 1999). This middle Callovian unit is lowermost in the formation, and is *ca.* 17m in thickness as exposed at its type section in the King's Dyke Pit (Whittlesey, Cambridgeshire; TL 248 967; Figs. 5.3 & 5.4). It is largely comprised of compacted, organic-carbon rich and highly fossiliferous shale, interspersed with thin shell-rich beds (shell-beds). The bulk of the organic matter is of marine, phytoplanktonic origin (Belin & Kenig 1994; Martill *et al.* 1994). The carbonate has both primary (e.g. nannofossils, foraminifera, bivalves and ammonites) and diagenetic components (MacQuaker & Howell 1999).

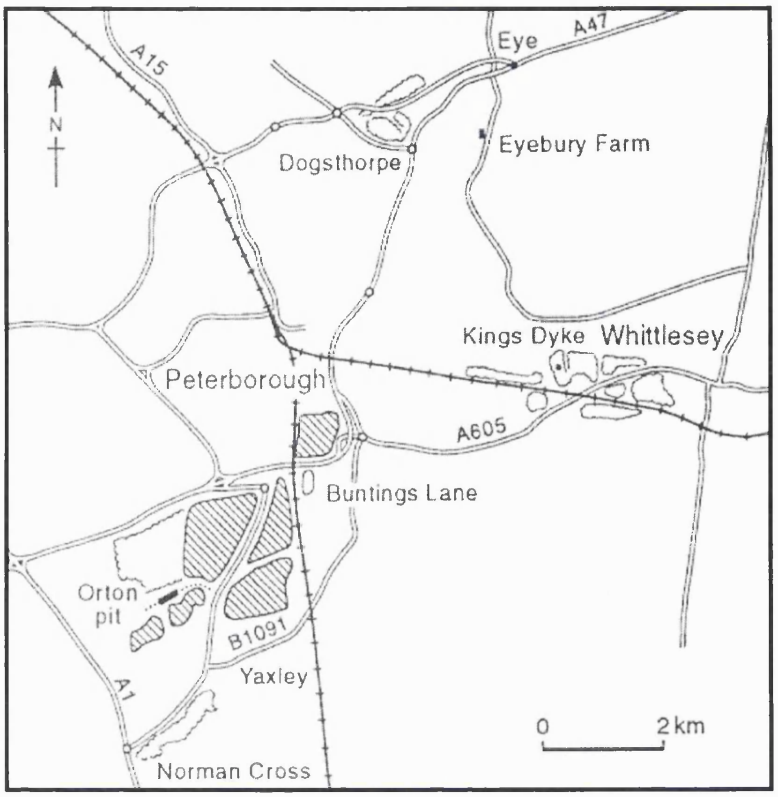

Fig. 5.3 Map showing the location of the King's Dyke Pit. Modified from Hudson & Martill (1994)

5.1.1 Sedimentary cycles

The lower part of the Peterborough Member is characterised by alternations between thick mudstone units and thin, distinct shell-beds. Above Hudson & Martill's (1994) Bed 19, the sequence exhibits decimetre-scale alternations between mudstone beds of subtly different type (Fig. 5.5). Shell-beds still occur, but are less distinct and less widely traceable than before. This part of the sequence has been the subject of speculation concerning Milankovitch cyclicity (Hudson & Martill 1994; Coe pers. comm. 1998), although no evidence of this has been produced to date.

5.1.2 Previous studies of Oxford Clay nannofossils

Nannofossils were first described from the Oxford Clay by Rood *et al.* (1971) and Medd (1971); these studies presented taxonomic and biostratigraphic data. Subsequently there have been a limited number of studies of nannofossils from

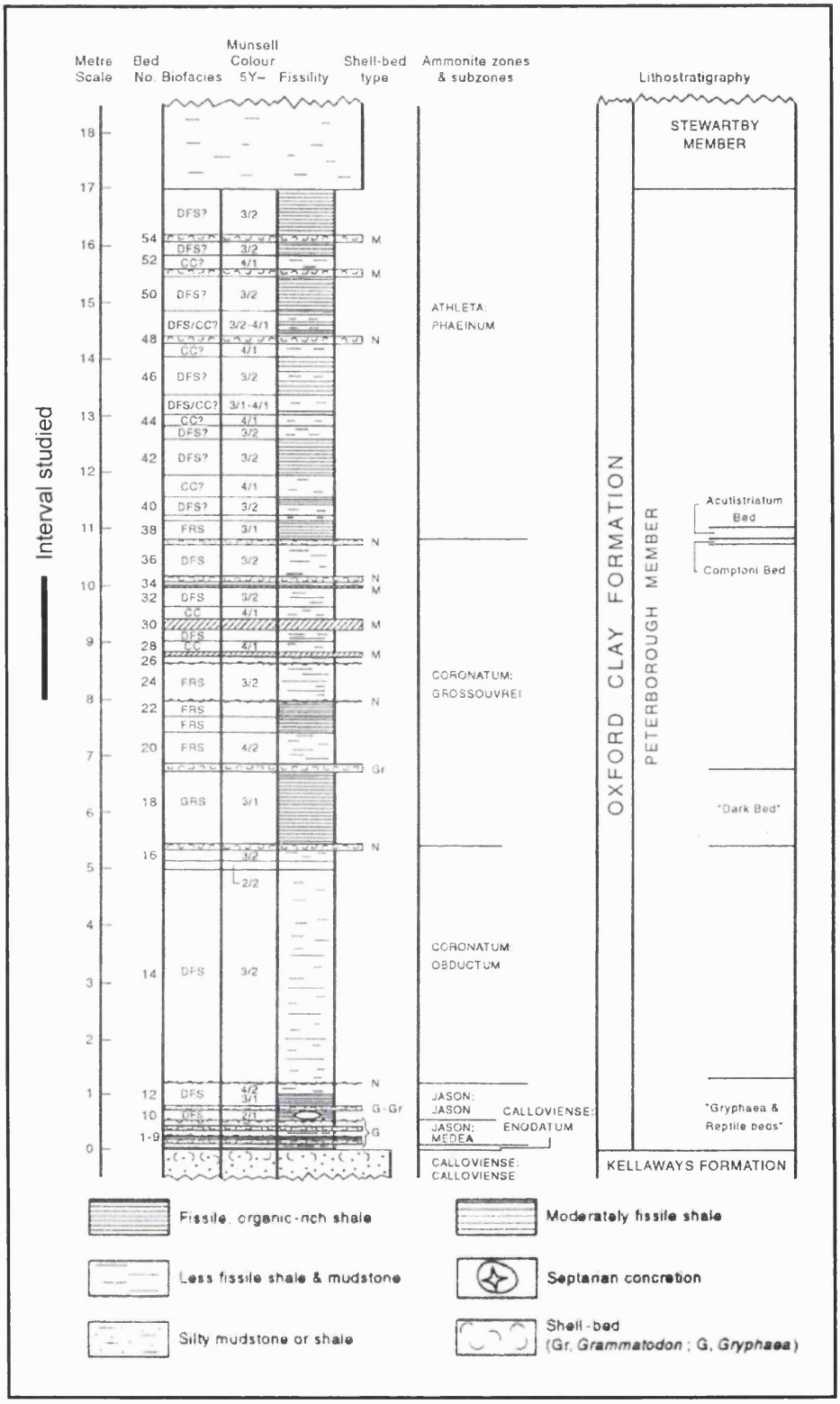

Fig. 5.4 Summary of the lithostratigraphy and ammonite stratigraphy of the Peterborough Member and part of the adjacent units at the King's Dyke Pit. DFS = deposit-feeder shale; N = nuculacean shell-bed; GRS = *Grammatodon*-rich shale; FRS = foraminifera-rich shale; CC = calcareous clay; M = *Meleagrinella* shell-bed. The interval subjected to high-resolution study is shown. Modified from Hudson & Martill (1994)

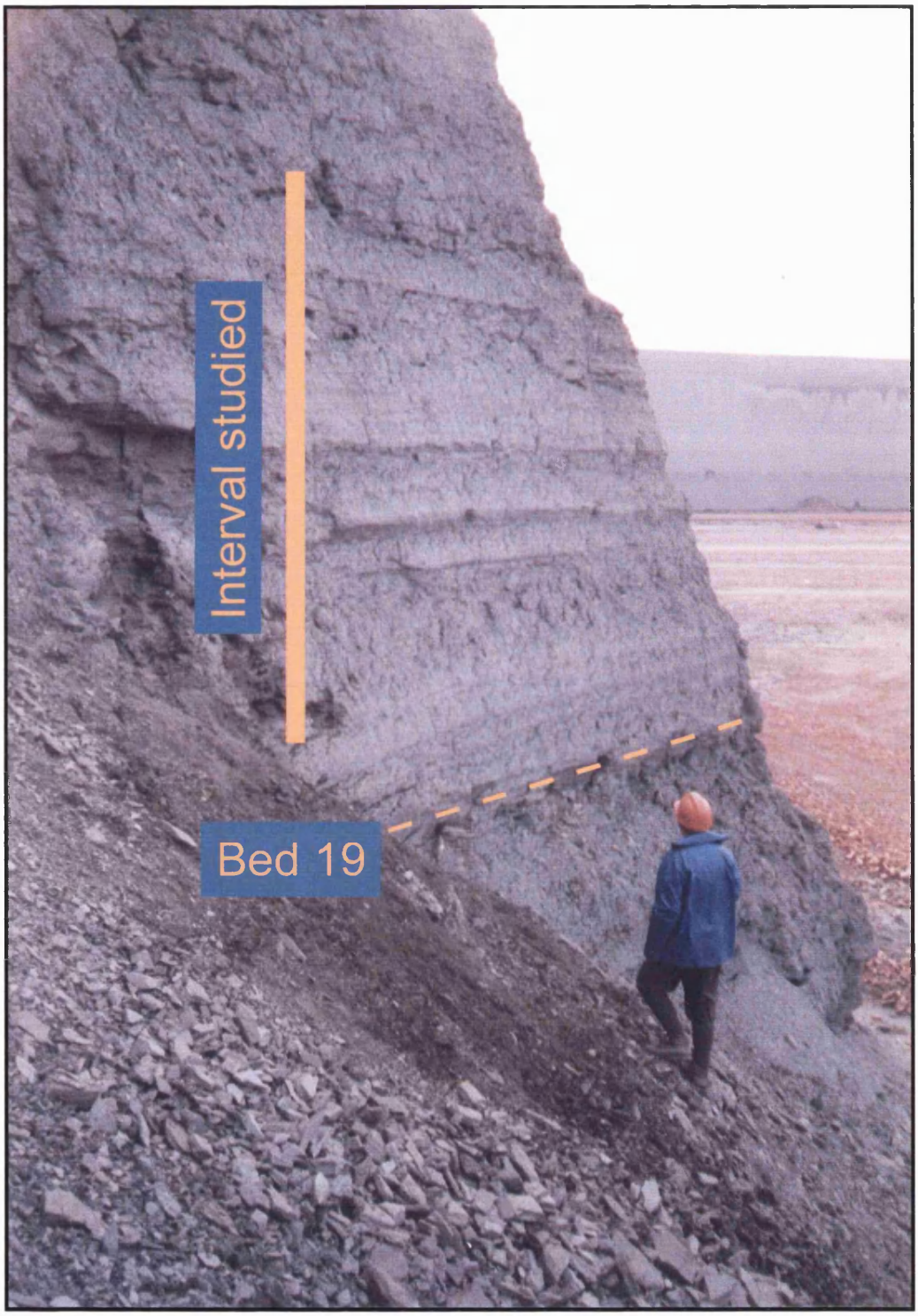

Fig. 5.5 Part of the exposure of the Peterborough Member at the King's Dyke Pit. Bed 19 and the interval subjected to high-resolution study are shown

this formation, and these have been primarily biostratigraphic in nature (Barnard & Hay 1974; Medd 1979, 1982; Bown *et al.* 1988). The single dedicated palaeoenvironmental approach is the brief, low-resolution study of Bown *in*

Martill *et al.* (1994). Where pertinent, the results of this study are discussed below.

5.2 MATERIALS AND METHODS

5.2.1 Sections studied

Reconnaissance study. Eight samples from various Oxford Clay intervals and sites were studied for the purpose of reconnaissance (Table 5.1). The intentions were to locate a section suitable for further, high-resolution study, and to allow consideration of the results of further study within the context of the Oxford Clay nannofloral succession as a whole. The samples represent the full stratigraphic interval exposed by the King's Dyke Pit, from the uppermost Kellaways Formation (directly below the Oxford Clay) to the base of the Stewartby Member. Also represented are single horizons of the Peterborough Member as exposed in the Quest Pit (Stewartby, Bedfordshire; TL 030 420), the Weymouth Member in the Cleveland Farm Pit (Ashton Keynes, Wiltshire; SP 070 943), and the Weymouth Member in Brown's Pit (Stanton Harcourt, Oxfordshire; SP 413 047). These samples were provided by Angela Coe (Open University; King's Dyke Pit samples) and Paul Bown (UCL; all other samples).

High-resolution study. The King's Dyke Pit section of the Peterborough Member was chosen for high-resolution study on the grounds that it is accessible, unweathered (the pit is still worked) and the subject of speculation concerning orbital-climatic forcing (Section 5.1.1). Furthermore, reconnaissance demonstrated the presence of an abundant, well-preserved nannoflora in this section (Section 5.3.1).

Forty-five samples were collected at 5cm intervals from a 2.20m interval between Beds 24 and 34. A sampling interval of 5cm was employed in order to ensure adequate representation of the decimetre-scale bedding.

Lithostratigraphy		Ammonite zone		Site (pit)	Sample	Preservation	Nannofossils	*Watznaueria* coccospheres	*Watznaueria* protococcoliths	*W. britannica*	*W. fossacincta*	*C. margerelii*	*W. barnesae*	*Z. erectus*	*B. constans*	*E. gallicus*	*P. grassei*	*S. bigotii bigotii*	*S. hexum*	*W. manivitae*	*S. quadriarculla*	*A. cylindratus*	*A. harrisonii*	*B. dorsetensis*	*C. perforata*	*R. incompta*	*S. bigotii maximum*	*S. punctulata*	*A. atavus*	*Z. cf. Z. fissus*	Reworked: *C. magharensis*	*C. crassus*	*C. granulatus*	*M. elegans*	*P. liasicus distinctus*
Oxford Clay Fm	Weymouth Mbr	?mariae	?	Brown's	R8	E-1	A		C	A	C	C	C	C	C	C		P			P	P	P	P	P		P	P	P	P					
		mariae	scarburgense	Cleveland Farm	R7	X	A	P	C	A	C	C	P	C	C	C	C	C		P	C	C	P	P	P	P	P	P	P			P	P		
	Stewartby Mbr	athleta	phaeinum	King's Dyke	R6	E-1	C			C	P		P	P		P	P	P		P	P									P				
	Peterborough Mbr				R5	E-1	A		P	A	C	P	P		P		P			P												P		
		coronatum	grossouvrei	Quest	R4	E-1	A		P	C	C	P	P	C	P	P	P	P	P												P			P
				King's Dyke	R3	E-2	C	P		C	P	P	P	P																					
		jason	jason		R2	E-3	C	P		P	P	?diagenetically modified																							
Kellaways Fm		calloviense	calloviense		R1																													

Table 5.1 Oxford Clay nannofossil reconnaissance abundance data. Fm = Formation; Mbr = Member. Ammonite stratigraphy as presented by Bown *in* Martill *et al.* (1994). X = excellent, E-1 = slightly etched; E-2 = moderately etched; E-3 = heavily etched. Nannofossils = all taxa, excluding coccospheres, protococcoliths and reworked specimens. P = present (<1/field of view (FOV)); C = common (1-10/FOV); A = abundant (>10/FOV). The stratigraphic order of Samples R3 and R4, which represent the same ammonite subzone at different sites, is not known

5.2.2 Nannofossil data collection and analysis

All samples were studied using nannofossil data collection and analysis techniques described for the Belemnite Marls (Section 4.2.2), with the exception that (where possible) a minimum of 100 specimens was counted from each reconnaissance sample (a count of 100 specimens was sufficient for the qualitative evaluation required for reconnaissance). The standard minimum of 300 specimens was counted from each of the high-resolution samples. Taxon-specific conventions in data collection that are particular to this study are listed under the relevant taxonomic headings in Appendix 6.

5.2.3 Geochemical data collection

Wt%$CaCO_3$ and TOC data were also determined for the high-resolution King's Dyke Pit samples. Total C was measured using a Leco CS125 analyser (macrofossils were removed prior to analysis, in order to obtain values reflecting the composition of fines rather than the contribution of large bioclasts). TOC values were then found by re-measuring C after treating samples with 10% HCl, thus removing carbonate C. $CaCO_3$ was calculated by subtracting TOC values from those for total C. This work was carried out by Tony Osborne of the Wolfson Laboratory for Environmental Geochemistry, UCL.

5.3 RESULTS

All taxa encountered in the Oxford Clay are listed in Appendix 6; selected species are illustrated in Fig. 5.6. All data are listed in Appendix 7; data for selected parameters are illustrated in Table 5.1 and Fig. 5.7. The nannofossil biostratigraphy of the formation is discussed in Appendix 8.

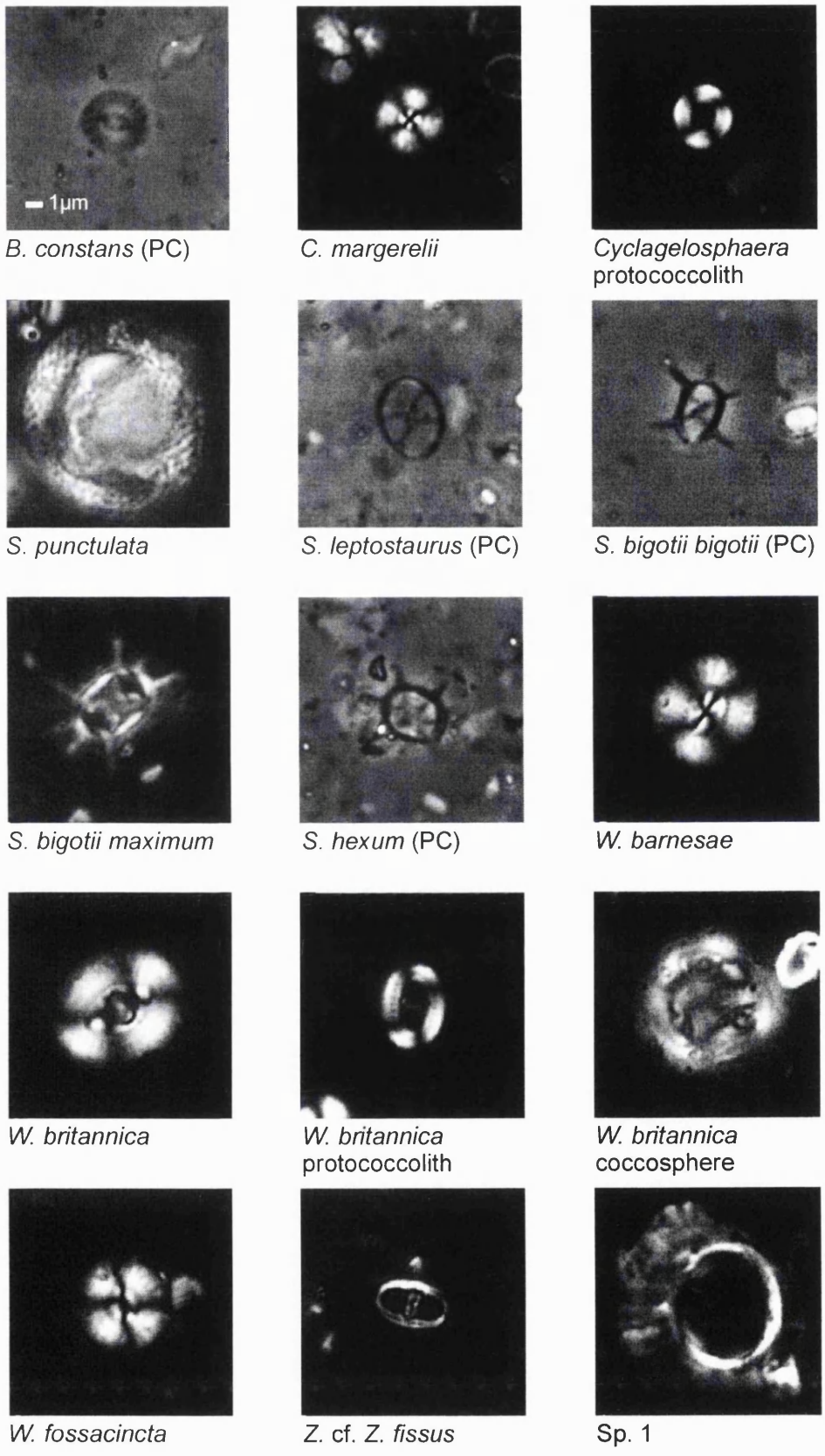

Fig. 5.6 Light micrographs of selected Oxford Clay nannofossils. Images captured in cross-polarised light, except where otherwise stated (PC = phase-contrast illumination)

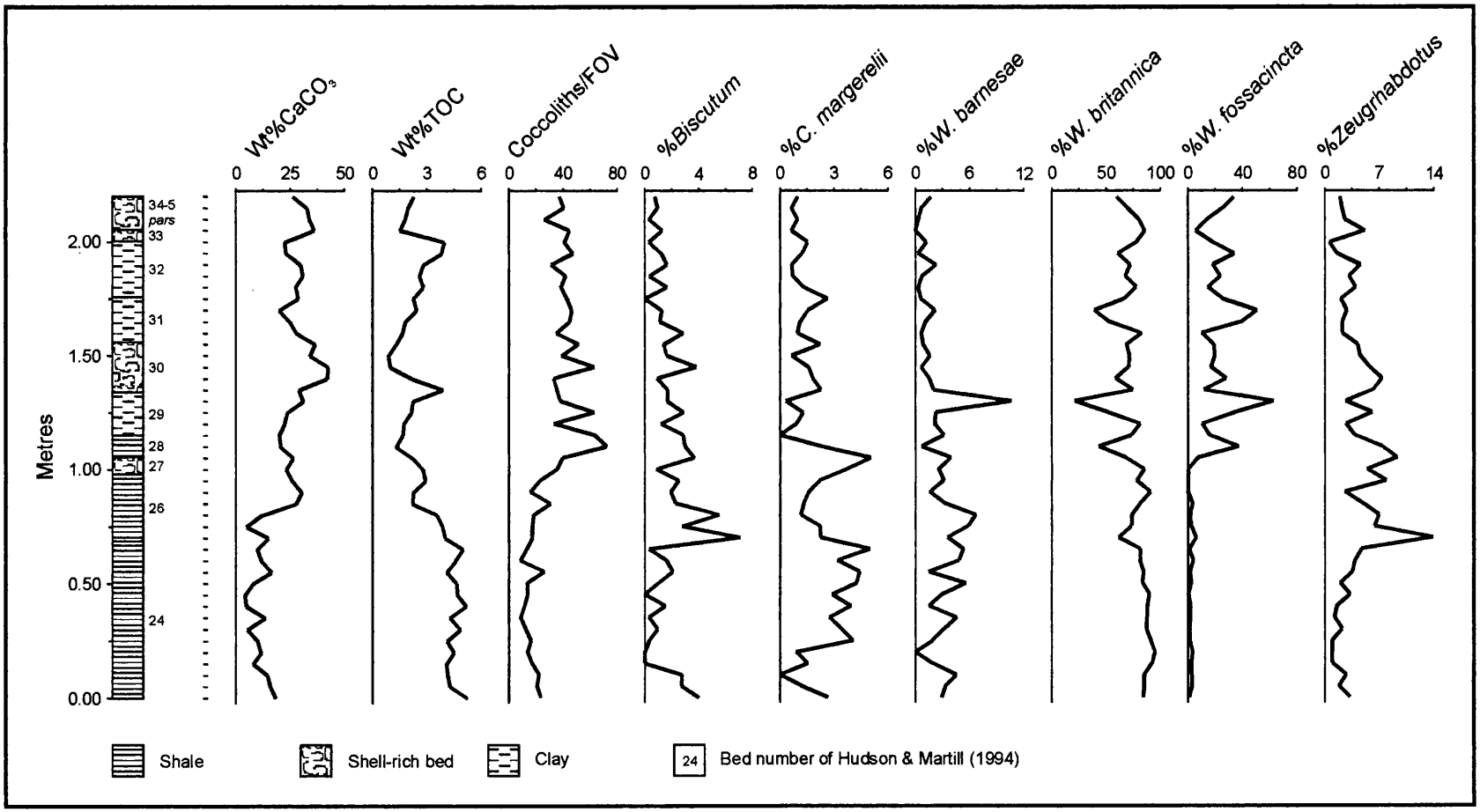

Fig. 5.7 Geochemical and nannofloral data from the King's Dyke Pit section of the Peterborough Member. Samples collected at 5cm intervals (shown)

5.3.1 Reconnaissance study

Most horizons sampled for reconnaissance purposes yielded abundant nannofloras. Preservation is generally good, particularly for sediments of this age; slight etching represents limited dissolution, consistent with the observation of MacQuaker (1994). However, Sample R1 appears to be barren of nannofossils, and Sample R2 is characterised by very low numbers of etched specimens (data from this sample were collected from 10 FOV).

The Peterborough and Stewartby Member nannofloras are characterised by low species diversity (this is true of the Peterborough Member as sampled from both the King's Dyke and Quest Pits). Assemblages are numerically dominated by *Watznaueria*, in particular *W. britannica*. Although diversity increases up-section, the lowermost Stewartby Member nannofloras are still essentially *Watznaueria* assemblages, with only a background presence of other taxa. The Weymouth Member (as sampled from both Brown's and Cleveland Farm Pits) records substantially increased diversity.

The Oxford Clay is characterised by unusually common protococcoliths (incomplete morphotypes representing early coccolith growth stages; Young & Bown 1991).

5.3.2 High-resolution study

As predicted from reconnaissance, all horizons sampled in the high-resolution study of the Peterborough Member yielded abundant, well-preserved nannofloras. These exhibit significant compositional fluctuations through the sequence, at both metre and decimetre scales. Substantial variations at these scales also characterise the carbonate and organic-carbon content of the sediments.

5.4 DISCUSSION

5.4.1 Reconnaissance study

Sedimentology and diagenesis. The abundance of nannofossils in most of the reconnaissance samples indicates that nannoplankton played a significant role in the genesis of the microcarbonate component of the Oxford Clay. Qualitative evaluation in the smear slides reveals that microcarbonate is largely accounted for by particles small enough to represent disintegrated nannofossils. Taking into account the good preservation of coccoliths and the rare occurrence of microspar, this suggests that the microcarbonate is largely of nannoplanktonic (and not diagenetic) origin.

However, Sample R1, which represents a carbonate-rich, concreted lithology, appears to contain no nannofossils. This suggests that diagenetic redistribution of carbonate led to nannofossil dissolution/recrystallisation in this horizon. Very low numbers of etched nannofossils in Sample R2 may also indicate the action of carbonate redistribution; calcareous concretions have been recorded from the horizon represented by this sample (Bed 10; Hudson & Martill 1994). The absent/impoverished nannoflora of the uppermost Kellaways Formation and lowermost Peterborough Member is thus more likely to represent the result of diagenetic destruction than low productivity/high background sedimentation rate. These horizons are clearly not eligible for nannofossil-based palaeoenvironmental analysis.

Nannofloral composition. Good preservation in most samples suggests that nannofloral fluctuations represent palaeoenvironmental controls. Given the preference of nannoplankton for oligotrophic, open-marine settings (Section 2.1.1), the oligotaxic assemblages characteristic of the Peterborough and Stewartby Members indicate that such conditions did not prevail in the Oxford Clay Sea during the interval represented (particularly as the period of Oxford Clay deposition saw the highest nannoplankton diversity in the Boreal Jurassic; Bown *et al.* 1992). The numerical dominance of *Watznaueria* is of interest in this respect. After its origination in the Bajocian, *Watznaueria* was essentially the dominant coccolith genus throughout the entire Mesozoic (Street & Bown 2000);

even so, its predominance throughout the Oxford Clay is striking. Such abundances of *Watznaueria* have previously been considered to be the result of deleterious preservation (and thus employed as a preservation index), based on the assumption that assemblages strongly affected by dissolution are enriched in these robust coccoliths (Roth & Bowdler 1981). There is however increasing evidence that 'floods' of *Watznaueria* in well-preserved sediments, such as those observed here, may represent primary palaeoenvironmental signals (Gale *et al.* 2000, Street & Bown 2000; Lees Burnett *et al.* in prep.).

It has previously been shown that the Peterborough Member records high surface-water fertility, based on the nature and abundance of the organic carbon and palaeontological evidence (Martill *et al.* 1994). This may have been connected with high levels of terrestrial run-off and restricted circulation in a shallow epeiric sea, largely surrounded by islands/larger landmasses and hundreds of kilometres from the nearest ocean (Hudson & Martill 1994). It appears from the results of the present study that high surface-water productivity may have persisted during initial deposition of the Stewartby Member, as nannofloral diversity remained low.

The Weymouth Member (as sampled from both Brown's and Cleveland Farm Pits) records dramatically increased diversity, even taking into account that the period of Oxford Clay deposition was characterised by steady nannoplankton diversification (Bown & Cooper 1998). The nannoflora is comparable with coeval assemblages from NW Europe and the proto-North Atlantic (Bown *in* Martill *et al.* 1994). It is of interest that *Biscutum* and *Zeugrhabdotus* become common (although *Watznaueria* remains dominant). Numerical relationships between these genera have provided useful indices of Cretaceous surface water fertility (Gale *et al.* 2000; Street & Bown 2000); *Watznaueria* is thought to have exhibited a preference for low-nutrient, open-marine settings, whilst *Biscutum* and *Zeugrhabdotus* proliferated during intervals of eutrophication. It is not at all clear however that these observations pertain to the Jurassic, or indeed to all marine settings. Recent work on the Kimmeridge Clay Formation (Upper Jurassic, UK; Lees Burnett *et al.* in prep.) has found that *Watznaueria* blooms occurred during intervals of high productivity, whilst *Biscutum* and *Zeugrhabdotus* abundances remained low. Certainly the increase in abundance of *Biscutum* and

Zeugrhabdotus through the Oxford Clay is not dramatic, and appears significant only as part of the general rise in nannofloral diversity. The Weymouth Member assemblages most probably record a transition towards open-marine environments more ecologically favourable to nannoplankton (diversity increased), albeit still characterised by relatively high productivity (*Watznaueria* still dominated).

Protococcoliths. The presence of Watznaueriacean protococcoliths throughout the Oxford Clay is of interest in the context of the high productivity suggested by overall nannofloral composition. Protococcoliths are not widely observed in either fossil or modern sediment-surface assemblages, even when incorrectly described as separate species (Young & Bown 1991). Culture work on the extant species *Emiliania huxleyi* allows a possible palaeoecological interpretation for their presence in the Oxford Clay. Protococcoliths are most common in samples from the exponential growth phase of cultures in high-nutrient media (Young & Bown 1991), the ecological analogue of these being bloom conditions. The relatively high occurrence of protococcoliths in the Oxford Clay may thus record Watznaueriacean blooms. Similar observations have been made in the Kimmeridge Clay (Young & Bown 1991; Lees Burnett *et al.* in prep.).

5.4.2 High-resolution study

Sedimentology and diagenesis. There is a clear relationship between coccolith abundance and carbonate content through the interval of the Peterborough Member subjected to high-resolution study. This further supports the observation (Section 5.4.1) that nannoplankton played a significant role in the genesis of the microcarbonate fraction of the Oxford Clay.

The Peterborough Member is characterised by a progressive increase in carbonate content. This has been interpreted in terms of a relative increase in coccolith input, as marine transgression increased the distance to siliciclastic sources (Kenig *et al.* 1994) and provided a more open-marine environment favourable to coccolithophores (Bown *in* Martill *et al.* 1994). The results of the present study are consistent with this model. A steady increase in microcarbonate occurs through the interval studied, relating to the lithological transition from

shale to clays and shell beds; this is accompanied by a rise in coccolith concentrations.

Nannofloral composition. The increasing coccolith content of the sediments is accompanied by a substantial rise in the %abundance of *Watznaueria fossacincta*, coupled with a decline in other members of the Watznaueriaceae (*Cyclagelosphaera margerelii*, *Watznaueria barnesae* and *W. britannica*). The ecological preferences of the individual species within this family are not currently known, and are the object of ongoing research (Street & Bown 2000; Lees Burnett *et al.* in prep.). If the palaeoenvironmental scenario outlined above is correct, this would suggest that *W. fossacincta* exhibited the typical coccolithophorid preference for distal, open-marine environments, whilst *Cyclagelosphaera margerelii*, *Watznaueria barnesae* and *W. britannica* all thrived in more unstable proximal settings. Given the limited interval studied here, this suggestion must for the time being remain purely speculative.

The essentially ubiquitous presence of *Biscutum*, *Watznaueria* and *Zeugrhabdotus* throughout the section allowed the productivity index *P* of Gale and other authors (e.g. Gale *et al.* 2000) to be calculated. The results do not yield further insights. This index has previously only been applied to Cretaceous nannofloras, and it may be that it relies on the ecological responses of the Cretaceous representatives of these taxa.

The nannofloral variation discussed above is present at the metre scale. There are also substantial fluctuations in the %abundances of all taxa at a smaller (decimetre) scale. In the absence of obvious correlation with geochemical and sedimentological parameters, the significance of these variations is not yet clear.

5.4.3 Relation of the results to previous studies

The results of the reconnaissance study (Section 5.4.1) are essentially consistent with those of Bown *in* Martill *et al.* (1994). However, Bown suggests that low nannofossil diversity in the Peterborough Member is a function of poor preservation in organic-rich sediments, and that there is a strong inverse relationship between organic-carbon content and nannofloral preservation and

abundance. In the present study nannofossil preservation was found to be good in all the high-resolution Peterborough Member samples, displaying little variation (despite substantial fluctuations in organic-carbon content). It is contended that low nannoplankton diversity in the Oxford Clay is a primary signal, related (together with organic-carbon enrichment) to high palaeosurface-water productivity. The inverse relationship between coccolith abundance and organic carbon probably reflects the largely nannoplanktonic origin of the variable microcarbonate component of the sediments.

5.4.4 Further work

Detection of regular sedimentary cyclicity in the Peterborough Member may be problematic, as the unit is not characterised by a consistent time-depth relationship. The low net accumulation rate suggested by the relative thinness of ammonite zones suggests that winnowing and/or sediment by-pass removed much in the way of fines into deeper parts of the basin (MacQuaker 1994). Temporal lithofacies variability may be the result of variations in the length of the transport path through time, due to delta-lobe switching updip in the fluvial source/relative sea-level change (as opposed to fluctuations in sediment input). Several lines of evidence indicate that sedimentation was episodic; intervals of rapid accumulation are attested to by articulated vertebrate skeletons, whilst shell-beds are thought to represent occasional removal of sediment by tempest events. The lithologically homogenous nature of much of the succession makes it difficult to assess the scale at which these types of variability are present.

Nonetheless, geochemical and nannofloral data from the Peterborough Member are characterised by substantial fluctuations at both metre and decimetre scales. These variations appear to be primary rather than diagenetic in origin, suggesting that these parameters are suitable for both further palaeoenvironmental study and time-series analysis.

6

The Black Ven Marls

6.1 INTRODUCTION TO THE FORMATION

The Black Ven Marls Formation (Dorset, southern UK) underlies the Belemnite Marls (Section 4.1), and represents the uppermost lower and upper Sinemurian sedimentary fill of the Wessex Basin (Hesselbo & Jenkyns 1995). It is well exposed in cliffs on the south coast of England (Fig. 6.1). The succession is *ca.* 43m in thickness (Fig. 6.2), and is comprised of a largely homogenous series of predominantly dark, organic-rich, millimetre-laminated shales and dark marls, broken at intervals by thin concretionary and tabular limestone bands. There are significant fluctuations in carbonate and organic-carbon contents throughout the sequence (Weedon & Jenkyns unpublished). Lang & Spath (1926) produced the first systematic bio- and litho-stratigraphic treatment of the Black Ven Marls; more recently, existing data have been integrated with new work by Hesselbo & Jenkyns (1995). Work of a sequence stratigraphic nature has also been presented by these authors (Hesselbo & Jenkyns 1998).

The palaeogeography of the site is essentially similar to that outlined for the Belemnite Marls, with the exception that the sediments of the Black Ven Marls were deposited in a more proximal setting, and may have been deltaic in origin (insects and plant remains have been recovered from the laminated limestone concretions of Lang & Spath's (1926) Bed 83 (Zeuner 1962; Wall 1965; Whalley 1985), suggesting that richly-vegetated land was not far away. This shift in palaeogeography between the proximal Black Ven Marls and the more distal Belemnite Marls is consistent with the eustatic sea-level rise thought to characterise the Early Jurassic (Donovan & Howarth *in* Bradshaw *et al.* 1992).

6.1.1 Sedimentary cycles

'Medium-scale' sedimentary cycles, approximating to AZs and ammonite sub-

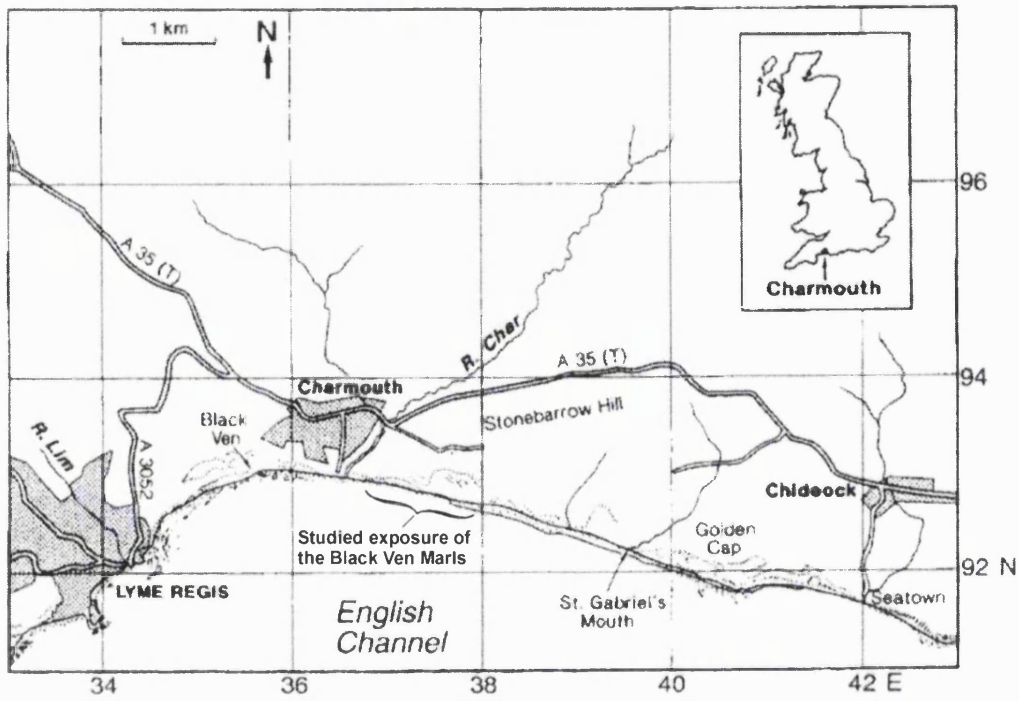

Fig. 6.1 Location of the Black Ven Marls exposure near Charmouth, southern UK. Numbers refer to the Ordnance Survey SY 100,000m grid square. Adapted from Weedon & Jenkyns (1999)

zones (ASZs) and thus representing *ca.* 0.5-3My (i.e. so-called 3rd-order or sequence cycles), are well-expressed in the Black Ven Marls by alternations of organic-rich and calcareous mudstones (Hesselbo & Jenkyns 1998). For instance, the calcareous mudstone that forms the top of the turneri AZ (birchi ASZ) is overlain by a thick (*ca.* 6m) succession of organic-rich, highly fossiliferous (e.g. containing ammonites, crinoids, fish and nests of rhychonellids; House 1989) paper-shales (the Obtusum Shale) belonging to the obtusum AZ (obtusum and stellare ASZs). The base of the Obtusum Shale is a minor erosion surface (Hesselbo & Jenkyns 1995) and the interval overlying the shale, which belongs to the upper part of the stellare ASZ, is a calcareous mudstone. In their sequence stratigraphy of the formation, Hesselbo & Jenkyns (1998) suggested that the Obtusum Shale was deposited during a relative sea-level rise or a highstand (although these authors acknowledge that the medium-scale sedimentary cycles in the formation cannot be definitively linked to relative sea-level changes in preference to changes in sediment supply).

The Black Ven Marls exhibits no clear evidence of Milankovitch cyclicity,

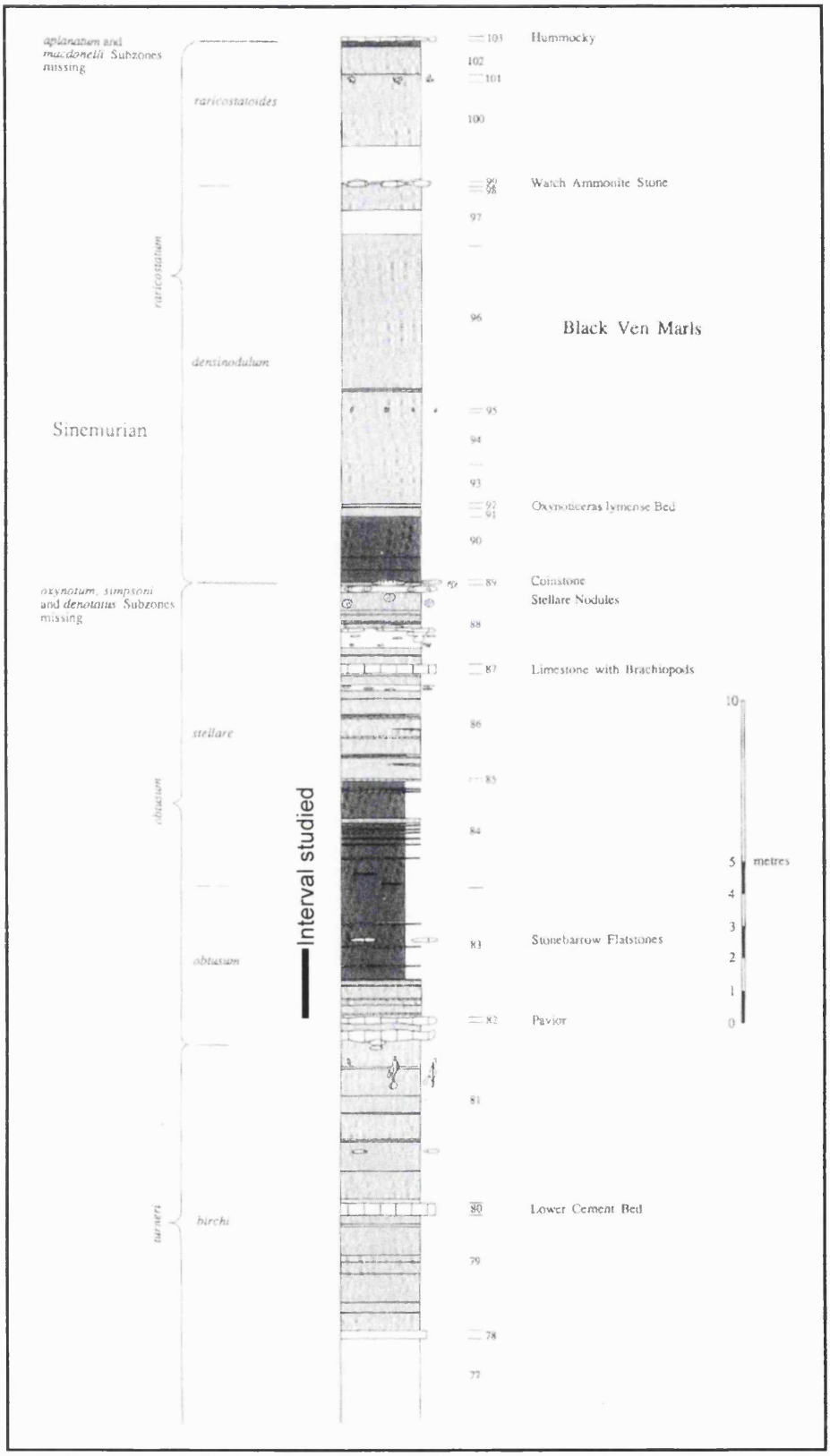

Fig. 6.2 Summary of the lithostratigraphy and ammonite stratigraphy of the Black Ven Marls (excluding Beds 76-7). Key as for Fig. 4.4. The interval studied is shown. Modified from Hesselbo & Jenkyns (1995)

unlike the underlying Blue Lias[1,2] (Waterhouse 1999; Weedon *et al.* 1999) and the overlying Belemnite Marls (Weedon & Jenkyns 1999; Ch. 4) Formations.

6.1.2 Previous studies of Black Ven Marls nannofossils

Rood *et al.* (1973) were the first to describe nannofossils from the Black Ven Marls; their taxonomic and biostratigraphic study was concerned with the Lower and Middle Jurassic as a whole. There have subsequently been a limited number of nannofossil studies of the Black Ven Marls, and these have also been primarily of a taxonomic and biostratigraphic nature; Barnard & Hay (1974) and Hamilton (1982) sampled the formation in their wider studies of the Jurassic, whilst Bown *in* Lord & Bown (1987) and Crux (1987a) present more detailed data for the formation itself. There has been no palaeoenvironmental approach to Black Ven Marls nannofacies to date.

6.2 MATERIALS AND METHODS

6.2.1 Sampling

The Black Ven Marls have been extensively sampled at 10cm intervals by Weedon & Jenkyns (unpublished) from the coastal cliff section below Stonebarrow Hill, east of Charmouth (Fig. 1; SY 368 930-SY 380 927). A sequence of 20 of these samples, representing a 2m interval through Beds 82-3, were employed in the current study. This interval spans the abrupt transition from

---

[1] The Blue Lias in fact underlies the Shales-with-Beef Formation (Hesselbo & Jenkyns 1995); however, the distinction between the latter and the overlying Black Ven Marls is arbitrary (not being based on significant lithological differences; Weedon pers. comm. 1999).

[2] A number of Milankovitch cycles in the Blue Lias were also sampled for nannofossils, for reconnaissance purposes. However, the Blue Lias has been severely altered by diagenetic processes (Weedon 1985); probably as a consequence, nannofossils are not well-represented in the limestone components of these cycles. It may therefore be impossible to assess the links between palaeoclimate and sedimentary cyclicity in the Blue Lias on the basis of nannofloral distribution (although there is still scope for investigation of those intervals of the formation which have been affected relatively little by diagenesis; Weedon pers. comm. 1999).

bioturbated marl to paper shale (Obtusum Shale) in the obtusum ASZ and thus represents part of a medium-scale sedimentary cycle (Section 6.1.1).

6.2.2 Data collection

Nannofloral data collection and analysis were carried out using procedures described for the Belemnite Marls, with the exception that specimens were counted from 10 FOV. This was deemed sufficient for the qualitative evaluation required.

A number of densely aggregated clusters of nannofossils were observed, which may represent faecal pellets. Their occurrence was recorded but no attempt was made to count their component taxa, as this would have compromised the consistency of the absolute abundance data.

Taxon-specific conventions in data collection that are particular to this study are listed under the relevant taxonomic headings in Appendix 3.

6.3 RESULTS

All taxa encountered in the Black Ven Marls are listed in Appendix 3, and those that are common in the formation are illustrated in Fig. 6.3. All data are listed in Appendix 9; selected data are illustrated in Figs. 6.4 and 6.5. The nannofossil biostratigraphy of the formation is discussed in Appendix 10.

Nannofloras were recovered from most of the horizons that were sampled, although abundances are low. Assemblage composition is typical of the Sinemurian of the Boreal Realm (Bown & Cooper 1998). Preservation is generally good, particularly for sediments of this age; slight etching represents limited dissolution. However, a number of samples yielded impoverished assemblages, and several appear to be barren of nannofossils.

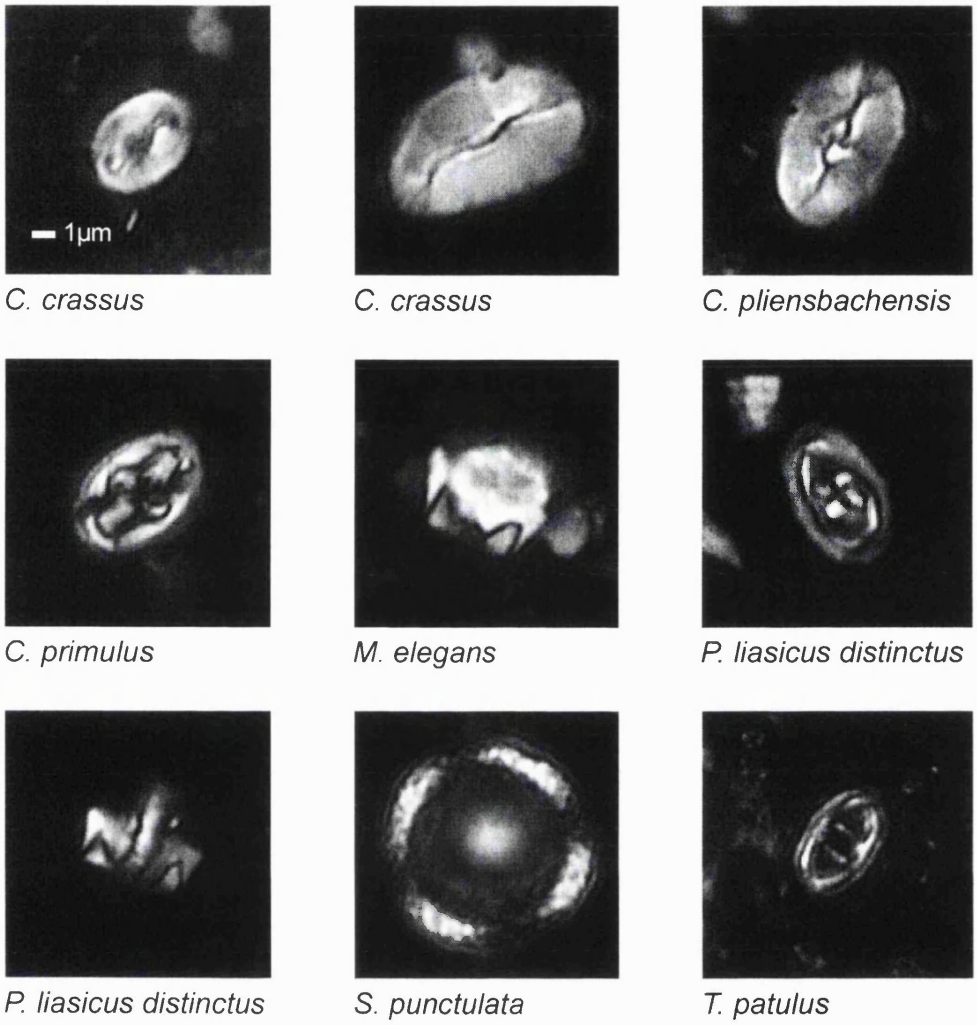

Fig. 6.3 Cross-polarised light micrographs of common Black Ven Marls nannofossils

6.4 DISCUSSION

Carbonate sedimentology and diagenesis

The presence of well-preserved nannofossils in most samples suggests that the sediments of the Black Ven Marls have not been subjected to extensive diagenetic modification. Nannofloral species richness is low, but this was characteristic of Early Jurassic assemblages (in the wake of the Triassic-Jurassic boundary extinctions; Bown & Cooper 1998). In general, nannofossil abundance appears to show some relationship with carbonate content, suggesting a largely nannoplanktonic origin for the Black Ven Marls microcarbonate fraction.

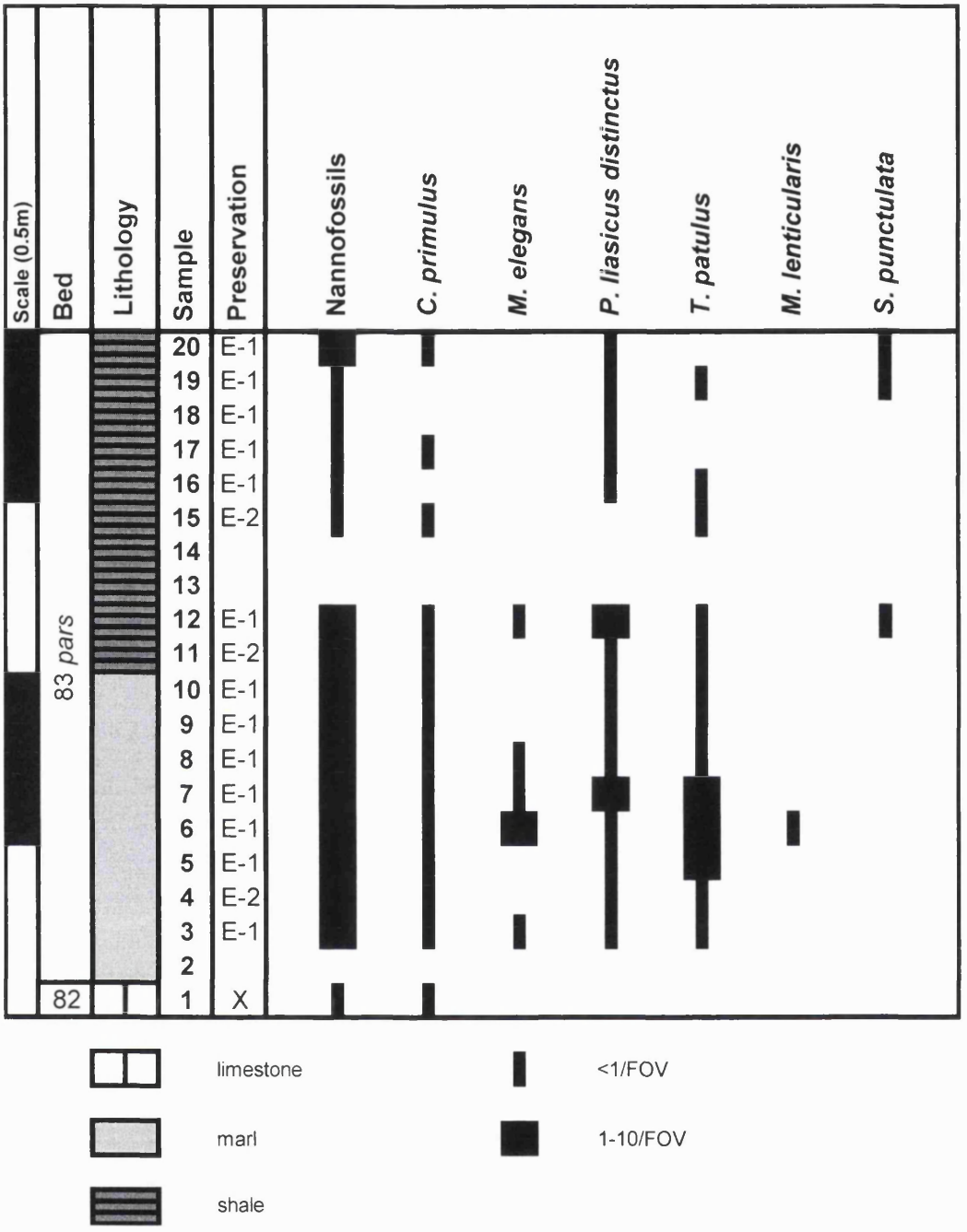

Fig. 6.4 Nannofloral distribution through a 2m interval in the obtusum ammonite zone of the Black Ven Marls. The lowermost sample represents the top of Bed 82; the sampling interval is 10cm. Bed numbers after Lang & Spath (1926)

Important exceptions are represented by Samples 1, 2, 13 and 14, all of which are characterised by impoverished/absent nannofloras. These samples were all collected from concretionary horizons or from immediately adjacent intervals (Sample 1 was collected from the Pavior limestone (Bed 82); Sample 14 corresponds to one of the thin carbonate-rich bands that punctuate the Obtusum

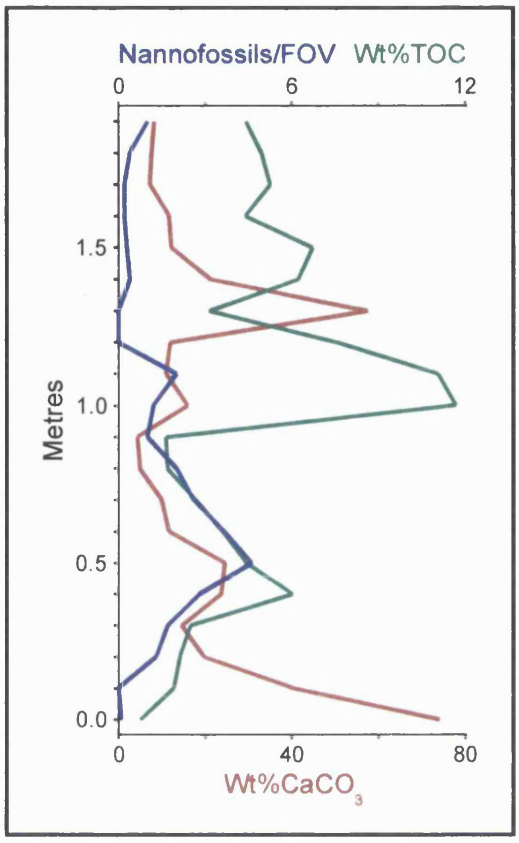

Fig. 6.5 Graph showing nannofossil abundance (specimens per field of view) and geochemical data from a 2m interval in the obtusum ammonite zone of the Black Ven Marls. The lowermost sample represents the top of Bed 82; the sampling interval is 10cm. Geochemical data from Weedon & Jenkyns (unpublished)

Shale); it thus appears that these assemblages record poor preservation, due to post-depositional carbonate redistribution.

Palaeoenvironmental analysis

If diagenesis is not responsible, the low nannofloral abundance throughout most of the section must represent a primary feature of the marine palaeoenvironment. The possible scenarios are low nannofloral productivity and/or high background sedimentation rate. Since nannoplankton are generally oligotrophic-adapted, the essentially 'normal' level of taxonomic evenness suggests that productivity was not particularly high. Even so, abundances are unusually low (e.g. in comparison with the Belemnite Marls). It thus appears that the background clay sedimentation rate was high, perhaps due to the proximity of the site to a near-shore, deltaic environment.

Samples 10 and 11 represent an abrupt transition from bioturbated marl to organic-rich paper-shale, and thus significant change in the depositional environment. Nannofossil abundance declines in the shale, although there appears to be little significant change in taxonomic composition (the slight decrease in species richness is almost certainly an artefact of counting from an impoverished assemblage). It is possible that the shale represents a period of enhanced precipitation and run-off, thus diluting the contribution of planktonic carbonate through increased terrestrial clay input. Rapid sedimentation may have ensured the fast burial and preservation of organic carbon. Fresh-water input, the development of a halocline and water-column stratification may also have resulted in very low/zero-oxygen conditions in bottom waters, allowing increased organic-carbon preservation and the development of fine lamination within the sediments through the inhibition of bioturbating organisms.

6.4.4 Further work

With the exception of the carbonate-rich beds and immediately adjacent horizons, both of which appear to represent diagenetic modification of sediment composition, the Black Ven Marls appears to be suitable for nannofloral palaeoceanographic analysis. Nannofossil abundance is low, but preservation analysis suggests that primary environmental signals are represented. As such, there is potential for investigating the genesis of the medium-scale lithological cycles. With the collection of higher-resolution time series it may also be possible to search for the Milankovitch cyclicity which characterises Lower Jurassic sediments both under- and overlying the formation. Nannofossil records of environmental cycles are not always accompanied by fluctuations in other lithological parameters (Erba *et al.* 1992), and may thus be present in lithologically monotonous sequences such as the Black Ven Marls. However, Milankovitch signals may well be absent, given the apparent exposure of the Black Ven Marls to near-shore processes and the presence of stratal gaps within the succession (Hesselbo & Jenkyns 1995).

7

Summary and Conclusions

7.1 SUMMARY

A summary of the main conclusions of this study is presented below:

7.1.1 The Belemnite Marls

- The carbonate cycles which characterise the Belemnite Marls do not appear to be pelagic in origin. Rather it may be that a relatively constant supply of nannoplanktonic carbonate was periodically diluted by major contributions of platform-derived carbonate mud into the basin. This observation is consistent with recent work on the genesis of other Mesozoic (including Lower Jurassic) rhythmites (Hinnov & Park 1999; Mattioli *et al.* 2000).

- Orbitally-forced sedimentary cycles in the Belemnite Marls (Weedon & Jenkyns 1999) are accompanied by fluctuations in nannofossil species diversity. These fluctuations do not appear to be taphonomic in origin; rather, they may record variations in surface-water nutrification, perhaps driven by a shifting intensity of vertical mixing in the water-column. Such a palaeoenvironmental model is not universally applicable to Mesozoic marine rhythmites (e.g. Watkins 1989; Thierstein & Roth 1991; Erba *et al.* 1992; Mutterlose & Ruffel 1999; da Gama 2000; Scarparo Cunha 2000). However, interpretations which are broadly similar to those advanced here have been proposed for some sections (e.g. Mattioli 1997; Windley 1995; Herrle & Hemleben 2000).

- *Crepidolithus crassus* may have been an ecological opportunist in the early Pliensbachian of the Boreal Realm, flourishing during intervals of high surface-water fertility, whilst *C. pliensbachensis* and *Mitrolithus elegans* may

have been specialists, exhibiting a preference (typical of extant nannoplankton) for low-fertility conditions. *Parhabdolithus liasicus* and *Similiscutum cruciulus* may have been somewhat oriented towards elevated nutrient conditions during certain intervals. Ecological preferences appear to have been subject to temporal (perhaps evolutionary) change; for instance, *Parhabdolithus liasicus* appears to have shifted through time towards a low-nutrient adaptation. *Schizosphaerella*, albeit a significant contributor to carbonate sedimentation, does not appear to have displayed Tethyan abundances or ecological affinities (Mattioli 1997) in the early Pliensbachian Boreal Realm.

- The nannofossil biostratigraphy of the Belemnite Marls presented here is consistent with the ammonite work of Palmer (1972). It also essentially concurs with less detailed nannofossil studies of the formation by Bown *in* Lord & Bown (1987), Crux (1987a) and Turner (1997).

7.1.2 The Oxford Clay

- Nannoplankton played a significant role in the genesis of the microcarbonate component of the Oxford Clay.

- In general, nannofloral composition is probably the result of palaeoenvironmental (as opposed to taphonomic) controls. High productivity (perhaps in connection with terrestrial run-off and restricted circulation) appears to have characterised the Callovian Oxford Clay Sea, as represented by the nannofloras of the Peterborough and lowermost Stewartby Members. The Weymouth Member most probably records an early Oxfordian transition towards more open-marine environments, albeit still characterised by relatively high surface-water nutrient conditions.

- The relatively high occurrence of protococcoliths in the Oxford Clay may record Watznaueriacean blooms. This is consistent with similar observations made in the Kimmeridge Clay Formation (Young & Bown 1991; Lees Burnett *et al.* in prep.).

- Nannofloral distribution through the Peterborough Member exhibits significant fluctuations at both metre and decimetre scales. Substantial variations at these scales also characterise the carbonate and organic-carbon content of the sediments. The metre-scale variations may be related to sea-level change. The significance of the decimetre-scale nannofloral variations is not yet clear; time-series analysis of these high-frequency fluctuations may prove useful in investigation of putative Milankovitch controls on Oxford Clay sedimentation (Hudson & Martill 1994; Coe pers. comm. 1998).

- The results of the present study of the Oxford Clay are essentially consistent with the established ammonite zonation (as presented by Bown *in* Martill *et al.* (1994)), and with the less detailed nannofloral stratigraphy and palaeoenvironmental analysis of Bown *in* Martill *et al.* (1994).

7.1.3 The Black Ven Marls

- The Black Ven Marls microcarbonate fraction is ascribed a largely nannoplanktonic origin.

- The nannofloras of the Black Ven Marls do not appear to have been subjected to extensive diagenetic modification (with the exception of those recovered from the occasional limestone horizons). The typically low-density assemblages may represent the high clay sedimentation rate of a proximal setting.

- The significant change in depositional environment recorded by the abrupt transition from bioturbated marl to the organic-rich Obtusum Shale is thought to represent a sequence cycle (Hesselbo & Jenkyns 1998). An accompanying decrease in nannofloral abundance suggests that the shale records a period of enhanced precipitation and run-off, thus diluting planktonic carbonate sedimentation through increased terrestrial clay input.

- The Black Ven Marls is suitable for further nannofloral palaeoenvironmental analysis, and there may be potential for detailed investigation of the genesis of the medium-scale lithological cycles (Hesselbo & Jenkyns 1998). It may also be possible to search for Milankovitch cyclicity which, although not visually evident in this formation, is known to characterise both under- and overlying Lower Jurassic sediments (Waterhouse 1999; Weedon & Jenkyns 1999; Weedon *et al.* 1999; Ch 4).

- The nannofossil biostratigraphy of the formation is essentially consistent with the ammonite zonation presented by Hesselbo & Jenkyns (1995). It also generally concurs with less detailed nannofossil studies of the formation by Bown *in* Lord & Bown (1987) and Crux (1987a).

7.2 GENERAL CONCLUSIONS

In addition to the points listed above, this study has generated some more general conclusions:

- Standard techniques of nannofossil preparation, data collection and analysis (Bown & Young 1998b) are confirmed as suitable not only for routine biostratigraphy but also (when applied consistently) for quantitative palaeoenvironmental study.

- The unusually high-resolution of the datasets collected for this study confirm that Boreal Jurassic strata are reasonably well-divided on the basis of nannofossil events (Bown & Cooper 1998).

- The role of nannofossils as useful cyclostratigraphic tools (Young *et al.* 1994) is confirmed. Nannofloral analysis of sediments which contain abundant, well-preserved assemblages may allow both quantification of sedimentary cycles and investigation of the underlying palaeoenvironmental processes involved in their genesis. In turn, responses to palaeoenvironmental fluctuations allow suggestions to be made concerning the little-known ecological preferences of

fossil nannoplankton. This thesis represents the first study to demonstrate the application of nannofloral time-series analysis to rhythmites dating from the Early Jurassic (and thus to the earliest stratigraphic range of nannoplankton; Bown & Young 1998a). Clearly nannofossils will play a significant role in the emerging science of cyclostratigraphy, itself one of the most innovative and promising new approaches to gather momentum within the Earth sciences in recent decades (Einsele *et al.* 1991).

Appendix 1

Sample Curation

The nannofossil slides generated for this study, and for which data are presented, together with the raw sediment samples collected from the Oxford Clay, are stored in the Department of Geological Sciences, UCL. The notation used in the labelling of these materials is presented in Table A1.1.

The sediment samples from the Belemnite Marls and the Black Ven Marls are held by Graham Weedon, Department of the Environment, Geography and Geology, University of Luton. The King's Dyke Pit Oxford Clay reconnaissance samples are held by Angela Coe, Department of Earth Sciences, Open University. The Oxford Clay slides from the Brown's, Cleveland Farm and Quest Pits were on loan from Paul Bown, Department of Geological Sciences, UCL.

Ben	Ben Walsworth-Bell
4 - X	Belemnite Marls - sample number
5 - (R) X	Oxford Clay - (reconnaissance) sample number
7 - X	Black Ven Marls - sample number

eg: Ben - 5 (R) 1

=

Ben Walsworth-Bell, Oxford Clay Reconnaissance Sample 1

Table A1.1 Notation used in the labelling of all samples as used in this study. To relate sample numbers to stratigraphic levels, see data tables in appendices

Appendix 2

Reproducibility of Data

Introduction

This study interprets nannofossil time series in terms of palaeoceanographic fluctuations. It is thus important to demonstrate the reproducibility of results generated by the preparation and data collection techniques outlined in Section 4.2.2[1].

Methods

Samples representing both Belemnite Marls dark marl (Sample A) and light marl (Sample B) beds were selected as end-member representatives of carbonate-poor/organic-rich and carbonate-rich/organic-poor sediments respectively (Weedon & Jenkyns 1999). This allowed the reproducibility of results from both of the major lithologies encountered in this study to be tested.

Five repeat counts of 300 specimens were made from a single preparation of Sample A, to test the precision of the data collection technique[2]. The results were processed to yield %abundance and abundance/FOV data.

To assess the precision of the simple smear preparation technique, 5 smear slides were prepared from both Samples A & B. Single counts of 300 were made from each of these preparations, and processed to yield %abundance and abundance/FOV data.

---

[1] This investigation of reproducibility was carried out in advance of data collection for this study. As such the techniques employed vary slightly from those outlined in Section 4.2.2 (e.g. *Schizosphaerella punctulata* is here included in all %abundance calculations). This does not compromise the significance of the results obtained here, as all further technique modifications were employed to improve precision in data collection.

[2] This procedure was carried out on only one sample, as results yielded by the counting technique are independent of lithology.

Results

Repeat counts. Results are presented in Table A2.1. The similarity between the 5 repeat counts is reasonable. Data for the taxon showing the highest discrepancy in %abundance (*Crepidolithus crassus*) exhibits an acceptable standard deviation of 2.15. Total nannofossil abundance/FOV exhibits a very low standard deviation of 0.59.

Data analysis	Count	Nannofossils	*C. crassus*	*C. pliensbachensis*	*C. primulus*	*M. elegans*	*M. lenticularis*	*P. liasicus distinctus*	*P. robustus*	*S. punctulata*	*T. patulus*	Sp. indet.
%abundance	1	n/a	72.31	7.69	0.00	10.46	1.54	4.92	0.00	2.15	0.92	0.00
	2		67.89	5.69	1.00	12.37	1.00	7.02	0.67	3.34	0.67	0.33
	3		67.77	8.31	1.33	9.97	0.33	4.98	0.33	4.65	2.33	0.00
	4		68.13	6.56	0.63	15.00	0.31	3.44	0.31	3.44	2.19	0.00
	5		71.29	5.94	0.66	11.55	0.99	4.95	0.33	2.31	1.98	0.00
Mean			69.48	6.84	0.72	11.87	0.84	5.06	0.33	3.18	1.62	0.07
Standard deviation			**2.15**	**1.13**	**0.50**	**1.98**	**0.52**	**1.28**	**0.24**	**1.01**	**0.76**	**0.15**
Abundance/FOV	1	10.48	7.58	0.81	0.00	1.10	0.16	0.52	0.00	0.23	0.10	0.00
	2	11.50	7.81	0.65	0.12	1.42	0.12	0.81	0.08	0.38	0.08	0.04
	3	10.03	6.80	0.83	0.13	1.00	0.03	0.50	0.03	0.47	0.23	0.00
	4	10.32	7.03	0.68	0.06	1.55	0.03	0.35	0.03	0.35	0.23	0.00
	5	10.10	7.20	0.60	0.07	1.17	0.10	0.50	0.03	0.23	0.20	0.00
Mean		10.49	7.28	0.71	0.08	1.25	0.09	0.54	0.04	0.33	0.17	0.01
Standard deviation		**0.59**	**0.41**	**0.10**	**0.05**	**0.23**	**0.06**	**0.17**	**0.03**	**0.10**	**0.07**	**0.02**

Table A2.1 Data generated to test reproducibility of repeat counts from a single smear slide (Sample A). FOV = field of view

Repeat preparations. Results are presented in Table A2.2. The similarity between counts from the 5 repeat preparations is reasonable. Data for the taxon showing the highest discrepancy in %abundance (*Crepidolithus crassus* in Sample A) exhibits a reasonably low standard deviation of 4.01. Total nannofossil abundance/FOV shows a higher discrepancy in Sample A than in Sample B, albeit with a reasonably low standard deviation of 1.67.

Discussion

The results presented above indicate that the methods employed in this study yield

Data analysis	Sample	Slide	Nannofossils	*Calyculus* sp.	*C. crassus*	*C. pliensbachensis*	*C. primulus*	*M. elegans*	*M. lenticularis*	*P. liasicus distinctus*	*P. robustus*	*S. punctulata*	*S. cruciulus*	*T. patulus*	Sp. indet.
%abundance	A	1	n/a	0.00	72.31	7.69	0.00	10.46	1.54	4.92	0.00	2.15	0.00	0.92	0.00
		2		0.33	68.54	5.96	1.99	9.93	0.33	7.95	0.00	2.32	0.00	1.99	0.66
		3		0.00	70.53	7.21	0.00	8.46	1.25	7.21	0.31	3.13	0.00	1.88	0.00
		4		0.00	61.79	6.87	1.49	14.03	0.30	9.25	0.00	1.79	0.00	3.28	1.20
		5		0.29	67.34	6.88	0.86	13.75	1.15	5.73	0.00	2.29	0.00	1.72	0.00
	Mean			0.12	68.10	6.92	0.87	11.33	0.91	7.01	0.06	2.34	0.00	1.96	0.37
	Standard deviation			**0.17**	**4.01**	**0.63**	**0.89**	**2.45**	**0.57**	**1.73**	**0.14**	**0.49**	**0.00**	**0.85**	**0.62**
	B	1		0.88	52.65	5.29	3.82	13.82	0.29	12.65	0.29	5.29	0.59	2.94	1.47
		2		0.50	49.75	4.48	2.74	16.92	0.50	12.19	0.25	8.21	0.25	3.48	0.75
		3		0.66	52.32	4.64	0.99	15.89	0.00	8.94	0.00	8.61	1.32	4.30	2.32
		4		1.27	51.58	6.65	3.16	14.24	0.00	11.08	0.63	6.33	0.32	3.16	1.58
		5		0.00	55.59	3.62	0.99	19.08	0.66	10.20	0.33	6.58	0.33	1.64	0.99
	Mean			0.66	52.38	4.93	2.34	15.99	0.29	11.01	0.30	7.00	0.56	3.11	1.42
	Standard deviation			**0.47**	**2.12**	**1.13**	**1.29**	**2.13**	**0.29**	**1.50**	**0.23**	**1.38**	**0.45**	**0.97**	**0.61**
Abundance/field of view	A	1	10.48	0.00	7.58	0.81	0.00	1.10	0.16	0.52	0.00	0.23	0.00	0.10	0.00
		2	10.07	0.03	6.90	0.60	0.20	1.00	0.03	0.80	0.00	0.23	0.00	0.20	0.07
		3	10.63	0.00	7.50	0.77	0.00	0.90	0.13	0.77	0.03	0.33	0.00	0.20	0.00
		4	13.40	0.00	8.28	0.92	0.20	1.88	0.04	1.24	0.00	0.24	0.00	0.44	0.16
		5	13.42	0.04	9.04	0.92	0.12	1.85	0.15	0.77	0.00	0.31	0.00	0.23	0.00
	Mean		11.60	0.01	7.86	0.80	0.10	1.34	0.10	0.82	0.01	0.27	0.00	0.23	0.05
	Standard deviation		**1.67**	**0.02**	**0.82**	**0.13**	**0.10**	**0.48**	**0.06**	**0.26**	**0.01**	**0.05**	**0.00**	**0.13**	**0.08**
	B	1	10.30	0.09	5.42	0.55	0.39	1.42	0.03	1.30	0.03	0.55	0.06	0.30	0.15
		2	9.57	0.05	4.76	0.43	0.26	1.62	0.05	1.17	0.02	0.79	0.02	0.33	0.07
		3	7.55	0.05	3.95	0.35	0.08	1.20	0.00	0.68	0.00	0.65	0.10	0.33	0.18
		4	10.90	0.14	5.62	0.72	0.34	1.55	0.00	1.21	0.07	0.69	0.03	0.34	0.17
		5	8.94	0.00	4.97	0.32	0.09	1.71	0.06	0.91	0.03	0.59	0.03	0.15	0.09
	Mean		9.45	0.07	4.95	0.47	0.23	1.50	0.03	1.05	0.03	0.65	0.05	0.29	0.13
	Standard deviation		**1.29**	**0.05**	**0.65**	**0.16**	**0.15**	**0.20**	**0.03**	**0.26**	**0.02**	**0.09**	**0.03**	**0.08**	**0.05**

Table A2.2 Data generated to test reproducibility of single counts from repeat smear slide preparations of two samples

data of adequate precision. They compare favourably with results obtained in similar experiments by other authors, including those testing the reproducibility of the allegedly higher-precision random settling technique (e.g. Geisen *et al.* 1999).

The greater standard deviation generated by single counts from repeat preparations as opposed to repeat counts of the same preparation probably represents the degree of sampling error introduced by obtaining sediment from the different stratigraphic levels represented by even the smallest sample (Samples A and B represent uncrushed hand-specimens). Considering the acceptable levels of this standard deviation, the decimetre/metre scale of the bedding phenomena and the prevalence of bioturbation in the sequences under investigation, and the 'channel' sampling technique employed for the Belemnite Marls time-series

analysis, such sampling error is not considered to be problematic in the context of this study.

No significant difference was observed in the reproducibility of data obtained from the two major lithologies under study. This suggests that the different physical properties of the samples (e.g. grain size and its effect on sediment dispersal on the slide) are not responsible for variations in the nannofloral data.

Appendix 3

Belemnite Marls and Black Ven Marls Taxonomic List

All nannofossil taxa encountered during this study of the Belemnite Marls are listed below, and discussed where necessary. All taxonomic references listed in this thesis are provided by Bown (1998b). Figure numbers refer to this thesis.

Bussonius prinsii (Noël 1973) Goy 1979

Calyculus Noël 1973

Crepidolithus crassus (Deflandre 1954) Noël 1965 (Figs. 4.9 & 6.3)

C. granulatus Bown 1987

C. pliensbachensis Crux 1985; emend. Bown 1987 (Figs. 4.9 & 6.3)

Crucirhabdus primulus Prins *ex* Rood *et al.* 1973; emend. Bown 1987 (Figs. 4.9 & 6.3)

Mitrolithus elegans Deflandre 1954 (Figs. 4.9 & 6.3)

This species bears a lamellar spine which is uniquely susceptible to disaggregation, and spine fragments are common through much of the Belemnite Marls. Relative levels of nannofossil disarticulation have previously been applied as quantitative indices of preservation (e.g. Matsuoka 1990). In this study the number of *M. elegans* spines was recorded, and the ratio between *M. elegans* coccoliths and spine fragments investigated as a possible index of nannofossil attrition.

M. lenticularis Bown 1987

For the purposes of time-series analysis, *M. elegans* and *M. lenticularis* were grouped together as *M. elegans*. Distinguishing between these species is problematic (impossible in plan view; in side view, it appears from specimens observed in the Belemnite Marls that these taxa represent end-members of a continuous morphological spectrum).

Orthogonoides hamiltoniae Wiegand 1984

In the Belemnite Marls study nannolith (*O. hamiltoniae* and *Schizosphaerella punctulata*) data were collected in addition to a minimum count of 300 coccoliths. These species are of uncertain taxonomic affiliation, and it is thus important to consider their population dynamics separately from those of the coccolithophores.

Parhabdolithus liasicus Deflandre 1952

P. liasicus distinctus Bown 1987 (Figs. 4.9 & 6.3)

P. liasicus liasicus Bown 1987

For the purposes of time-series analysis, *P. liasicus distinctus* and *P. liasicus liasicus* data

were grouped together as *P. liasicus*. *P. liasicus liasicus* is rare and sporadic in its occurrence through the Belemnite Marls, and cannot always be distinguished from *P. liasicus distinctus* in the absence of the spine. As sub-species, these taxa would have responded to the same environmental parameters.

P. robustus Noël 1965 (Fig. 4.9)

Schizosphaerella punctulata Deflandre & Dangeard 1938 (Figs. 4.9 & 6.3)

See entry under *O. hamiltoniae*.

The *S. punctulata* data represent the number of whole (i.e. bi-valved) specimens observed. This was achieved by counting whole specimens, single valves and fragments representing as little as half a valve. Given the ubiquitous abundance of small fragments of this species, this was found to be the most meaningful method of quantifying its distribution. Thus population counts record whole tests, as opposed to the coccolith data where numerous specimens represent a single coccosphere (it is not possible to establish the number of coccospheres represented by the coccolith counts, as the ratio between liths and spheres is not known).

Similiscutum cruciulus de Kaenel & Bergen 1993 (Fig. 4.9)

The species *S. cruciulus* is here applied in a slightly broader sense than that of de Kaenel & Bergen (1993), to include all sub-circular to elliptical forms with variable central-area widths which may or may not reveal a central-area axial cross (*sensu* Bown & Cooper 1998). Such a grouping is supported by the recent morphometric analysis of Mattioli *et al.* (2000).

Sollasites Black 1967

Stradnerlithus Black 1971

Tubirhabdus patulus Rood *et al.* 1973 (Figs. 4.9 & 6.3)

Appendix 4

Belemnite Marls Data

The raw nannofossil data generated for the Belemnite Marls study are listed in Table A4.1, together with the geochemical data of Weedon & Jenkyns (1999).

Table A4.1 (Next page) Nannofossil count data generated for the Belemnite Marls, together with the corresponding geochemical data of Weedon & Jenkyns (1999). The nannofossil stratigraphy of the formation is shown. Ammonite stratigraphy based on Palmer (1972). Bed numbers follow Lang *et al.* (1928). O-1 = slightly overgrown; O-2 = moderately overgrown. • = inferred range, based on first (▁▲) and last (▔▼) occurrences

Metres	Ammonite zone		Bed	Sample	Wt%$CaCO_3$	Wt%TOC	Fields of view	Preservation	*M. elegans* spines	*C. crassus*	*C. pliensbachensis*	*C. primulus*	*M. elegans*	*M. lenticularis*	*P. liasicus distinctus*	*S. punctulata*	*T. patulus*	*P. robustus*	*O. hamiltoniae*	*P. liasicus liasicus*	*S. cruciulus*	*Stradnerilithus* sp.	*C. granulatus*	*Calyculus* sp.	*Solisaltes* sp.	*B. prinsii*	Nannofossil zone
12.90				**103**	59.65	0.80	16	O-2	49	114	24	11	44	*	107	11	3	*	1	1	1	1	*	*	*	*	
12.87				**102**	69.36	0.51	35	O-2	39	162	21	7	42	*	79	10	13	*	*	*	2	*	*	*	*	*	
12.84				**101**	71.05	0.46	26	O-2	38	161	19	12	36	*	75	18	5	*	*	*	2	*	*	*	*	*	
12.81				**100**	73.96	0.36	33	O-2	56	181	16	5	39	*	75	6	6	*	*	*	*	*	*	*	*	*	
12.78				**99**	74.99	0.53	35	O-2	40	230	13	2	35	1	40	10	3	*	*	*	*	*	*	*	*	*	
12.75				**98**	77.11	0.40	44	O-2	35	201	10	5	30	3	56	17	1	1	*	*	2	*	*	1	*	*	
12.72			111e	**97**	75.16	0.44	28	O-2	31	200	6	9	35	1	62	10	5	1	*	*	*	*	*	*	*	*	
12.69				**96**	71.21	0.62	20	O-2	43	182	19	5	45	*	60	7	9	*	*	*	3	*	*	*	1	*	
12.66				**95**	70.38	0.50	17	O-2	55	181	18	5	44	3	55	23	4	*	*	*	3	*	*	*	*	*	
12.63				**94**	69.01	0.56	20	O-2	46	181	5	7	42	*	55	14	11	*	*	*	1	1	*	*	*	*	
12.60				**93**	66.89	0.74	18	O-2	40	168	14	6	36	2	63	24	18	*	*	*	*	*	*	*	*	*	
12.57				**92**	66.18	0.63	17	O-2	49	218	15	11	48	3	59	23	17	1	*	*	2	*	*	*	*	*	
12.54				**91**	63.98	0.98	19	O-2	43	186	22	7	42	1	43	8	18	*	*	*	*	*	*	*	*	*	
12.51				**90**	52.65	1.39	16	O-2	36	180	13	8	34	*	70	8	12	*	1	1	*	*	*	*	*	*	
12.48			111d	**89**	52.47	1.78	15	O-2	34	185	20	7	44	1	80	5	17	*	2	*	*	*	*	*	*	*	
12.45				**88**	53.58	2.23	13	O-2	26	169	26	6	36	3	61	6	11	*	*	*	*	*	*	1	*	1	
12.42				**87**	64.72	0.93	9	O-2	28	180	13	8	33	1	80	4	17	*	*	*	*	*	*	*	*	*	
12.39				**86**	68.08	0.86	16	O-2	15	194	12	3	24	2	63	2	6	*	*	*	*	*	*	*	*	*	
12.36			111c	**85**	71.43	0.37	17	O-2	28	211	12	3	23	2	67	8	7	*	*	*	*	*	*	*	*	*	
12.33				**84**	71.76	0.56	17	O-2	32	208	12	3	24	5	53	3	9	1	2	*	2	*	*	*	1	1	
12.30				**83**	65.81	0.67	16	O-2	15	215	4	6	29	3	66	6	10	1	*	2	*	*	*	*	*	*	
12.27				**82**	61.11	1.02	15	O-2	20	195	17	4	21	1	80	6	12	*	*	*	*	*	*	*	*	2	
12.24				**81**	58.78	0.95	12	O-2	25	199	11	13	21	1	72	11	9	1	*	*	1	*	*	*	*	*	
12.21				**80**	54.75	1.15	9	O-2	23	193	20	15	28	2	65	9	9	*	*	*	*	*	*	*	*	*	
12.18				**79**	52.96	1.43	8	O-2	36	159	26	10	28	*	77	8	7	*	*	*	*	*	*	*	*	*	
12.15				**78**	55.41	1.32	12	O-2	34	159	28	12	27	*	67	4	13	*	*	*	*	*	*	1	*	*	
12.12				**77**	57.80	1.30	11	O-2	33	180	29	4	36	*	71	8	6	*	*	1	*	*	*	*	*	*	
12.09			111b	**76**	61.71	0.97	9	O-2	28	182	18	10	28	*	77	4	5	*	*	*	*	*	*	*	*	*	
12.06				**75**	63.81	1.27	9	O-2	22	181	21	7	26	*	82	6	6	*	*	*	*	*	*	*	*	*	
12.03				**74**	65.01	0.88	10	O-2	24	198	15	12	21	*	58	9	8	*	*	*	*	*	*	*	*	*	
12.00				**73**	66.06	0.72	11	O-2	27	185	27	14	39	*	84	15	8	*	*	*	*	*	*	1	*	*	
11.97				**72**	65.08	0.66	9	O-2	29	186	14	19	37	1	57	7	13	*	*	*	*	*	*	*	*	1	
11.94				**71**	61.51	1.13	11	O-2	27	190	22	7	30	*	71	5	9	*	*	*	*	*	*	*	*	1	
11.91				**70**	62.91	1.01	12	O-2	28	177	17	14	39	1	55	3	19	*	*	*	*	*	*	*	*	*	
11.88				**69**	64.54	1.00	11	O-2	32	195	14	7	19	1	57	6	13	*	*	*	*	*	*	*	*	*	
11.85				**68**	66.85	0.81	8	O-2	20	197	20	12	31	*	63	10	13	*	*	*	*	*	*	*	*	*	
11.82				**67**	67.77	0.66	16	O-2	28	199	6	7	20	*	88	7	5	*	*	*	*	*	*	*	*	*	
11.79				**66**	68.80	0.57	13	O-2	22	218	15	8	22	*	77	7	9	*	*	*	*	*	*	*	*	*	
11.76			111a	**65**	70.42	0.50	15	O-2	25	226	10	2	26	*	57	10	11	*	*	*	*	*	*	*	*	*	
11.73				**64**	70.75	0.39	24	O-2	28	194	7	11	15	1	73	4	2	*	*	*	*	*	*	*	*	*	
11.70				**63**	70.59	0.49	16	O-2	35	191	23	11	40	*	76	3	13	*	1	*	*	*	*	*	*	*	
11.67				**62**	70.58	0.68	14	O-2	20	210	11	6	15	*	75	4	7	*	*	*	1	*	*	*	*	*	
11.64				**61**	72.08	0.44	20	O-2	17	191	14	13	13	*	81	6	4	1	*	*	*	*	*	*	*	*	
11.61				**60**	69.48	0.59	14	O-2	6	194	15	4	5	*	99	3	4	*	*	*	*	*	*	*	1	*	
11.58				**59**	68.36	0.54	12	O-2	3	193	19	12	5	*	115	9	7	*	*	*	*	*	*	*	*	*	
11.55				**58**	54.46	1.34	8	O-2	3	137	8	8	4	*	141	9	11	*	*	*	*	*	*	*	*	*	
11.52				**57**	49.26	2.02	13	O-2	1	170	14	21	4	*	122	6	10	1	*	*	*	*	*	*	*	1	
11.49				**56**	46.69	2.73	10	O-2	2	168	18	13	2	*	129	6	13	*	*	*	*	*	*	*	*	1	
11.46				**55**	43.52	3.59	13	O-2	2	169	21	7	1	*	98	2	14	*	*	1	3	*	*	*	*	*	
11.43				**54**	43.49	4.82	12	O-2	1	118	10	14	1	*	157	11	20	*	1	*	*	*	*	*	*		
11.40				**53**	41.83	4.07	13	O-2	1	105	22	12	2	*	163	16	8	*	1	*	*	*	*	*	*		
11.37				**52**	41.97	4.02	19	O-2	1	101	26	13	3	*	152	4	20	*	1	*	*	*	*	*	*		
11.34				**51**	42.83	3.63	19	O-2	6	120	30	21	5	*	199	19	25	*	4	*	*	*	*	*	*		
11.31				**50**	42.08	3.46	16	O-2	6	118	37	27	6	*	150	10	21	*	2	*	*	*	*	*	*		
11.28				**49**	43.17	3.09	12	O-2	14	116	32	11	17	*	133	4	14	*	4	*	*	*	*	*	*		
11.25				**48**	42.20	2.83	10	O-2	24	97	36	27	14	*	116	3	20	*	*	*	*	*	*	*	*		
11.22				**47**	45.30	2.57	12	O-2	33	124	50	31	18	1	117	19	13	*	1	1	*	*	*	*	*		
11.19				**46**	43.91	2.60	16	O-2	39	96	37	21	28	*	119	13	12	*	1	*	*	*	*	*	*		
11.16				**45**	47.45	2.93	14	O-2	47	120	51	14	23	*	115	14	4	*	1	*	*	*	*	*	1		
11.13				**44**	47.95	2.69	14	O-1	19	143	32	20	18	1	118	13	6	*	3	*	*	*	1	*	*		
11.10				**43**	48.03	2.40	11	O-2	24	148	44	18	26	*	85	12	13	*	*	*	*	*	*	*	*		
11.07			110b	**42**	42.97	3.44	15	O-2	26	95	37	24	30	*	123	25	15	*	2	*	*	*	*	*	*		
11.04				**41**	40.95	4.17	19	O-2	36	105	33	7	36	*	111	15	8	*	3	*	*	*	*	*	*		
11.01				**40**	39.33	3.97	16	O-2	23	104	47	19	15	*	149	16	10	*	2	*	*	*	*	*	*		
10.98				**39**	39.01	3.64	16	O-2	12	98	32	19	12	*	131	7	9	*	*	1	*	*	*	*	*		
10.95				**38**	38.77	3.35	17	O-1	19	106	49	37	20	*	153	12	8	*	*	*	*	*	*	*	*		
10.92				**37**	37.71	2.83	21	O-2	27	84	41	29	20	*	128	17	8	*	1	2	*	*	*	*	*		
10.89				**36**	37.56	2.77	16	O-2	27	63	55	29	38	*	146	10	16	*	3	*	*	*	*	*	1		
10.86				**35**	43.99	2.49	14	O-1	22	50	38	23	29	*	164	14	16	*	1	*	*	*	*	*	*		
10.83				**34**	46.93	2.55	21	O-2	30	33	47	37	20	*	142	12	20	*	3	1	*	*	*	1	*		
10.80				**33**	51.14	1.91	17	O-2	39	58	52	31	25	*	112	16	32	*	4	1	*	*	*	1			
10.77				**32**	50.07	2.01	23	O-2	46	57	47	11	31	1	153	21	19	*	*	*	*	*	*				
10.74				**31**	44.91	2.79	28	O-2	81	50	48	14	32	*	139	16	23	*	1	*	*	*	*				
10.71				**30**	45.39	3.05	18	O-2	50	47	64	17	64	*	120	40	22	*	3	*	*	*	1				
10.68				**29**	45.52	3.26	20	O-2	50	37	44	17	53	1	106	9	38	*	5	*	*	1					
10.65				**28**	39.16	5.88	22	O-2	28	37	34	20	43	1	150	19	40	*	1	*	*						
10.62				**27**	39.62	4.47	29	O-2	75	61	55	10	31	*	160	39	28	*	3	*	*						
10.59				**26**	35.33	3.81	19	O-2	42	46	48	42	28	1	151	25	27	*	1	*	*						
10.56				**25**	40.04	2.58	15	O-2	42	51	56	28	35	1	142	11	13	*	*	*	*						
10.53				**24**	51.33	1.32	20	O-1	44	51	64	24	36	*	131	17	16	*	1	1	*						
10.50				**23**	52.20	1.37	29	O-2	65	95	54	10	29	*	120	21	17	*	*	*	*						
10.47				**22**	54.23	1.26	25	O-2	48	90	53	14	21	1	109	19	14	*	*	*	*						
10.44			110a	**21**	55.34	1.26	13	O-2	32	81	49	22	22	2	117	22	17	*	*	*	1						
9.57				**20**	37.38	3.80	38	O-2	74	48	44	39	52	1	94	23	21	1	*	2	2						
7.26				**19**	34.12	3.78	17	O-1	30	23	26	41	42	*	138	16	34	*	*								
4.83				**18**	39.00	3.31	22	O-2	52	20	88	29	65	1	102	26	11	*	1								
2.55				**17**	39.95	4.72	28	O-2	16	27	1	20	32	*	209	35	24	*	2								
2.37				**16**	55.61	2.41	32	O-1	22	12	70	20	36	*	108		28	26	*								
2.34				**15**	59.98	1.63	31	O-1	18	9	78	19	37	*	110		33	14	*								
2.31				**14**	57.67	1.70	28	O-1	9	15	77	18	35	*	103		27	25	*								
2.28				**13**	56.21	2.45	25	O-1	22	28	38	25	43	*	103		18	45	*								
2.25				**12**	55.86	2.21	25	O-1	10	19	45	26	32	*	108		32	38	*								
2.22				**11**	54.90	2.84	27	O-1	18	18	68	18	38	*	94		26	38	*								
2.19				**10**	52.42	4.34	24	O-1	10	17	62	16	45	*	88		30	42	*								
2.16				**9**	45.46	2.18	23	O-1	20	17	88	9	48	*	86		22	50	*								
2.13				**8**	43.44	2.65	23	O-1	16	14	83	12	45	*	73		24	49	*								
2.10				**7**	45.32	3.03	25	O-1	13	11	83	11	53	*	76		18	48	*								
2.07				**6**	47.96	3.37	23	O-1	21	6	85	22	31	*	77		34	45	1								
2.04				**5**	50.33	3.09	26	O-1	32	18	75	20	24	*	94		28	41									
2.01				**4**	51.27	2.90	32	O-1	14	10	79	25	25	*	112		20	29									
1.98				**3**	54.62	3.22	31	O-1	12	20	70	18	28	*	117		33	14									
1.95				**2**	55.91	3.49	30	O-1	37	12	83	14	20	*	108		37	26									
0.21			104	**1**	61.93	1.20	19	O-2	17	24	12	50	57	5	145	80	22										

jamesoni *pars* | *polymorphus pars* | bayloni | 108 | data not collected | NJ3 | NJ4a *pars* | *S. cruciulus*

Metres	Ammonite zone											Bed	Sample	Wt%$CaCO_3$	Wt%TOC	Fields of view	Preservation	*M. elegans* spines	*C. crassus*	*C. pliensbachensis*	*C. primulus*	*M. elegans*	*M. lenticularis*	*P. liasicus distinctus*	*S. punctulata*	*T. patulus*	*P. robustus*	*O. hamiltoniae*	*P. liasicus liasicus*	*S. cruciulus*	*Stradnerlithus* sp.	*C. granulatus*	*Calyculus* sp.	*Solisasites* sp.	*B. prinsii*	Nannofossil zone
15,51													190	38,68	2,07	18	O-2	14	206	8	5	28	•	80	5	11	•	•	•	9	•	•	•	•	•	
15,48													189	49,97	0,66	18	O-2	17	220	3	8	8	•	60	4	7	•	•	•	10	•	•	•	•	•	
15,45													188	55,14	0,80	23	O-2	22	220	2	5	7	•	47	7	10	•	•	•	21	•	•	•	•	•	
15,42													187	59,62	0,62	18	O-2	6	234	•	4	10	•	37	1	16	•	•	•	8	•	•	•	•	•	
15,39													186	64,14	0,59	22	O-2	12	210	2	8	6	•	59	2	14	1	•	•	11	•	•	•	•	•	
15,36													185	67,55	0,59	37	O-2	15	271	4	12	12	•	67	1	12	1	•	•	7	•	•	•	•	•	
15,33													184	66,76	0,75	23	O-2	14	275	4	10	8	•	47	6	3	•	•	•	3	•	•	•	•	2	
15,30													183	70,12	0,51	14	O-2	9	240	1	3	6	•	44	9	6	•	•	•	1	•	•	•	•	•	
15,27													182	69,19	0,48	26	O-2	8	239	4	3	6	•	45	2	9	•	•	•	9	•	•	•	•	•	
15,24													181	59,82	0,61	22	O-2	11	207	4	2	6	•	57	•	18	3	•	•	13	•	•	•	1	1	
15,21													180	52,92	0,92	13	O-2	11	204	8	7	13	•	68	1	19	1	•	1	4	•	•	•	4	•	
15,18													179	44,35	1,75	13	O-1	9	216	8	11	23	•	37	4	11	•	1	•	4	•	•	•	•	1	
15,15													178	35,45	3,66	13	O-2	23	196	25	10	17	•	35	4	9	•	•	•	9	•	•	•	•	•	
15,12													177	46,85	1,90	16	O-2	22	216	21	2	11	•	66	4	19	•	•	•	8	1	1	•	•	•	
15,09													176	52,72	1,20	21	O-2	24	185	11	10	20	•	52	4	14	•	•	1	16	•	•	•	1	1	
15,06													175	59,32	0,99	20	O-2	22	189	2	4	28	•	54	2	17	•	•	•	9	1	•	•	•	2	
15,03													174	59,82	0,83	20	O-2	26	197	1	11	16	•	70	10	25	1	•	•	14	1	•	•	•	1	
15,00													173	66,87	0,55	33	O-2	42	221	1	10	18	•	42	3	22	•	•	•	15	•	•	•	•	•	
14,97													172	69,72	0,51	39	O-1	38	238	1	6	21	1	50	5	15	•	•	•	10	•	1	•	•	•	
14,94													171	70,90	0,40	42	O-2	28	211	2	8	22	•	44	4	11	•	•	•	4	•	•	•	2	•	
14,91													170	70,62	0,47	46	O-2	22	234	1	5	23	•	32	9	6	•	•	•	•	•	•	•	•	•	
14,88													169	69,84	0,40	49	O-2	27	206	2	6	20	•	57	2	9	•	•	•	11	•	•	•	•	•	
14,85													168	63,06	0,35	27	O-1	24	204	•	13	28	•	65	7	8	•	•	•	8	•	•	•	1	1	
14,82													167	60,81	0,45	30	O-1	29	203	6	8	26	•	70	4	10	1	•	•	5	•	2	•	•	•	
14,79													166	46,77	1,52	28	O-2	34	197	3	8	25	•	65	4	10	•	•	•	2	•	2	•	•	•	
14,76													165	39,97	1,96	18	O-2	44	200	2	11	33	•	88	3	18	•	2	•	4	•	•	1	•	•	
14,73													164	45,12	1,58	11	O-2	29	195	6	9	28	•	72	6	8	•	1	1	6	•	•	1	•	•	
14,70													163	52,15	0,92	11	O-1	18	223	8	21	11	•	50	6	12	•	2	2	10	•	•	•	•	•	
14,67													162	54,81	0,89	11	O-2	15	222	2	12	14	•	62	2	4	•	•	•	10	•	•	•	•	•	
14,64													161	59,92	0,63	15	O-2	9	236	2	14	14	•	50	12	12	•	•	•	2	•	•	•	•	•	
14,61													160	63,67	0,63	26	O-2	20	222	2	9	14	•	53	7	14	•	•	•	5	•	•	•	•	•	
14,58													159	65,70	0,52	22	O-2	19	201	3	8	32	•	60	4	6	•	•	•	3	•	•	•	•	•	
14,55													158	68,05	0,33	20	O-2	14	205	2	5	17	•	78	6	7	•	•	•	1	•	•	•	•	1	
14,52													157	66,02	0,47	26	O-2	35	197	9	9	27	•	60	24	11	•	•	•	2	•	•	•	•	•	
14,49													156	60,33	0,62	10	O-2	29	210	3	5	27	•	50	6	8	•	•	•	2	•	•	•	•	•	
14,46													155	47,23	1,45	18	O-2	73	146	21	12	57	•	69	23	11	•	1	1	2	•	•	•	•	•	
14,43													154	41,82	2,03	15	O-2	92	123	15	7	75	•	111	8	7	•	1	•	•	•	1	•	•	•	
14,40													153	40,37	2,25	11	O-2	70	93	7	10	86	•	100	16	7	•	•	•	1	•	•	•	•	•	
14,37													152	45,97	1,75	16	O-2	78	191	2	18	38	•	90	4	12	•	1	•	1	•	•	•	•	•	
14,34													151	47,62	1,22	15	O-2	46	197	3	20	49	•	77	4	15	•	4	•	•	•	•	•	•	•	
14,31													150	50,47	0,94	12	O-2	41	176	2	14	25	•	75	2	12	•	1	•	•	•	•	•	•	•	
14,28													149	52,02	0,80	13	O-2	30	182	4	22	43	•	77	18	8	•	3	•	•	•	•	•	•	•	
14,25													148	52,05	0,96	12	O-2	43	167	3	16	24	•	81	6	18	•	•	1	1	•	•	•	•	•	
14,22													147	47,92	1,50	16	O-1	60	159	7	26	42	•	82	10	23	•	5	•	•	•	•	•	•	•	
14,19													146	45,49	1,94	15	O-1	83	166	13	8	42	•	84	12	11	1	•	•	•	•	•	•	•	1	
14,16													145	42,25	1,81	20	O-2	68	137	7	10	50	•	82	10	19	•	8	•	•	•	•	•	•	•	
14,13													144	41,27	2,10	12	O-2	86	118	18	11	65	2	72	13	18	2	2	•	•	•	•	•	•	•	
14,10													143	38,11	2,48	19	O-2	101	92	17	11	75	•	96	22	21	•	9	•	•	•	•	1	•	•	
14,07													142	35,07	2,70	21	O-1	139	95	23	19	74	1	114	12	21	•	6	•	•	•	•	•	•	•	
14,04													141	37,02	2,30	30	O-1	131	74	23	7	87	•	98	11	20	1	•	•	•	•	3	•	•	•	
14,01													140	37,84	2,02	38	O-1	108	80	28	12	78	•	105	8	28	•	•	•	1	•	3	•	•	•	
13,98													139	39,79	1,83	33	O-1	88	98	17	11	66	•	96	17	18	1	1	•	•	•	3	•	•	•	
13,95													138	40,53	2,05	23	O-1	86	129	3	12	50	•	92	16	25	1	7	•	2	•	•	•	•	•	
13,92													137	40,47	3,54	34	O-1	63	133	6	5	42	•	106	15	39	•	•	•	•	•	•	•	•	•	
13,89													136	45,37	3,73	18	O-2	34	146		6	29	•	97	3	31	•	•	•	•	•	•	•	•	•	
13,86													135	47,40	2,12	15	O-2	37	235	1	7	27	•	47	4	12	•	•	•	•	•	1	•	•	•	
13,83													134	46,66	2,18	23	O-1	55	190	6	4	28	•	74	2	28	•	•	•	•	•	•	•	•	•	
13,80													133	44,82	2,76	18	O-2	56	110	4	•	42	•	109	11	38	•	•	•	•	•	•	•	•	•	
13,77													132	43,98	3,50	31	O-2	74	71	8	8	57	•	116	14	36	4	1	•	•	•	•	•	•	•	
13,74													131	41,63	4,59	29	O-2	58	54	4	2	64	•	159	12	33	•	•	•	•	•	4	•	•	•	
13,71													130	43,10	4,35	34	O-1	47	37	12	20	47	•	164	22	39	•	•	1	•	•	3	•	•	•	
13,68													129	39,37	3,86	22	O-1	60	45	28	10	49	2	144	6	37	•	1	•	•	•	•	•	•	•	
13,65													128	35,59	3,96	34	O-1	63	60	23	9	70	1	123	15	23	•	2	•	•	•	•	•	•	•	
13,62													127	39,92	2,92	25	O-1	30	97	21	12	45	1	136	6	22	•	2	•	•	•	1	•	•	•	
13,59													126	48,35	1,48	24	O-1	34	170	19	6	42	1	130	2	18	•	3	1	•	•	•	•	•	•	
13,56													125	54,13	1,05	22	O-1	34	162	24	9	33	•	74	4	6	•	•	•	•	1	•	•	•	•	
13,53													124	56,56	1,05	30	O-1	33	155	23	12	21	•	84	5	24	1	1	•	•	•	•	•	•	2	
13,50													123	56,61	0,93	13	O-1	24	89	37	22	46	•	94	29	10	•	•	•	2	•	•	•	•	1	
13,47													122	57,24	0,92	33	O-1	44	102	42	12	36	•	87	3	31	•	•	•	•	•	•	•	•	•	
13,44													121	50,59	1,37	19	O-2	36	87	28	24	34	•	121	16	27	•	5	•	3	•	•	1	•	3	
13,41													120	47,27	1,51	24	O-2	26	65	43	8	37	•	133	13	31	2	5	•	•	•	•	•	•	•	
13,38													119	40,08	2,04	27	O-2	34	90	46	19	24	•	114	21	29	•	3	•	•	•	•	•	•	•	
13,35													118	38,33	1,79	25	O-2	19	107	49	19	17	•	131	16	26	•	2	•	1	•	•	•	•	•	
13,32													117	42,02	1,47	22	O-1	26	120	50	15	14	•	80	23	29	•	4	1	•	•	•	•	•	1	
13,29													116	43,57	1,65	21	O-2	37	62	49	18	35	•	115	10	23	•	6	•	•	•	•	•	•	•	
13,26													115	47,91	1,22	26	O-2	30	122	35	11	25	•	91	15	20	2	1	•	•	•	•	•	•	•	
13,23													114	50,27	1,02	20	O-1	17	143	50	22	35	•	95	27	24	•	2	•	•	•	•	•	•	•	
13,20													113	55,37	0,74	25	O-2	25	164	17	8	23	•	82	7	18	•	•	1	•	•	•	1	•	1	
13,17													112	56,39	0,82	23	O-1	20	142	22	23	27	•	96	7	15	•	4	•	•	•	•	1	•	•	
13,14													111	57,79	1,07	20	O-1	46	164	20	10	46	•	87	16	10	•	2	•	•	•	•	•	•	•	
13,11													110	57,00	0,89	14	O-2	43	209	20	4	29	•	48	5	3	1	•	•	•	•	•	•	•	•	
13,08													109	57,31	0,77	18	O-1	54	175	21	15	43	•	79	16	11	•	•	•	•	•	•	•	•	2	
13,05													108	56,48	0,82	16	O-2	43	148	19	11	35	•	84	9	7	•	•	•	1	•	•	•	•	•	
13,02													107	53,21	0,83	15	O-1	41	182	6	13	40	1	73	13	9	•	•	•	1	•	•	•	1	2	
12,99													106	52,33	0,87	14	O-2	24	157	13	5	29	•	94	9	13	1	•	•	•	•	•	•	•	1	
12,96													105	52,08	0,89	16	O-2	28	142	13	9	42	•	106	14	7	•	•	2	•	•	•	•	•	•	
12,93													104	55,21	0,65	17	O-2	36	164	25	6	45	•	110	21	9	•	•	1	•	•	•	•	•	•	

Metres	Ammonite zone		Bed	Sample	Wt%$CaCO_3$	Wt% TOC	Fields of view	Preservation	*M. elegans* spines	*C. crassus*	*C. pliensbachensis*	*C. primulus*	*M. elegans*	*M. lenticularis*	*P. liasicus distinctus*	*S. punctulata*	*T. petulus*	*P. robustus*	*O. hamiltoniae*	*P. liasicus liasicus*	*S. cricutus*	*Stradnerithus* sp.	*C. granulatus*	*Calyculus* sp.	*Sollasites* sp.	*B. prinsii*	Nannofossil zone
23.46			120	266	27.90	3.54	35	O-1	93	12		31	203	1	42	31	12				1			1	2		NJ4b
22.80				265	29.36	5.62	25	O-1		52	1	26	•	•	58	36	8	4			154			1	3	1	
22.59				264	49.32	1.55	39	O-2	5	15	2	31	5	•	73	11	16	26			136			5	•	1	
22.56				263	45.59	3.25	25	O-1		17	1	31	1	•	63	36	10	22			166			4	•	•	
22.53				262	32.85	5.39	14	O-2		7	•	25	•	•	59	20	7	6			203			2	•	•	
22.50			119	261	40.22	6.02	21	O-2		15	7	47	•	1	75	35	2	21			177			5	•	•	
22.47				260	45.40	6.01	26	O-2	1	15	3	18	•	•	30	38	7	12			225		1	5	•	•	
22.44				259	46.21	5.59	25	O-2		28	3	44	1	•	77	35	14	33			198		•	1	•	•	
22.41				258	36.93	6.29	21	O-2		15	1	34	5	•	54	30	17	20		1	195		•	2	•	•	
22.38				257	37.37	5.54	18	O-2		71	5	53	2	•	52	24	6	24		1	202		•	•	•	•	
22.35				256	57.74	1.48	18	O-2		94	3	45	2	•	93	25	22	37		2	127		8	•	•	1	
22.32				255	44.83	3.29	12	O-1		155	3	27	3	•	57	23	29	24		4	150		3	•	2	•	
22.29				254	43.65	3.87	9	O-1	1	131	3	27	•	•	34	9	16	12		2	101		•	•	•	•	
22.26				253	47.92	2.97	12	O-2	1	128	1	20	•	•	40	8	28	10		•	91		2	•	•	•	
22.23				252	52.14	1.47	13	O-1		133	1	22	2	•	39	10	18	8	1	1	82		2	•	•	•	
22.20			118d	251	55.12	1.03	18	O-1		92	1	38	1	•	51	27	30	10	•	•	117	1	2	1	•	1	
22.17				250	58.37	1.08	26	O-2		47	•	42	3	•	51	16	26	11	•	•	132	•	4	1	2	1	
22.14				249	59.49	1.11	22	O-1	1	64	3	28	4	•	65	35	19	13	•	2	113	•	1	1	3	6	
22.11				248	50.99	1.87	19	O-2	2	66	•	45	2	•	40	18	24	10	•	•	119	•	1	3	1	1	
22.08				247	48.14	1.93	16	O-2	1	88	4	28	7	•	85	18	35	11	•	•	96	1	4	•	2	•	
22.05				246	50.66	1.89	16	O-2		96	•	37	3	•	43	19	37	15	•	•	76	•	•	•	2	•	
22.02				245	57.19	1.40	10	O-2	1	164	4	32	6	•	88	21	34	17	•	•	51	•	•	•	1	•	
21.99				244	57.36	1.49	10	O-2		105	4	45	3	•	82	17	26	26	•	1	67	•	6	•	1	•	
21.96				243	45.30	2.19	14	O-2		48	3	26	5	•	76	11	28	24	•	•	119	•	2	•		1	
21.93				242	43.54	2.17	10	O-1		37	2	38	1	•	74	37	21	24	•	1	97	•	4	•	2	•	
21.90				241	41.69	2.14	19	O-2	1	56	3	30	5	•	57	28	24	19	•	•	136	•	•	•	•	•	
21.87				240	38.03	2.64	10	O-2	1	48	2	30	1	•	52	12	24	20	•	•	166	•	1	1	•	•	
21.84				239	42.03	1.90	13	O-2	1	43	2	39	•	•	36	13	22	19	•	1	166	•	2	•	•	•	
21.81				238	45.62	1.75	14	O-1	1	57	5	53	10	•	89	21	31	20	•	•	125	•	7	•	•	1	
21.78			118c	237	48.67	1.53	16	O-2		52	3	51	8	•	105	22	39	17	•	•	160	1	5	•	2	1	
21.75				236	45.53	1.72	22	O-1	2	49	5	35	9	•	63	19	9	22	•	•	135	•	2	1	1	•	
21.72				235	30.14	2.64	15	O-2		58	11	20	•	•	84	12	26	6	•	2	126	•	3	•	1	•	
21.69				234	33.99	2.28	9	O-2		29	6	51	1	•	83	12	38	9	2	2	109	•	9	•	•	•	
21.66				233	39.57	1.97	11	O-1		36	11	26	1	•	56	10	40	13	•	2	113	•	•	•	3	•	
21.63				232	44.77	1.90	17	O-1	4	41	4	30	5	•	67	17	59	18	•	•	102	•	•	•	1	•	
21.60				231	41.34	1.85	11	O-1	1	67	3	42	3	1	68	14	41	14	1	•	98	•	3	•	•	2	
21.57				230	35.63	2.30	13	O-2	1	66	7	37	3	1	44	4	16	11	•	•	136	•	1	•	1	•	
21.54				229	36.98	2.21	10	O-1	1	25	8	39	13	1	85	12	15	15	•	•	142	•	•	•	•	•	
21.51			118b	228	43.72	1.76	15	O-1	2	31	1	28	14	3	66	16	38	17	•	1	165	•	1	•	•	2	
21.48				227	47.92	1.55	9	O-1		23	•	42	16	2	66	26	15	14	•	2	146	•	•	•	1	•	
21.45				226	51.76	1.46	28	O-2		78	5	40	1	•	96	25	19	60	•	•	138	•	•	•	•	•	
21.42			118a	225	51.97	1.48	15	O-2	1	47	5	21	•	•	55	17	16	27	1	•	132	•	1	2	1	•	
20.40				224	36.17	3.36	9	O-2	5	251	•	6	8	•	21	1	5	1	1	•	21	•	•	•	•	•	
19.20			116	223	44.32	2.21	7	O-2	7	254	3	4	14	1	38	5	11	2	•	•	26	•	•	•	•	•	
17.88			115	222	45.83	1.57	15	O-2	29	231	18	9	22	•	33	12	•	3	•	•	17	•	•	•	•	•	
16.77				221	43.01	2.61	22	O-1	15	146	24	18	16	•	57	23	8	8	•	•	38	•	•	1	•	•	
16.41				220	58.00	0.70	19	O-2	15	199	12	8	10	•	50	7	18	1	•	•	24	•	•	•	•	•	
16.38				219	56.04	1.10	22	O-2	22	144	15	9	19	•	71	7	13	•	•	•	32	•	•	•	•	1	
16.35				218	49.96	1.45	25	O-1	25	144	13	18	28	•	62	9	24	•	•	•	29	•	•	•	•	•	
16.32				217	41.72	2.43	25	O-1	42	158	16	10	29	•	57	6	10	•	•	•	27	1	•	•	•	1	
16.29				216	37.42	5.13	27	O-2	57	109	33	12	56	•	61	10	8	•	•	•	31	•	•	•	•	1	
16.26				215	31.85	5.21	19	O-2	50	133	28	12	54	•	56	14	15	2	•	•	19	•	•	•	•	1	
16.23				214	37.27	2.35	13	O-2	25	198	5	7	35	•	52	6	7	•	1	•	13	•	•	•	•	1	
16.20				213	39.32	1.91	17	O-2	22	238	2	7	17	•	43	6	7	•	•	•	8	•	•	1	•	1	
16.17				212	51.01	1.04	20	O-2	24	223	10	11	20	•	39	12	6	•	•	•	22	•	•	•	•	1	
16.14				211	52.64	0.94	23	O-2	29	203	13	7	20	•	47	5	6	•	•	•	17	•	•	•	•	•	
16.11				210	54.95	0.90	24	O-2	33	157	20	7	36	•	73	6	15	•	•	•	14	•	•	•	•	•	
16.08				209	50.67	1.44	21	O-1	46	160	28	15	51	•	73	3	17	•	•	•	26	•	•	•	1	•	
16.05				208	42.22	2.46	23	O-2	53	89	44	15	52	•	75	7	7	•	2	•	17	•	•	•	3	•	
16.02				207	38.70	2.83	39	O-1	77	86	67	14	61	•	85	14	6	•	2	•	10	•	•	•	•	•	
15.99			114	206	39.60	2.29	30	O-1	41	69	36	13	44	•	114	19	11	•	4	•	21	•	•	1	•	•	
15.96				205	39.94	2.46	25	O-2	40	72	52	16	54	•	98	18	10	•	1	•	2	•	•	•	•	•	
15.93				204	41.95	1.97	32	O-2	42	138	41	21	33	•	71	14	6	•	4	•	8	•	•	•	•	•	
15.90				203	46.28	1.83	38	O-1	40	118	16	15	28	•	97	17	9	1	2	1	17	•	•	•	•	•	
15.87				202	46.44	1.87	42	O-1	38	86	20	23	27	•	92	11	20	•	8	•	36	•	•	•	•	•	
15.84				201	48.42	1.76	44	O-2	49	151	20	22	45	•	134	21	25	2	5	•	24	•	•	•	•	•	
15.81				200	53.14	1.24	41	O-2	57	138	3	11	33	•	73	5	22	•	2	•	24	•	•	1	•	•	
15.78				199	53.82	0.96	39	O-1	42	132	7	14	20	•	73	16	22	•	2	•	21	•	1	•	1	•	
15.75				198	49.41	1.23	18	O-1	24	151	5	13	21	•	94	23	16	•	•	•	9	•	•	3	•	•	
15.72				197	45.95	1.51	37	O-2	37	161	3	10	28	•	85	11	16	•	2	•	12	•	•	•	•	•	
15.69				196	43.47	1.68	32	O-2	43	160	8	9	32	•	74	13	21	•	•	•	18	•	•	•	•	•	
15.66				195	40.02	1.90	30	O-1	41	205	9	2	26	•	54	24	8	•	1	•	4	•	•	1	•	•	
15.63				194	32.36	2.78	25	O-1	39	188	1	10	27	•	66	7	8	•	5	•	1	1	•	•	•	•	
15.60				193	31.53	3.15	14	O-2	41	207	4	3	31	•	43	4	13	•	•	•	3	•	•	•	•	•	
15.57				192	30.08	3.11	20	O-1	31	207	8	8	44	•	81	5	19	1	1	•	1	•	•	•	•	•	
15.54				191	35.72	2.53	16	O-2	36	193	17	8	27	•	53	3	15	•	1	•	1	•	•	•	•	•	

Ibex: jamesoni pars; brevispina pars; jamesoni; valdani; masseanum

NJ4a pars

P. robustus & *C. pliensbachensis*

Appendix 5

Biostratigraphy of the Belemnite Marls

Introduction and methods

In addition to the time series, the entire thickness of the Belemnite Marls was sampled for biostratigraphic purposes. Samples were collected at *ca.* 2m intervals from the lower and middle parts of the formation. A sampling interval of *ca.* 1m was applied to the upper interval (Bed 114 and above), compensating for the decreased sedimentation rate (Weedon & Jenkyns 1999) and maximising the chances of detecting nannofossil subzone NJ4b (Bown & Cooper 1998) within the condensed ibex AZ. Samples were collected from dark marl horizons, as species diversity is higher here than in the light marls (Section 4.3.2); the accuracy of establishing the stratigraphic ranges of taxa was thus optimised. Marker species inceptions/extinctions were confirmed by additional traverses of slides made from horizons below/above. The data are interpreted using the most recent nannofossil zonation scheme available (Bown & Cooper 1998; Fig. A5.1).

Results

The abundance and diversity of well-preserved nannofossils throughout the Belemnite Marls allows a useful nannofossil stratigraphy of the formation to be established (Table A4.1). The lower part of the formation, from the basal beds (as represented by Bed 103) to Bed 110a, falls within nannofossil zone (NZ) NJ3. This is based on the presence of *Crepidolithus crassus* and the absence of *Similiscutum cruciulus*. The presence of *Orthogonoides hamiltoniae* supports this interpretation (its absence in the basal beds is probably an artefact of its rarity throughout the formation).

The remaining beds (110a-121) are assigned to NJ4, based on the presence of *Similiscutum cruciulus* and the absence of *Lotharingius hauffii* and *Biscutum finchii*. This interval may be divided into NJ4a & b, using the LO of

Parhabdolithus robustus in Bed 119. Supporting evidence for the presence of NJ4a is the FO of *Bussonius prinsii*, which originates in this subzone (at least in the Tethyan Realm; de Kaenel *et al.* 1996). The LO of *Crepidolithus pliensbachensis*, which approximates the base of NJ4b, does indeed coincide here with that of *Parhabdolithus robustus*.

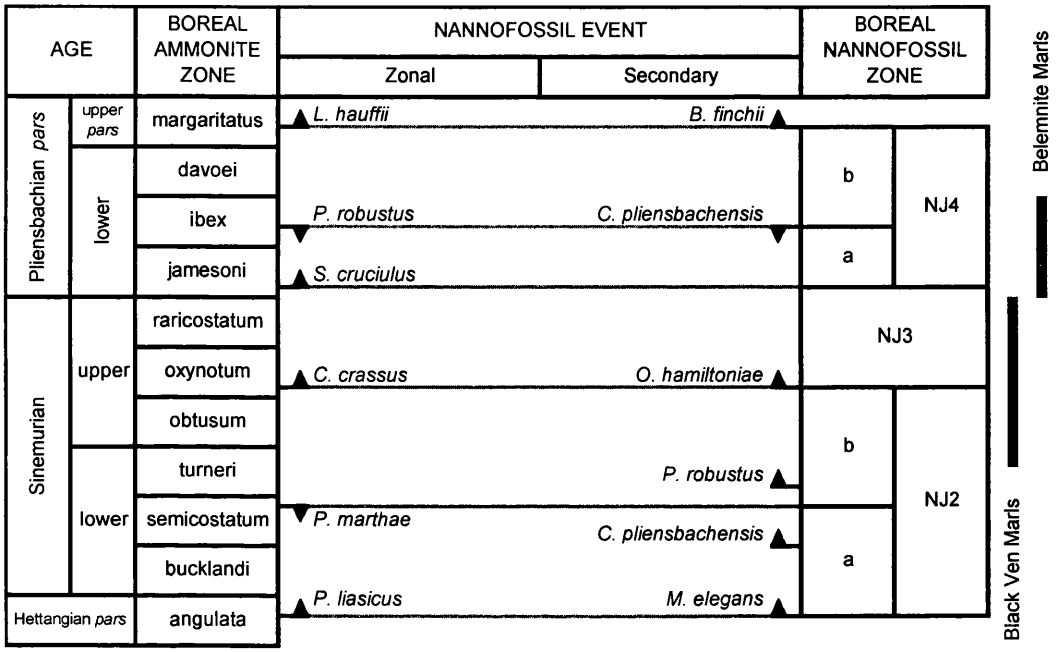

Fig. A5.1 Biostratigraphic events and zones discussed in relation to the Belemnite Marls and the Black Ven Marls. The intervals represented by the Belemnite Marls and the Black Ven Marls are indicated. ▲ = first occurrence; ▼ = last occurrence. Modified from Bown & Cooper (1998)

Discussion

This nannofossil stratigraphy of the Belemnite Marls is consistent with the ammonite stratigraphy of Palmer (1972). It also essentially concurs with the most recent nannofossil studies of the formation (Bown *in* Lord & Bown 1987; Crux 1987a; Turner 1997), with the exception of the following points: (1) Both Crux and Turner place the FO of *Similiscutum cruciulus* (Crux's *Biscutum dubium*; Turner's *B. ellipticum*) lower in the formation. The rarity of this species early in its range makes this event hard to place with confidence. (2) Both Bown and Crux found rare *Parhabdolithus robustus* (Crux's *P. zweilii*) in formations overlying the Marls. This is likely to represent reworking/contamination/misidentification, as the LO of this species is now recognised as a marker event within the ibex AZ

(which does not extend above the Belemnite Marls). Futhermore, Crux records *P. robustus* as rare in Bed 118, whereas the present study finds this species to be common/abundant on his scale in all samples from this horizon. Crux's abundance estimates and range for this species may reflect confusion between this taxon and *P. liasicus distinctus*, which looks somewhat similar when very overgrown. (3) Crux did not record the LO of *Crepidolithus pliensbachensis* within the Marls, probably because the uppermost horizon he sampled is lower than that examined here. However, his observation that this species does not range into the overlying formation supports the present study in its assertion that subzone NJ4b is represented by the uppermost Belemnite Marls. (4) Crux records the (sometimes 'abundant') presence of *C. cavus* in all of his Belemnite Marls samples. This species was not encountered in the present study. Bown (1987) considers claims for such early occurrences as spurious, due to contamination/misidentification. In this instance the latter seems likely. If it is assumed that all specimens assigned by Crux to *C. cavus* are in fact *C. crassus* (a species displaying considerable morphological variation; Bown 1987), this would explain his assertion that *C. crassus* is normally 'rare' in the Belemnite Marls (it is essentially always common, and often the dominant species). (5) The presence of *Orthogonoides hamiltoniae* in the Belemnite Marls is not recorded by Crux. This may be because this species was erected only several years before his study, and is rare in this formation (it does not preserve well and is generally rare in Boreal sediments; Bown pers. comm. 2000). (6) *Zeugrhabdotus erectus* was not encountered during this study. The FO of this species is controversial; whilst Crux (1987a) places it in the late Toarcian, Bown & Cooper (1998) tentatively locate it in the early Pliensbachian. Specimens were observed in the Belemnite Marls by Turner.

In general, the limited differences between the results of these studies demonstrate the advantages of high-resolution sampling (Crux sampled only 8 horizons within the Belemnite Marls, whilst Turner sampled 25) and large population counts (neither Crux nor Turner discuss their methods in detail, but it is likely that fewer specimens were observed per sample). As a whole, these results affirm that the lower Pliensbachian of the Boreal Realm is reasonably well-divided using nannofossil events (although nannofossils do not provide the biostratigraphic resolution that ASZs (not discussed here) allow).

In addition, it is worth noting the relationships between the following observations of Bown *et al.* (1988) and those of the present study: (1) Bown *et al.* note that (a) *Parhabdolithus robustus* enjoys its most consistent and abundant distribution within NJ4a, (b) *Schizosphaerella punctulata* is an important component of Lower Jurassic assemblages, (c) the Early Jurassic nannoplankton were essentially cosmopolitan in distribution, although *Mitrolithus jansae* (the dominance of which is a striking feature of Tethyan assemblages of Sinemurian to Toarcian age) is rarely observed in higher latitudes, and the endemic Tethyan Mazaganellaceae are not found in the Boreal Realm below the uppermost Toarcian (having first appeared in the Sinemurian Tethys). All these observations are supported by the present study. (2) Bown *et al.* found *Crepidolithus granulatus* to be associated with NJ4b. This species was not observed within this subzone in the Belemnite Marls, although this may be due to limited sampling of this interval on account of its poor representation within the section, and/or palaeobiogeography (this species is much more common in coeval Portugese sediments; Bown pers. comm. 2000).

Finally, the following observations are of interest: (1) The FO of *Similiscutum cruciulus* represents the origin of the Biscutaceae. This is a distinctive and significant bioevent (Bown & Cooper 1998), as it records the appearance of the placolith morphology (coccoliths with two sub-horizontal shields, separated by a tube) in the Boreal Realm, radically different in appearance to the muroliths (coccoliths with a wall-like, sub-vertical rim) which characterise all earlier coccolith assemblages. *S. cruciulus* begins to dominate numerically in the upper part of the Belemnite Marls (a significant increase of this species within the ibex AZ has also been noted by Perilli in the Tudanca and Santotis sections (Basque-Cantabrian area, northern Spain; pers. comm. 2000); it may be that this represents a biostratigraphically useful event). Placoliths have essentially been the dominant component of coccolith assemblages ever since. (2) The appearance of *Calyculus* in the Belemnite Marls is essentially coeval with that of *Sollasites*, whilst it is believed that the latter taxon is ancestral to the former (Crux 1987b). The ranges of these taxa as observed here may be an artefact of their rarity. (3) *Mitrolithus lenticularis* has been described as predominantly Tethyan in distribution (e.g. Bown & Cooper 1998). This is supported by the present study, where this taxon was found to be rare. (4) Holococcoliths are coccoliths constructed from minute,

simple equidimensional crystallites, as opposed to the elaborate and variably-shaped crystal units of heterococcoliths. The earliest holococcoliths yet discovered date from the Pliensbachian (Bown 1993), and it is thought that they have been produced since the inception of coccolithophorid biomineralisation (based on phylogenetic evidence; Young pers. comm. 2000); they represent a significant component of modern surface-water assemblages. However, none have ever been described from the Belemnite Marls. This is probably due to the low preservation potential of holococcoliths, as their crystallite components are susceptible to disaggregation. As such their fossil record is sparse, and their Early Jurassic representatives were only preserved in exceptional Lagerstätte-type deposits. It is likely that at least a small fraction of the microcarbonate in any heterococcolith-bearing sediment was cryptogenically sourced from holococcoliths. (5) No coccospheres have been described from the Belemnite Marls. Most early Pliensbachian taxa were muroliths; typically, muroliths do not interlock efficiently, and coccospheres constructed in this fashion disintegrate soon after death (although partial murolith coccospheres have been observed from the Jurassic; Rood *et al.* 1971). *Similiscutum cruciulus*, the single taxon bearing interlocking placoliths that is common in the Belemnite Marls, may have been too small to withstand disaggregation. Monospecific clusters of coccoliths representing collapsed murolith coccospheres are sometimes found in Jurassic sediments (e.g. Bown 1993); these were not observed in the Belemnite Marls, perhaps due to the extensive bioturbation of the sediments.

Appendix 6

Oxford Clay Taxonomic List

All nannofossil taxa encountered during this study of the Oxford Clay are listed below, and discussed where necessary. Figure numbers refer to this thesis.

Anfractus harrisonii Medd 1979

Axopodorhabdus atavus (Grün *et al.* 1974) Bown 1987

A. cylindratus (Noël 1965) Wind & Wise *in* Wise & Wind 1977

Biscutum constans (Górka 1957) Black *in* Black & Barnes 1959 (Fig. 5.6)

B. dorsetensis (Varol & Girgis 1994) Bown & Cooper 1998

Bussonius prinsii (Noël 1973) Goy 1979

Calyculus Noël 1973

***Calyculus* sp.**

Carinolithus magharensis (Moshkovitz & Ehrlich 1976) Bown 1987

Crepidolithus crassus (Deflandre 1954) Noël 1965

C. granulatus Bown 1987

C. perforata (Medd 1979) Grün & Zweili 1980

Crucirhabdus primulus Rood *et al.* 1973

Cyclagelosphaera Noël 1965

Morphotypes previously assigned to *C. tubulata* (Grün & Zweili 1980) Cooper 1987 are thought to be *Cyclagelosphaera* protococcoliths (Fig. 5.6; Lees Burnett *et al.* in prep.). The specimens observed most likely represent *C. margerelii*, as no other species in this genus was observed in the Oxford Clay. These protococcoliths are easily distinguished from their fully-formed counterparts on the basis of the central area, which is open in the former and closed in the latter.

Cyclagelosphaera margerelii Noël 1965 (Fig. 5.6)

Some *Cyclagelosphaera* specimens observed here are larger and thicker than 'classic' *C. margerelii* (this large morphotype is the *Cyclagelosphaera* sp. 1 of Bown *in* Martill *et al.* (1994); Bown pers. comm. (1999)). However, given an apparent spectrum of size variability in these and other members of the Watznaueriaceae, together with a lack of other morphological differences, these were included under *C. margerelii* in the present study.

Discorhabdus striatus Moshkovitz & Ehrlich 1976

Ethmorhabdus gallicus Noël 1965

Lotharingius crucicentralis (Medd 1971) Grün & Zweili 1980

Mitrolithus elegans Deflandre *in* Deflandre & Fert 1954

M. jansae (Wiegand 1984b) Bown *in* Young *et al.* 1986

Octopodorhabdus decussatus (Manivit 1961) Rood *et al.* 1971

Parhabdolithus liasicus distinctus Bown 1987

P. marthae Deflandre *in* Deflandre & Fert 1954

Podorhabdus grassei Noël 1965

Polypodorhabdus escaigii Noël 1965

Pseudoconus enigma Bown & Cooper 1989b

Retecapsa incompta Bown 1987

Schizosphaerella punctulata Deflandre & Dangeard 1938 (Fig. 5.6)

Staurolithites leptostaurus (Cooper 1987a) Bown & Cooper 1998 (Fig. 5.6)

S. quadriarculla (Noël 1965) Wilcoxon 1972

Stephanolithion bigotii bigotii Deflandre 1939 (Fig. 5.6)

S. bigotii maximum Deflandre 1939 (Fig. 5.6)

S. hexum Rood & Barnard 1972 (Fig. 5.6)

Triscutum Dockerill 1987

?*Triscutum* sp.

A single specimen of ?*Triscutum* bearing an axial cross in its central area was observed. An axial cross is not known to be characteristic of any species in this genus.

T. beaminsterensis Dockerill 1987

T. expansus (Medd 1979) Dockerill 1987

Tubirhabdus patulus Rood *et al.* 1973

The large, thick coccolith rim and enlarged spine girth of specimens observed here are characteristic of the modified morphotype of this species that appeared in the Middle Jurassic (Bown & Cooper 1998; Bown pers. comm. 2000).

Watznaueria Reinhardt 1964

Although it is possible to recognise *Watznaueria* coccospheres in the LM (Fig. 5.6), species identification is often problematic due to the difficulty of resolving small-scale morphological features on the surface of such thick particles. *Watznaueria* coccospheres were thus excluded from routine population counts (this also prevented over-representation of *Watznaueria* coccolith abundances, as this genus is frequently represented by intact coccospheres (Appendix 8), each of which contain numerous liths).

Watznaueria protococcoliths have been identified as such by Young & Bown (1991) and Lees Burnett *et al.* (in prep.). Most lack developed morphological features and cannot be assigned to species. Exceptional are those with an incomplete bar in the central area, which must belong to *W. britannica* (Fig. 5.6).

Watznaueria barnesae (Black *in* Black & Barnes 1959) Perch-Nielsen 1968 (Fig. 5.6)

W. britannica (Stradner 1963) Reinhardt 1964 (Fig. 5.6)

This species is very variable in size and central area morphology in the Oxford Clay, ranging from very small (several microns) with a small central area filled by the bar, to

medium/large (e.g. 7 or 8μm) with a large central area spanned by the bar. It has been suggested that such large specimens (as observed in Kimmeridgian sediments) represent a distinct population (Lees Burnett *et al.* in prep.); however, the apparently continuous spectrum of variability in size observed in this study may be the result of intra-species variation. Rarely, specimens possess a bar which bifurcates at both ends. These are thought to represent a late stage of *W. britannica* coccolithogenesis (Lees Burnett *et al.* in prep.).

W. fossacincta (Black 1971) Bown *in* Bown & Cooper 1989 (Fig. 5.6)

Late growth stages of *W. fossacincta* are not easily discerned from fully formed coccoliths, on account of the variable size of the central area in relation to the coccolith rim which characterises this species. Count data may thus include some protococcoliths and marginally over-represent the abundance of this taxon.

W. manivitiae Bukry 1973

Zeugrhabdotus erectus (Deflandre *in* Deflandre & Fert 1954) Reinhardt 1965

Z. erectus shows unusual variability in size in the Oxford Clay. The rim of this species shows an inconsistently bicyclic appearance in XPL, and the transverse bar varies substantially in brightness; these observations may be a factor of coccolith size and/or preservation.

Z.* cf. *Z. fissus (Fig. 5.6)

The transverse bar of some Oxford Clay zeugrhabdotids exhibits a light microscope image which splits along its long axis when rotated in XPL; this is not characteristic of *Z. erectus*. These specimens are labelled with reference to *Z. fissus* Grün & Zweili 1980, albeit the bar of *Z. fissus* does not exhibit the brightness in XPL shown by these specimens (Bown pers. comm. 2000), and the interval studied here pre-dates the range of this species (middle Oxfordian-?upper Valanginian; Bown & Cooper 1998).

Sp. 1 (Fig. 5.6)

These are large (*ca.* 10 x 12μm), broadly elliptical placoliths of uncertain taxonomic affinity. The central area is of normal width to wide. Little further morphological detail could be ascertained as only several, badly-preserved specimens were observed.

Appendix 7

Oxford Clay Data

The raw nannofossil and geochemical data generated for the Oxford Clay study are listed in Tables A7.1 and A7.2.

Lithostratigraphy		Ammonite zone		Site (pit)	Sample	Fields of view	Preservation	*Watznaueria* coccospheres	*Watznaueria* protococcoliths	*W. britannica*	*W. fossacincta*	*C. margerelii*	*W. barnesae*	*Z. erectus*	*B. constans*	*E. gallicus*	*P. grassei*	*S. bigotii bigotii*	*S. hexum*	*W. manivitae*	*S. quadriarculla*	*A. cylindratus*	*A. harrisonii*	*B. dorsetensis*	*C. perforata*	*R. incompta*	*S. bigotii maximum*	*S. punctulata*	*A. atavus*	*Z.* cf. *Z. fissus*	Reworked: *C. magharensis*	Reworked: *C. crassus*	Reworked: *C. granuletus*	Reworked: *M. elegans*	Reworked: *P. liasicus distinctus*	Nannofossil zone
Oxford Clay Fm	Weymouth Mbr	?mariae	?	Brown's	R8	3	E-1		3	71	13	4	7	21	15	3		1			2	2	1	2	2		1	1	1	1						
		mariae	scarburgense	Cleveland Farm	R7	3	X	1	4	61	15	5	2	19	28	9	4	3		1	3	4	2	1	3	1	1	1			1	1			NJ14
	Stewartby Mbr	athleta	phaelnum	King's Dyke	R6	20	E-1			99	8	•	9	6	•	3	3	4		1	1									2					
	Peterborough Mbr				R5	14	E-1		1	171	29	3	3	•	3	•	1	•		2													1		? NJ13
		coronatum	grossouvrei	Quest	R4	11	E-1		1	97	14	4	3	11	7	1	1	1	5												1			1	
				King's Dyke	R3	17	E-2	1		98	1	1	1	1																					
		jason	jason		R2	10	E-3	1		8	2																								?
Kellaways Fm		calloviense	calloviense		R1	10																													

S. bigotii maximum ▲

Table A7.1 Nannofossil count data generated for the Oxford Clay reconnaissance study. The nannofossil stratigraphy of the formation is shown. Mbr = Member. Ammonite stratigraphy as presented by Bown *in* Martill *et al.* (1994). X = excellent; E-1 = slightly etched; E-2 = moderately etched; E-3 = heavily etched. • = inferred range, based on first (▁▲) and last occurrences. The stratigraphic order of Samples R3 and R4, which represent the same ammonite subzone at different sites, is not known

Metres	Bed	Sample	Wt%$CaCO_3$	Wt%TOC	Fields of view	Preservation	*Watznaueria* coccospheres	*Cyclagelosphaera* protococcoliths	*Watznaueria* protococcoliths	*A. helvetica*	*A. cylindratus*	*B. constans*	*C. margerelii*	*E. gallicus*	*P. grassei*	*S. bigotii bigotii*	*T. beaminsterensis*	*W. barnesae*	*W. britannica*	*W. fossacincta*	*Z. erectus*	*D. criotus*	*S. hexum*	*T. patulus*	*W. manivitiae*	*B. dorsetensis*	*L. crucicenralis*	*S. quadriarculla*	*P. escaigli*	*T. expansus*	*C. perforata*	*Z.* cf *Z. fissus*	*L. contractus*	*A. atavus*	*R. octofenestra*	*R. incompta*	Reworked: *B. finchii*	Reworked: *C. crassus*	Reworked: *C. primulus*	Reworked: *M. elegans*	Reworked: *P. liasicus distinctus*	Reworked: *S. speciosum octum*	Nannofossil zone
0,95		**20**	25,93	2,93	14	E-1	1		6	3	1	8	7	•	6	3	•	10	249	1	25		1	•	•	1	•	1			1	1										
0,90		**19**	30,35	2,25	20	E-1	1		3	•	2	5	5	•	1	2	•	5	284	•	8			•	•	1	•	1				1	1			1						
0,85	26	**18**	27,60	2,19	10	E-1			2	•	•	7	4	2	3	4	•	10	249	10	14			1	•	•	•	1				•	1									
0,80		**17**	11,92	3,56	19	E-1		1	2	•	•	19	4	•	5	4	•	23	255	6	24			2	•	1	•	•				•	•				2					
0,75		**16**	5,00	3,86	21	E-1	1		4	•	5	9	8	1	2	6	•	21	263	8	20			4	•	1	1	•				1	1					2				
0,70		**15**	14,93	4,00	18	E-1		2	6	•	5	21	7	•	5	6	•	11	191	18	40			•	•	1	1	•				1	1					1				
0,65		**14**	9,84	4,98	25	E-2	1			•	•	1	16	•	1	3	•	17	261	3	14			•	•	•	•	•				2	1									
0,60		**13**	11,67	4,58	38	E-2	1	3	2	•	•	5	10	1	•	3	•	15	253	12	11			•	•	•	•	•				•	1									
0,55		**12**	16,43	4,09	13	E-1		1	2	•	1	6	15	•	3	2	•	5	285	6	11			1	•	1	1	•				1	3									
0,50		**11**	7,92	4,63	23	E-1			4	•	1	3	13	1	1	•	•	17	254	7	6			2	•	•	•	•				•	3									
0,45		**10**	4,17	4,68	23	E-2				•	•	•	9	•	•	1	•	9	279	1	10			•	•	1	•	•				1	•									
0,40		**9**	4,84	5,17	29	E-1	1	1	4	•	•	5	13	•	1	3	•	5	289	7	5			•	•	1	•	•				•	•									
0,35	24	**8**	13,59	4,26	38	E-2	1		2	•	•	1	9	•	1	1	•	15	285	6	4			•	•	1	•	•			1	•	•				1					
0,30		**7**	5,34	4,84	26	E-2	2		5	•	2	3	11	•	1	1	•	10	277	3	7	1		•	•	1	•	2				2	•				2					
0,25		**6**	10,09	4,11	20	E-1	2		1	•	•	1	13	•	1	•	•	6	290	4	3	•		•	•	1	•	•				1	•					1				
0,20		**5**	11,59	4,48	25	E-1			3	•	•	•	3	•	•	•	•	•	320	11	3	•		•	•	1	•	•				•	•						1			
0,15		**4**	8,00	4,07	19	E-2		1	2	•	2	•	5	•	•	•	1	6	296	7	3	•		•	•	•	1	•				•	•							1		
0,10		**3**	14,51	4,13	15	E-1	1		2	•	2	8	•	•	1	1	•	15	281	9	9	1		•	•	•	1	1				•	•								1	
0,05		**2**	15,93	4,27	16	E-1		1	4	1	2	9	4	•	1	1	•	11	280	10	6	1		1	1	•	•	1				1	1									
0,00		**1**	18,26	5,23	16	E-1	1		2	1	2	15	10	1	1	1	2	11	315	4	12			1	1	•	•	1				1	1									
NJ13 *pars*																																										

Table A7.2 Nannofossil count data and geochemical data generated for the high-resolution Peterborough Member study. The nannofossil stratigraphy of the interval is shown.

E-1 = slightly etched; E-2 = moderately etched. • = inferred range, based on first and last occurrences

Metres	Bed	Sample	Wt%CaCO$_3$	Wt%TOC	Fields of view	Preservation	*Watznaueria* coccospheres	*Cyclagelosphaera* protococcoliths	*Watznaueria* protococcoliths	*A. cylindratus*	*B. constans*	*C. margerelii*	*P. grassei*	*E. gallicus*	*S. bigotii bigotii*	*W. barnesae*	*W. britannica*	*W. fossacincta*	*Z. erectus*	*T. beaminsterensis*	*S. hexum*	*T. patulus*	*W. manivitiae*	*B. dorsetensis*	*L. crucicenralis*	*S. quadriarculla*	*T. expansus*	*C. perforata*	*Z.* cf *Z. fissus*	*L. contractus*	*A. atavus*	*L. sigillatus*	*A. depravatus*	*B. novum*	*C. granulatus*	*H. cuvillieri*	*Lotharingius* sp.	Reworked: *C. crassus*	Reworked: *C. primulus*	Reworked: *M. elegans*	Reworked: *M. jansae*	Reworked: *P. liasicus distinctus*	Nannofossil zone
2,20	34	45	26,10	2,27	11	E-1		1	6	1	3	4				7	243	136	8						1							4											
2,15	&	44	32,68	1,96	8	E-1	1		6	•	3	2	1			2	226	82	7						•							•										1	
2,10	35	43	33,77	1,80	12	E-1				1	•	3	1			1	251	43	8					1	•	3		1				•											?
2,05	33	42	36,02	1,50	7	E-1			10	1	4	2	2	1		•	267	18	16					•	•	1		•				•											
2,00		41	22,51	3,96	8	E-1			6	•	1	5	•	•		4	254	59	2		1	1		•	•	•		•				•											
1,95		40	23,01	3,81	7	E-1		1	7	1	4	4	•	•		1	200	111	5		•	•		•	•	•		•				2					1						
1,90	32	39	29,68	2,80	10	E-1			7	•	4	2	•	•	2	7	222	56	14		•	1		1	•	•		•				•					•						
1,85		38	30,68	2,58	7	E-1			8	1	1	2	•	2	2	2	197	69	9		•	•		•	•	•	1	•				3				2	1						
1,80		37	27,52	2,79	8	E-1	1		4	•	5	4	1	•	1	1	237	45	12		•	•		•	•	•	•	•				•				•							
1,75		36	28,52	2,24	8	E-1		1	4	1	•	9	2	•	•	2	226	87	7		1	1		•	2	•	•	•				•	1			1		1	1	1			
1,70	31	35	19,93	2,43	7	E-1			9	2	4	5	1	•	1	7	127	163	9		•	•		•	2	•	•	•				2	•										
1,65		34	24,76	1,81	10	E-1		1	6	1	4	5	•	•	1	5	237	176	10		•	•	1	1	4	•	1	•				2	•										
1,60		33	27,77	1,65	9	E-1			4	1	8	3	•	•	1	2	261	32	7		•	•	•	1	•	•	•	•				•	•	1	1					1			
1,55		32	36,44	1,30	7	E-1	1		5	1	5	8	1	1	3	3	247	68	15		•	•	1	•	•	3	•	1			1	•	•							1			NJ13 *pars*
1,50		31	34,02	0,87	8	E-1			2	•	5	2	•	1	•	5	222	61	14		•	•	•	•	•	•	•	•			•	•	•										
1,45	30	30	42,44	0,98	5	E-1			3	•	12	5	•	1	1	2	223	53	18		•	•	•	•	•	•	•	•			•	•	•										
1,40		29	41,94	2,15	10	E-1	1	1	3	1	2	6	1	•	•	5	192	92	24		•	1	•	1	2	•	•	•			•	1	•										
1,35		28	29,02	3,88	10	E-1			14	•	6	8	•	2	•	7	265	41	22		•	1	1	•	•	1	•	•			•	•	1										
1,30		27	31,02	2,23	8	E-1				•	5	1	•	•	•	32	63	189	8		•	•	•	•	•	•	•	•			•	3									1		
1,25	29	26	23,60	2,13	5	E-1		1	2	1	9	4	1	1	•	7	162	108	19		•	•	•	•	•	2	•	•			•												
1,20		25	22,43	1,72	10	E-1			5	2	4	3	1	•	1	7	269	35	9		•	•	•	•	•	•	•	•			•												
1,15		24	19,93	1,67	5	E-1		1	6	•	8	•	1	1	1	10	232	49	11		•	•	•	1	•	•	•	•	1		1												
1,10	28	23	20,68	1,29	6	E-1		1	6	7	13	10	3	4	7	3	188	161	32		•	•	•	•	•	5	•	•	•		1								1				
1,05		22	26,35	2,19	9	E-1		3	4	5	13	18	1	•	1	14	242	26	32	1	•	•	1	•	•	•	•	•	1	1	•												
1,00	27	21	23,01	2,76	10	E-1			7	2	3	13	2	•	•	9	299	1	19	1	1	•	1	•	•	•	•	1	•	•	•							2					

Appendix 8

Biostratigraphy of the Oxford Clay

Introduction and methods

The Oxford Clay data were subjected to biostratigraphic analysis using the most recent nannofossil zonation scheme available (Bown & Cooper 1998; Fig. A8.1). Marker species ranges were confirmed by additional traverses of slides made from horizons below/above F/LOs.

A number of taxa only were observed during additional scanning of slides for image capture purposes (Table A8.1). In the interests of maintaining standardised observational procedures for palaeoenvironmental analysis, these are not recorded in Appendix 7 or discussed in Chapter 5. However, where relevant, they are considered in the discussion below.

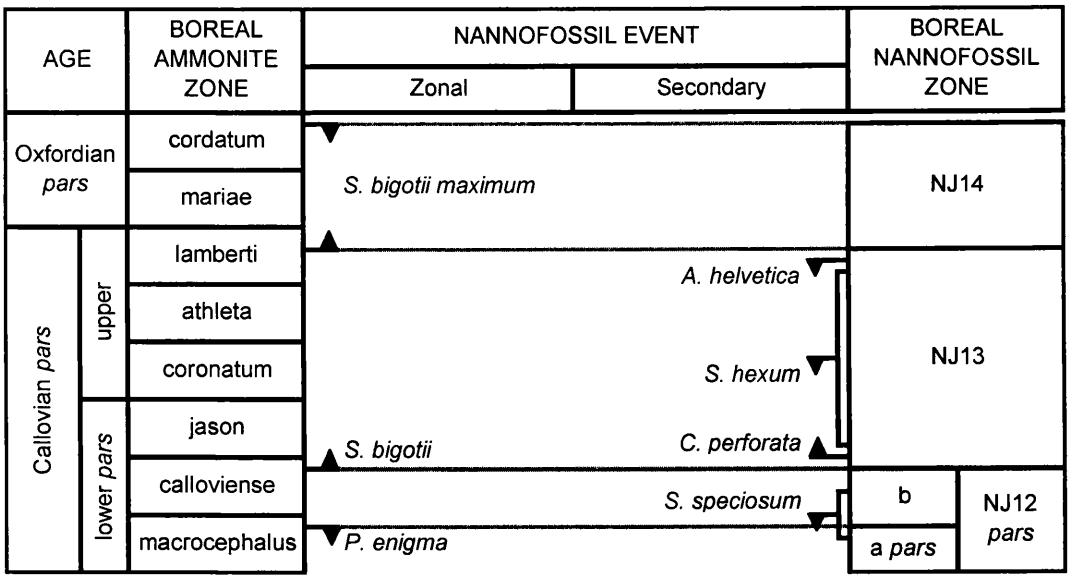

Fig. A8.1 Biostratigraphic events and zones discussed in relation to the Oxford Clay. ▲ = first occurrence; ▼ = last occurrence. Modified from Bown & Cooper (1998)

Lithostratigraphy (Member)	Ammonite zone		Site (pit)	Sample	*A. atavus*	*A. cylindratus*	*D. striatus*	*L. crucicentralis*	*O. decussatus*	*P. grassei*	*P. escaigii*	*S. punctulata*	*S. leptostaurus*	*T. beaminsterensis*	*T. expansus*	*?Triscutum* sp.	Reworked							
																	B. prinsii	*Calyculus* sp.	*C. crassus*	*C. primulus*	*M. jansae*	*P. liasicus distinctus*	*P. marthae*	*P. enigma*
Weymouth	?mariae	?	Brown's	R8	P	•	•	P	•	P	•	•	•	P	P	P	•	•	P	•	•	•	•	•
	mariae	scarburgense	Cleveland Farm	R7	•	•	P	P	P	•	P		P	P	P	•	P	P	•	P	P	P	P	P
Peterborough	coronatum	grossouvrei	Quest	R4	•	P	•	•	•	•	•	P	•	•	•	•	P	•	•	•	•	•	•	•

Table A8.1 Additional Oxford Clay nannofossil distribution data, collected from the reconnaissance samples but outside the scope of the methods of this study. Ammonite stratigraphy as presented by Bown *in* Martill *et al.* (1994). P = present (<1/field of view); • = presence/absence recorded during reconnaissance (Table A7.1)

Results

Nannofossil biostratigraphy of the King's Dyke Pit section is rendered problematic by taxonomically depauperate assemblages throughout the section. Sample R6 can however be assigned to nannofossil zone NJ13, based on the presence of *Stephanolithion bigotii bigotii* and the absence of *S. bigotii maximum* (Table A7.1). The high-resolution samples (with the exception of Samples 42-45) all represent this zone, according to the ranges of *Stephanolithion bigotii bigotii* and *S. hexum* (Table A7.2); rare occurrences of *Ansulasphaera helvetica* and *Crepidolithus perforata* support this interpretation. Samples 42-45 can be tentatively assigned to NJ13, on account of their stratigraphic position below Sample R6.

Sample R4 can also be assigned to NJ13 on the basis of the presence of *Stephanolithion bigotii bigotii* and *S. hexum*, and the absence of *S. bigotii maximum*. In the absence of marker species, Sample R5 is tentatively assigned to NJ13, on account of its stratigraphic position between Samples R3 and R6. Samples R7 and R8 belong to NJ14, as *S. bigotii maximum* is found in both. The absence of *S. hexum* in these samples is consistent with this observation.

Discussion

The nannofossil stratigraphy of the Oxford Clay is commensurate with the established ammonite zonation (as presented by Bown *in* Martill *et al.* (1994) and Hudson & Martill (1994)) and with the most recent nannofossil study of the formation (Bown *in* Martill *et al.* 1994). In addition, the following observations are of interest: (1) The polytaxic assemblages in Samples R7 and R8 are consistent with Bown & Cooper's (1998) observation that the highest diversities of Jurassic nannofossils from northern Europe are recorded from NJ14. (2) The first occurrence of *Staurolithites leptostaurus* has been placed in the Kimmeridgian (Bown & Cooper 1998). Its presence in Sample R7 suggests that the range of this species should be revised to include rare occurrences as early as the earliest Oxfordian (mariae AZ). (3) Whilst the Watznaueriaceae are numerically dominant in all assemblages studied here, specimens of the genus *Lotharingius* (which belongs to this family) are rare. This is characteristic of this

taxon at this stratigraphic level (Bown pers. comm. 2000). (4) *Watznaueria* coccospheres display unique preservation potential throughout the Mesozoic, on account of the abundance of this genus and its large, robustly interlocking coccoliths. Coccospheres of *Watznaueria*, and no other genus, were observed in this study. (5) Most samples contain a small component of reworked taxa. These are predominantly Lower Jurassic in origin, and presumably represent erosion of older sediments into the basin. This is consistent with Bown & Cooper's (1998) assertion that reworked Lower and Middle Jurassic nannofossils are common in sections representing NJ14 from England and France. Based on the results of this study (and those of Bown *in* Martill *et al.* (1994)), it may well be that this observation should be extended to include English sections representing NJ13. (6) The extinction of *Schizosphaerella punctulata* has been tentatively placed in the Bathonian, whilst it is acknowledged that rare occurrences continue through the Kimmeridgian (Bown & Cooper 1998). It is not known whether this extended distribution records reworking or a depleted but surviving population. Good preservation of the rare specimens of this species in the Oxford Clay does not provide evidence of survival, as the preservation of reworked taxa has not been adversely affected.

Appendix 9

Black Ven Marls Data

The raw nannofossil data generated for the Black Ven Marls study, together with the corresponding geochemical data of Weedon & Jenkyns (unpublished), are listed in Table A9.1.

Metres	Ammonite zone		Sample	Wt%$CaCO_3$	Wt%TOC	Fields of view	Preservation	?Faecal pellets	*C. primulus*	*M. elegans*	*P. liasicus distinctus*	*T. patulus*	*M. lenticularis*	*S. punctulata*	*C. crassus*	*C. pliensbachensis*	Nannofossil zone	
30.9	raricostatum	rari.	29			10	E-1		6		10			8		1		
27.4			28			10	E-1		15		17	2		12	1	3	NJ3	*C. crassus*
23.8		densi.	27			10	E-1		12	1	40	3		6	2	•		
20.9			26			10	E-1		5	•	39	1		7	4	1		▲
16.9			25			10	E-1		1	1	11	1		1				
14.9			24			10	E-1		5	1	14	2		1				
10.3		stell.	23			10			•	•	•	•		•				
7.8			22			10	E-1		1	•	•	1		•				
2.5			21			10			•	•	•	•		•				
1.9	obtusum	obtusum	20	8.21	4.40	10	E-1		5	•	4	•		1				
1.8			19	7.57	4.94	10	E-1		•	•	2	1		1				
1.7			18	7.23	5.24	10	E-1		•	•	2	•		•				
1.6			17	11.59	4.37	10	E-1		1	•	1	•		•				
1.5			16	12.12	6.72	10	E-1		•	•	2	1		•				
1.4			15	21.20	6.23	10	E-2		2	•	•	2		•				
1.3			14	57.48	3.13	10			•	•	•	•		•				
1.2			13	11.84	7.56	10			•	•	•	•		•				
1.1			12	10.91	11.06	10	E-1	2	2	1	11	5		1				
1.0			11	15.91	11.68	10	E-2		2	•	7	3						
0.9			10	4.35	1.64	10	E-1		2	•	5	3						
0.8			9	4.87	1.69	11	E-1		5	•	8	9						
0.7			8	9.90	2.67	10	E-1		4	8	7	7						
0.6			7	11.62	3.59	11	E-1		6	4	11	19						
0.5			6	24.52	4.41	10	E-1		6	14	9	16	1					
0.4			5	23.63	6.02	10	E-1	1	3	•	4	21						
0.3			4	14.49	2.49	10	E-2		7	•	3	7						
0.2			3	19.71	2.11	10	E-1		1	1	7	4						
0.1			2	40.30	1.91	10			•								?	
0.0			1	74.01	0.77	10	X		1									

Table A9.1 Nannofossil count data generated for the Black Ven Marls. The lowermost sample represents the top of Lang & Spath's (1926) Bed 82. The geochemical data corresponding to the high-resolution interval are provided (Weedon & Jenkyns unpublished), and the nannofossil stratigraphy of the formation is shown. Ammonite stratigraphy as presented by Hesselbo & Jenkyns (1995); stell. = stellare; densi. = densinodulum; rari. = raricostatoides. X = excellent; E-1 = slightly etched; E-2 = moderately etched. • = inferred range, based on first (▲) and last occurrences

Appendix 10

Biostratigraphy of the Black Ven Marls

Introduction and methods

In addition to the reconnaissance study, the entire thickness of the Black Ven Marls was sampled for biostratigraphic purposes. Samples were collected at intervals of several metres, avoiding diagenetically-altered carbonate-rich horizons. Marker species inceptions/extinctions were confirmed by additional traverses of slides made from horizons below/above. The data are interpreted using the most recent nannofossil zonation scheme available (Bown & Cooper 1998; Fig. A5.1).

Results

Nannofossils are scarce in/absent from Samples 1 and 2, and it is not possible to date the horizons represented using the data generated for this study (Table A9.1). Samples 3-25 belong to NJ2b, as indicated by the presence of *Mitrolithus elegans* and *Parhabdolithus liasicus*, together with the absence of *P. marthae*. The absence of *P. robustus* from these assemblages (and the Black Ven Marls as a whole) can be explained in terms of the sporadic distribution of this species in the early part of its range in the Liassic of Dorset (as observed in the Belemnite Marls; Appendix 5).

The remaining samples (26-9) represent NJ3, as *Crepidolithus crassus* is present and *Similiscutum cruciulus* is absent. The absence of *Orthogonoides hamiltoniae* from these assemblages is probably a function of the rarity of this species in Boreal sediments (Bown pers. comm. 2000; Appendix 5).

Discussion

The nannofossil biostratigraphy of the formation is thus essentially consistent with the ammonite zonation presented by Hesselbo & Jenkyns (1995; Table A9.1). However, the base of NJ3, which should coincide with the base of the raricostatum AZ in the Black Ven Marls (on account of the absence of the oxynotum AZ from the section) is 6m higher than expected. The FO of *Crepidolithus crassus*, which defines the base of NJ3, was placed even higher in the section by Bown *in* Lord & Bown (1987). It may be that this event does not provide a sufficiently reliable datum for NZ boundary definition. Bown & Cooper (1998) acknowledge that the appearance of *C. crassus* has been variably recorded in the literature, reflecting the presence of intermediate ancestral morphologies. Whilst this might explain the description of *C. crassus* from anomalously early horizons (e.g. the obtusum AZ; Crux 1987a), it does not account for the late appearance of this species as observed here.

Otherwise, the distribution of taxa through the Black Ven Marls as observed here is similar to that described by Bown *in* Lord & Bown (1987). It also compares well with the other most recent nannofossil study of the formation, that of Crux (1987a), with the exception of the following points: (1) Crux records *Annulithus arkelli* from all three AZs in the Black Ven Marls. This simple crystallite ring is considered to be of inorganic origin (Crux 1987a, Bown pers. comm. 1999), and was not observed in this study. (2) Crux records the presence of *Crepidolithus cavus* throughout the Black Ven Marls. This species was not encountered in the present study. Bown (1987) considers claims for such early occurrences as spurious, due to contamination/misidentification. It is unclear as to which of these factors was responsible for Crux's observations (he does not provide an illustration of this species); before the appearance of *C. crassus*, the other Sinemurian representatives of *Crepidolithus* are either rare in (*C. pliensbachensis*) or apparently absent from (*C. timorensis*) the formation, and other coeval taxa are morphologically dissimilar. Such consistent contamination is unlikely. The simplest conclusion would be that Crux's *C. cavus* specimens represent heavy etching of *C. crassus* and *C. pliensbachensis* coccoliths, resulting in an open central area. It may be that more specimens per sample were recorded by Crux

than in the current study (he does not discuss his methods in detail), resulting in a more consistent observation of the latter taxa.

Crux also records the presence of *Stradnerlithus primitus* (his *Chiastozygus primitus*) in all 3 AZs in the Black Ven Marls. This species was not observed in the present study, and may again reflect a more detailed investigation by Crux.

Finally, the following observations are of interest: (1) The absence of *Similiscutum* from the Black Ven Marls is consistent with the FO of this genus as located in the jamesoni AZ by Bown & Cooper (1998), and as observed in the Belemnite Marls (Appendix 5). This contradicts the assertion of de Kaenel *et al.* (1996) that *S. precarium* (*S. cruciulus* of Bown & Cooper 1998) originates in the raricostatum AZ. (2) A single specimen of *Mitrolithus lenticularis* was observed in the obtusum AZ, whilst the FO of this species has previously been placed in the younger raricostatum AZ (Bown & Cooper 1998). Given the rarity of this species in the Liassic of Dorset and the care exercised in sample collection and preparation, this is unlikely to represent contamination; rather it may be that this datum requires further scrutiny. It is possible that *M. lenticularis* merely represents an end-member of the spectrum of *M. elegans* morphological variability (as observed in the Belemnite Marls; Appendix 3), or a sub-species of *M. elegans*. In either case the ranges of these taxa should be similar; indeed their LOs both occur within the space of 3 AZs (Bown & Cooper 1998), and the current study locates the FO of *M. lenticularis* less than 4 AZs above that of *M. elegans* (Bown & Cooper 1998).

References

Alatalo RV 1981 Problems in the measurement of evenness in ecology *Oikos* 37: 199-204

Backman J & Raffi I 1997 Calibration of Miocene nannofossil events to orbitally tuned cyclostratigraphies from Ceara Rise *Proceedings of the Ocean Drilling Program, Scientific Results* 154: 83-99

Bailey I 2000 *Calcareous nannofossils of the Belemnite Marls of Dorset, England: their role in the production of carbonate cycles* MSci Thesis, University College London (unpublished)

Barnard T & Hay WW 1974 On Jurassic coccoliths: a tentative zonation of the Jurassic of southern England and northern France *Eclogae Geologicae Helvetiae* 67: 563-85

Belin S & Kenig F 1994 Petrographic analyses of organo-mineral relationships: depositional conditions of the Oxford Clay Formation (Jurassic), UK *Journal of the Geological Society* 151: 153-60

Berger WH 1976 Biogenous deep sea sediments: production, preservation and interpretation *In* Riley JP & Chester R (eds) *Chemical Oceanography*

Berger A, Loutre MF & Dehant V 1989 Influence of the changing lunar orbit on the astronomical frequencies of pre-Quaternary insolation patterns *Paleoceanography* 4: 555-64

Bown PR 1987 Taxonomy, biostratigraphy and evolution of Late Triassic-Early Jurassic calcareous nannofossils *Special Papers in Palaeontology* 38

Bown PR 1993 New holococcoliths from the Toarcian-Aalenian (Jurassic) of northern Germany *Senckenbergiania Lethaea* 73: 407-19

Bown PR 1998a Triassic *In* Bown (ed) *Calcareous Nannofossil Biostratigraphy* Chapman & Hall

Bown PR (ed) 1998b *Calcareous Nannofossil Biostratigraphy* Chapman & Hall

Bown PR, Burnett JA & Gallagher LT 1992 Calcareous nannoplankton evolution *Memorie di Scienze Geologiche* XLIII: 1-17

Bown PR & Cooper MKE 1998 Jurassic *In* Bown (ed) *Calcareous Nannofossil Biostratigraphy* Chapman & Hall

Bown PR, Cooper MKE & Lord AR 1988 A calcareous nannofossil biozonation scheme for the early to mid Mesozoic *Newsletters on Stratigraphy* 20: 91-114

Bown PR & Young JR 1998a Introduction *In* Bown (ed) *Calcareous Nannofossil Biostratigraphy* Chapman & Hall

Bown PR & Young JR 1998b Techniques *In* Bown PR (ed) *Calcareous Nannofossil Biostratigraphy* Chapman & Hall

Bradshaw MJ, Cope JCW, Cripps DW, Donovan DT, Howarth MK, Rawson PF, West IM & Wimbledon WA 1992 Jurassic *In* Cope JCW, Ingham JK & Rawson PF (eds) *Atlas of Palaeogeography and Lithofacies* Geological Society Memoir 13

Brand LE 1994 Physiological ecology of marine coccolithophores *In* Winter A & Siesser WG (eds) *Coccolithophores* Cambridge University Press

Bronnimann P 1955 Microfossils *incertae sedis* from the Upper Jurassic and Lower Cretaceous of Cuba *Micropaleontology* 1: 28-51

Burnett JA, Young JR & Bown PR 2000 Calcareous nannoplankton and global climate change *In* Culver SJ & Rawson PF (eds) *Biotic response to Global Climate Change: the last 145 Million Years* Cambridge University Press

Cachão M, Narciso Á, Silva A, CODENET team, Jordan R & Takahashi K 2000 The morphometric response of *Coccolithus pelagicus* to glacial-interglacial couplets during the last 4my *Journal of Nannoplankton Research* 22: 87

Cope JCW, TA Getty, MK Howarth, N Morton & HS Torrens 1980 A correlation of Jurassic rocks in the British Isles. Part 1: Introduction and Lower Jurassic *Geological Society Special Report* 14

Crux JA 1987a Early Jurassic calcareous nannofossil biostratigraphic events *Newsletters on Stratigraphy* 17: 77-100

Crux JA 1987b Concerning dimorphism in Early Jurassic coccoliths and the origin of the genus *Discorhabdus* Noël 1965 *Abhandlungen der Geologiches Bundesanstalt* 39: 51-5

Eades E, Versteegh G, Zonnenveld & Willems H 2000 Calcareous dinoflagellates as indicators of orbitally-driven climatic variation *Journal of Nannoplankton Research* 22: 95

Einsele G & Ricken W 1991 Limestone-marl alternation – an overview *In* Einsele G, Ricken W & Seilacher A (eds) *Cycles and Events in Stratigraphy* Springer-Verlag

Einsele G, Ricken W & Seilacher A (eds) 1991 *Cycles and Events in Stratigraphy* Springer-Verlag

Erba E, Castradori D, Guasti G & Ripepe M 1992 Calcareous nannofossils and Milankovitch cycles: the example of the Albian Gault Clay Formation (southern England) *Palaeogeography, Palaeoclimatology, Palaeoecology* 93: 47-69

Fischer AG, Boer PL de & Premoli-Silva I 1990 Cyclostratigraphy *In* Ginsburg RN & Beaudoin B (eds) *Cretaceous Resources, Events and Rhythms* Kluwer

Fleet AJ, Clayton CJ, Jenkyns HC & Parkinson DN 1987 Liassic source rock deposition in western Europe *In* Brooks J & Glennie K (eds) *Petroleum Geology of North West Europe* Graham & Trotman

Frakes LA, Francis JE & Syktus JI 1992 *Climate Modes of the Phanerozoic* Cambridge University Press

Gama da R 2000 *Calcareous nannoplankton palaeoecology from the Cenomanian-Turonian of Tarfaya, Morocco* MSc thesis, University College London (unpublished)

Gale AS 1998 Cyclostratigraphy *In* Doyle P & Bennett MR (eds) *Unlocking the Stratigraphical Record: Advances in Modern Stratigraphy* John Wiley & Sons Ltd

Gale AS, Smith AB, Monks NEA, Young JR, Howard A, Wray DS & Huggett JM 2000 Marine biodiversity through the Late Cenomanian-Early Turonian: palaeoceanographic controls and sequence stratigraphic biases *Journal of the Geological Society* 157: 745-57

Geisen M, Bollmann J, Herrle JO, Mutterlose J & Young JR 1999 Calibration of the random settling technique for calculation of absolute abundances of calcareous nannoplankton *Micropaleontology* 45: 437-42

Gibbs S 2000 Pliocene to Early Pleistocene evolution of nannofossil assemblages in response to palaeoceanographic changes *Journal of Nannoplankton Research* 22: 101

Gradstein FM, Agterberg FP, Ogg JG, Hardenbol J, Veen P van, Thierry J & Huang Z 1994 A Mesozoic timescale *Journal of Geophysical Research* 99: 24051-74

Hallam A 1975 *Jurassic Environments* Cambridge University Press

Hamilton G 1977 Early Jurassic calcareous nannofossils from Portugal and their biostratigraphic use *Eclogae Geologicae Helvetiae* 70: 575-97

Hamilton GB 1982 Triassic and Jurassic calcareous nannofossils *In* Lord AR (ed) *A Stratigraphical Index of Calcareous Nannofossils* British Micropalaeontological Society Series

Herrle JO & Hemleben C 2000 A new proxy to estimate orbitally-induced productivity cycles in mid-Cretaceous sediments *Journal of Nannoplankton Research* 22: 106-7

Hesselbo SP & Jenkyns HC 1995 A comparison of the Hettangian to Bajocian successions of Dorset and Yorkshire *In* Taylor PD (ed) *Field Geology of the British Jurassic* Geological Society 105-50

Hesselbo SP & Jenkyns HC 1998 British Lower Jurassic sequence stratigraphy *In* Graciansky PC, Hardenbol J, Jacquin T, Farley MB & Vail PR (eds) *Mesozoic and Cenozoic Sequence Stratigraphy of European Basins* Society of Economic Paleontologists and Mineralogists Special Publication 60: 561-81

Hill MO 1973 Diversity and evenness: A unifying notation and its consequences *Ecology* 54: 427-32

Hinnov LA & Park JJ 1999 Strategies for assessing Early-Middle (Pliensbachian-Aalenian) Jurassic cyclochronologies *Philosophical Transactions of the Royal Society of London* 357: 1831-59

House M 1989 *Geology of the Dorset Coast* Geologists' Association Guide

Hudson JD 1994 Oxford Clay studies *Journal of the Geological Society* 151: 111-2

Hudson JD & Martill DM 1991 The Lower Oxford Clay: production and preservation of organic matter in the Callovian (Jurassic) of central England *In* Tyson RV & Pearson TH (eds) *Modern and Ancient Continental Shelf Anoxia* Geological Society Special Publication 58: 363-79

Hudson JD & Martill DM 1994 The Peterborough Member (Callovian, Middle Jurassic) of the Oxford Clay Formation at Peterborough, UK *Journal of the Geological Society* 151: 113-24

Imbrie J & Imbrie K 1979 *Ice Ages: Solving the Mystery* Harvard University Press

Ineson JR, Schiøler P, Jutson DJ & Sheldon E 2000 Mid-Cretaceous of the Danish Central Graben: implications for sequence stratigraphic analysis of chalks *Journal of Nannoplankton Research* 22: 108

Jacobs DK & Sahagian DL 1995 Milankovitch fluctuations in sea level and recent trends in sea-level change: ice may not always be the answer *In* Haq BU (ed) *Sequence Stratigraphy and Depositional Response to Eustatic, Tectonic and Climatic Forcing* Kluwer Academic Publishers

Kälin O & Bernouilli D 1984 *Schizosphaerella* Deflandre and Dangeard in Jurassic deep water carbonate sediments, Mazagan continental margin (Hole 547B) and Mesozoic Tethys *Initial Reports of the Deep Sea Drilling Project* 79: 411-35

Kaenel E de, Bergen JA & von Salis Perch-Nielsen K 1996 Jurassic calcareous nannofossil biostratigraphy of Western Europe. Compilation of recent studies and calibration of bioevents *Bulletin de la Societé Géologique de France* 167: 15-28

Kenig F, Hayes JM, Popp BN & Summons RE 1994 Isotopic biogeochemistry of the Oxford Clay Formation (Jurassic), UK *Journal of the Geological Society* 151: 139-52

Knappertsbusch M 2000 3-D animated views of the morphological evolution of the coccolithophorid *Calcidiscus leptoporus* from the Early Miocene to Recent *Journal of Nannoplankton Research* 22: 117

Kutzbach JE 1994 Idealised Pangean climates: sensitivity to orbital change *In* Klein GD (ed) *Pangea: Paleoclimate, Tectonics and Sedimentation During Accretion, Zenith and Breakup of a Supercontinent* Geological Society of America Special Paper 288: 41-44

Lang WD & Spath LF 1926 The Black Marl of Black Ven and Stonebarrow, in the Lias of the Dorset coast *Quarterly Journal of the Geological Society* 82: 144-87

Lang WD, Spath LF, Cox LR & Muir-Wood HM 1928 The Belemnite Marls of Charmouth, a series in the Lower Lias of the Dorset Coast *Quarterly Journal of the Geological Society* 84: 179-257

Lees Burnett JA, Bown PR, Young JR, Riding JA (in prep) Late Jurassic phytoplankton responses to environmental change: a Kimmeridge Clay Formation case study *Rapid Global Geological Events Project*

Lord AR & Bown PR (eds) 1987 *Mesozoic and Cenozoic Stratigraphical Micropalaeontology of the Dorset Coast and Isle of Wight, Southern England* British Micropalaeontological Society Guide Book 1

Ludwig JA & Reynolds JF 1988 *Statistical Ecology: a Primer on Methods and Computing* Wiley

MacLeod N, Rawson PF, Forey PL, Banner FT, Boudagher-Fadel MK, Bown PR, Burnett JA, Chambers P, Culver S, Evans SE, Jeffery C, Kaminski MA, Lord AR, Milner AC, Milner AR, Morris N, Owen E, Rosen BR, Smith AB, Taylor PD, Urquhart E & Young JR 1997 The Cretaceous-Tertiary biotic transition *Journal of the Geological Society* 154: 265-92

MacQuaker JHS 1994 A lithofacies study of the Peterborough Member, Oxford Clay Formation (Jurassic), UK: an example of sediment bypass in a mudstone succession *Journal of the Geological Society* 151: 161-72

MacQuaker JHS & Howell JK 1999 Small-scale (<5.0m) vertical heterogeneity in mudstones: implications for high-resolution stratigraphy in siliciclastic mudstone successions *Journal of the Geological Society* 156: 105-12

Mann ME & Lees J 1996 Robust estimation of background noise and signal detection in climatic time series *Climate Change* 33: 409-45

Martill DM, Taylor MA & Duff KL 1994 The trophic structure of the biota of the Peterborough Member, Oxford Clay Formation (Jurassic), UK *Journal of the Geological Society* 151: 173-94

Matsuoka H 1990 A new method to evaluate dissolution of calcium carbonate in deep sea sediments *Palaeontological Society of Japan, Transactions and Proceedings* 157: 430-4

Mattioli E 1997 Nannoplankton productivity and diagenesis in the rhythmically-bedded Toarcian-Aalenian Fiuminuta Section (Umbria-Marche Appenines, Central Italy) *Palaeogeography, Palaeoclimatology, Palaeoecology* 130: 113-33

Mattioli E, Reboulet S, Pittet B, Proux O & Baudin F 2000 Calcareous nannoplankton and ammonoid abundance in Valanginian limestone-marl couplets: a dominance of carbonate dilution or productivity? *Journal of Nannoplankton Research* 22: 123-4

Mattioli E, Young JR, Bown PR & Pittet B 2000 Morphometric analyses on the Early Jurassic Biscutaceae *Journal of Nannoplankton Research* 22: 124-5

Medd AE 1971 Some Middle and Upper Jurassic Coccolithophoridae from England and France *Proceedings II Planktonic Conference Rome 1970* 2: 821-845

Medd AE 1979 The Upper Jurassic coccoliths from the Haddenham and Gamlingay boreholes (Cambridgeshire, England) *Eclogae Geologicae Helvetiae* 72: 19-109

Medd AE 1982 Nannofossil zonation of the English Middle and Upper Jurassic *Marine Micropalaeontology* 7: 73-95

Munnecke A, Westphal H, Elrick M & Reijmer JJG in press The mineralogical composition of precursor sediments of calcareous rhythmites - a new approach *International Journal of Earth Sciences*

Mutterlose J & Ruffell 1999 Milankovitch-scale palaeoclimate changes in pale-dark bedding rhythms from the Early Cretaceous (Hauterivian and Barremian) of eastern England and northern Germany *Palaeogeography, Palaeoclimatology, Palaeoecology* 154: 133-60

Okada H & Matsuoka M 1996 Lower-photic nannoflora as an indicator of the late Quaternary monsoonal palaeo-record in the tropical Indian Ocean *In* Moguilevsky A & Whatley R (eds) *Microfossils and Oceanic Environments* University of Wales, Aberystwyth Press

Palmer CP 1972 A revision of the zonal classification of the Lower Lias of the Dorset coast in southwest England *Newsletters on Stratigraphy* 2: 45-54

Pienaar RN 1994 Ultrastructure and calcification of coccolithophores *In* Winter A & Siesser WG (eds) *Coccolithophores* Cambridge University Press

Quinn PS 1999 A note on the behaviour of calcareous nannofossils during the firing of ceramics *Journal of Nannoplankton Research* 21: 31-2

Quinn PS 2000 *'Ceramic micropalaeontology': the analysis of microfossils in archaeological ceramics with special reference to its application in the southern Aegean* PhD thesis, University of Sheffield (unpublished)

Raffi I 1999 Precision and accuracy of nannofossil biostratigraphic correlation *Philosophical Transactions of the Royal Society* 357: 1975-93

Ricken W 1991 Variation of sedimentation rates in rhythmically bedded sediments. Distinction between depositional types *In* Einsele G, Ricken W & Seilacher A (eds) *Cycles and Events in Stratigraphy* Springer-Verlag

Rood AP, Hay WW & Barnard T 1971 Electron microscope studies of Oxford Clay coccoliths *Eclogae Geologicae Helvetiae* 64: 245-72

Rood AP, Hay WW & Barnard T 1973 Electron microscope studies of Lower and Middle Jurassic coccoliths *Eclogae Geologicae Helvetiae* 66: 365-82

Roth PH 1983 Jurassic and Lower Cretaceous calcareous nannofossils in the Western North Atlantic (Site 534): biostratigraphy, preservation, and some observations on biogeography and palaeoceanography *Initial Reports of the Deep Sea Drilling Project* 76: 587-621

Roth PH 1994 Distribution of coccoliths in oceanic sediments *In* Winter A & Siesser WG (eds) *Coccolithophores* Cambridge University Press

Roth PH & Bowdler J 1981 Middle Cretaceous calcareous nannoplankton biogeography and oceanography of the Atlantic ocean *In* Warme JE, Douglas RG & Winterer EL (eds) The Deep Sea Drilling Project: a decade of progress *Society of Economic Paleontologists and Mineralogists Special Publication* 32: 517-46

Salis von K 1995 Calcareous nannofossils in the arts *In* Poulsen NE (ed) *6th International Nannoplankton Association Conference Programme and Abstract Volume*

Scarparo Cunha AA 2000 Dry-wet climatic cycles in the Turonian sequences of the Sergipe (NE Brazilian continental margin) and Angola (SW African continental margin) Basins *Journal of Nannoplankton Research* 22: 93

Shackleton NJ, McCave IN & Weedon GP (eds) 1999 Astronomical (Milankovitch) calibration of the geological time-scale *Philosophical Transactions of the Royal Society* 357

Sellwood BW 1970 The relation of trace fossils to small scale sedimentary cycles in the British Lias *In* Crimes TP & Harper JC (eds) *Trace Fossils* Seel House Press

Sellwood BW 1972 Regional environmental changes across a Lower Jurassic stage boundary in Britain *Palaeontology* 15: 125-57

Sellwood BW & Jenkyns HC 1975 Basins and swells and the evolution of an epeiric sea (Pliensbachian-Bajocian of Great Britain) *Geological Society of London Journal* 131: 373-88

Steinmetz JC 1994 Sedimentation of coccolithophores *In* Winter A & Siesser WG (eds) *Coccolithophores* Cambridge University Press

Street C & Bown PR 2000 Palaeobiogeography of Early Cretaceous (Berriasian-Barremian) Calcareous Nannoplankton *Marine Micropaleontology* 39: 265-91

Thierstein HR 1980 Selective dissolution of Late Cretaceous and earliest Tertiary calcareous nannofossils: experimental evidence *Cretaceous Research* 2: 165-76

Thierstein HR, Geitzenauer KR & Molfino B 1977 Global synchroneity of Late Quaternary coccolith datum levels: validation by oxygen isotopes *Geology* 5: 400-4

Thierstein HR & Roth PH 1991 Stable isotopic and carbonate cyclicity in Lower Cretaceous deep-sea sediments: dominance of diagenetic effects *Marine Geology* 97: 1-34

Thomsen E 1989 Seasonal variation in Boreal Early Cretaceous calcareous nannofossils *Marine Micropaleontology* 15: 123-52

Turner A 1997 *Biostratigraphy of the Belemnite Marls Using Nannofossil Assemblages* BSc Project Report, University of Luton (unpublished)

Volin S, Eshet Y, Kisch H 1998 Microfossils help in deciphering a complex metamorphic and paleogeographic enigma *7th International Nannoplankton Association Conference Programme and Abstracts Volume*

Walker DT 1991 *Cyclic Sedimentation in the Pliensbachian of the Wessex Basin* PhD Thesis, University of Reading (unpublished)

Wall D 1965 Microplankton, pollen and spores from the Lower Jurassic in Britain *Micropaleontology* 11: 151-90

Waterhouse HK 1999 Regular terrestrially derived palynofacies cycles in irregular marine sedimentary cycles, Lower Lias, Dorset *Journal of the Geological Society* 156: 1113-24

Watkins DK 1989 Nannoplankton productivity fluctuations and rhythmically-bedded pelagic carbonates of the Greenhorn Limestone (Upper Cretaceous) *Palaeogeography, Palaeoclimatology, Palaeoecology* 74: 75-86

Weedon GP 1985 Hemipelagic shelf sedimentation and climatic cycles: the basal Jurassic (Blue Lias) of South Britain *Earth and Planetary Science Letters* 76: 321-35

Weedon GP 1991 The spectral analysis of stratigraphic time series *In* Einsele G, Ricken W & Seilacher A (eds) *Cycles and Events in Stratigraphy* Springer-Verlag

Weedon GP 1993 The recognition and stratigraphic implications of orbital forcing of climate and sedimentary cycles *In* Wright VP (ed) *Sedimentology Review* Blackwell

Weedon GP in prep *Analysing Stratigraphic Records of Environmental Cycles* Cambridge University Press

Weedon GP & Jenkyns HC 1990 Regular and irregular climatic cycles and the Belemnite Marls (Pliensbachian, Lower Jurassic, Wessex Basin) *Journal of the Geological Society* 147: 915-8

Weedon GP & Jenkyns HC 1999 Cyclostratigraphy and the Early Jurassic time scale: data from the Belemnite Marls, Dorset, Southern England *Geological Society of America Bulletin* 111: 1823-40

Weedon GP, Jenkyns HC, Coe AL, Hesselbo SP 1999 Astronomical calibration of the Jurassic time-scale from cyclostratigraphy in British mudrock formations *Philosophical Transactions of the Royal Society* 357: 1787-813

Whalley PES 1985 The systematics and palaeogeography of the Lower Jurassic insects of Dorset, England *Bulletin of the British Museum (Natural History), (Geology)* 39: 107-89

Windley DE 1995 *Calcareous Nannofossil Applications in the Study of Cyclic Sediments of the Cenomanian* PhD thesis, University College London (unpublished)

Winter A, Jordan RW & Roth PH 1994 Biogeography of living coccolithophores in ocean waters *In* Winter A & Siesser WG (eds) *Coccolithophores* Cambridge University Press

Young JR 1990 Size variation of Neogene *Reticulofenestra* coccoliths from Indian Ocean DSDP cores *Journal of Micropalaeontology* 9: 71-86

Young JR 1994 Functions of coccoliths *In* Winter A & Siesser WG (eds) *Coccolithophores* Cambridge University Press

Young JR, Bergen JA, Bown PR, Burnett JA, Fiorentino A, Jordan RW, Kleijne A, Niel BE van, Ton Romein AJ & Salis K von 1997 Guidelines for coccolith and calcareous nannofossil terminology *Palaeontology* 40: 875-912

Young JR & Bown PR 1991 An ontogenetic sequence of coccoliths - *Watznaueria fossacincta* in the Kimmeridge Clay (U. Jurassic, England) *Palaeontology* 34: 843-50

Young JR, Bown PR & Burnett JA 1994 Palaeontological perspectives *In* Green JC & Leadbeater BSC (eds) *The Haptophyte Algae* Systematics Association Special Volume 51

Zeuner FE 1962 Fossil insects from the Lower Lias of Charmouth, Dorset *Bulletin of the British Museum (Natural History), (Geology)* 7: 155-71